2022

Non-Canonical Odor Coding Ensures Robust Mosquito Attraction to Humans

Margaret Herre

Non-Canonical Odor Coding Ensures Robust Mosquito Attraction to Humans

A Thesis Presented to the Faculty of

The Rockefeller University

in Partial Fulfillment of the Requirements for

the degree of Doctor of Philosophy

by

Margaret Herre

June 2022

Non-Canonical Odor Coding Ensures Robust Mosquito Attraction to Humans

Margaret Herre, Ph.D.
The Rockefeller University 2022

Aedes aegypti mosquitoes spread deadly diseases, including dengue, Zika, yellow fever, and chikungunya. Only female mosquitoes bite, and they do so because they require a blood-meal for reproduction. *Aedes aegypti* prefer to bite human hosts, which contributes to their effectiveness as a deadly disease vector. Mosquitoes rely heavily on chemosensory cues, including carbon dioxide (CO_2) emitted from breath and human body odor, which is a mixture of more than 200 different individual odorants. Although the exact odor profile of people varies considerably, *Aedes aegypti* are incredibly reliable in finding humans to bite, despite widespread efforts to by humans to mask our odor. Even mosquitoes with genetic mutations that eliminate entire families of chemosensory receptors are still able to find and bite humans. It remains unknown how the mosquito olfactory system is seemingly infallible in its ability to detect humans for taking a blood meal.

In the well-studied olfactory systems of *Drosophila melanogaster* and *Mus musculus*, individual olfactory sensory neurons express a single type of olfactory receptor and project their axons to discrete regions, called glomeruli, in the antennal lobe or olfactory bulb, respectively. This organization is believed to be a widespread motif in olfactory systems and has been established dogma since the mid-2000s and is hypothesized to permit the brain to parse which subpopulation of olfactory neurons is activated by a given odor. To understand how human odor is encoded in the mosquito

olfactory system, we developed a CRISPR-Cas9-based genetic knock-in strategy in *Aedes aegypti* and generated a suite of transgenic mosquito strains that label populations of olfactory sensory neurons. Surprisingly, we find that the olfactory system of *Aedes aegypti* does not have the expected “one-receptor-to-one-neuron-to-one-glomerulus” organization seen in other insects. Rather, there are many more receptors than glomeruli. We frequently observe co-expression of multiple chemosensory receptors within individual olfactory sensory neurons and individual glomeruli are commonly innervated by olfactory sensory neurons expressing different receptors.

What is the functional consequence of this unconventional organization? To understand how co-expression of multiple chemosensory families affects human odor detection by mosquitoes, we examined a minimal mixture that drives host seeking behavior. Mosquitoes are attracted to the combination of the two human-derived, cues CO_2 and lactic acid. We found that the same neurons that sense CO_2 also sense volatile amines, including triethyl amine. These amines are detected by separate chemosensory receptor genes and we discovered that these cues can be interchanged to drive attraction in the presence of lactic acid. This sensory organization, in which multiple receptors that respond to very different types of chemicals are co-expressed, suggests a redundancy in the odor code at the level of the olfactory sensory neurons for cues that signal the presence of a human to bite. We speculate that this design supports the robust human host-seeking seen in this olfactory specialist.

For Shawna

ACKNOWLEDGMENTS

Thank you to my friends, family, colleagues, and mentors for your unwavering support, enthusiasm, patience, and kindness. You have sustained me and you gave this journey meaning.

Thank you to my graduate mentor, Leslie Vosshall. You have pushed me to be more confident, to think about the important questions without losing sight of the details, to be more assertive and also be more patient with myself. I have had space to make mistakes and grow into the scientist and person I aspire to be. From you I have learned how to be a steadfast advocate for my colleagues, community, and my science. You are an unforgettable, extraordinary mentor who will leave a lasting impact on me that will extend far beyond how to design the best experiment, generate beautiful figures, and captivate an audience.

I am grateful for my thesis committee, Dave Allis, Priya Rajasethupathy, and Mary Baylies, for your guidance and support. Your constructive feedback and genuine desire to help me succeed made FAC meetings an event where I emerged energized and inspired. Your thoughtful questions and insightful advice have shaped my career. Thank you, Priya, for always asking the next question that will keep me thinking. As an MD-PhD, I model my career path after yours. Thank you, Mary, for sharing the way you think about problems and for our conversations about my project outside of committee meetings. Your kindness and excitement about me as a scientist have been a source of strength. Thank you, Dave, for your steadfast support during my PhD as well as during my years as a research assistant. Your mentorship has been a throughline during my career at Rockefeller. Your intuition for the core issues of a problem, your sheer

enthusiasm for science, and your confidence in me are constant sources of hope and inspiration.

Thank you to Liqun Luo for serving as my external examiner. As I started to imagine how the mosquito olfactory system could be organized, I repeatedly retuned to your work as a paradigm for how to understand the logic of gene expression and wiring specificity in olfactory tissues. I am thrilled to have you serve as external examiner and I am grateful for the time you have committed to join me for my defense.

I am indebted to Lena Galkina for welcoming me into your lab when I had very little background or experience in science. Working in your lab changed my life, and I am grateful for your continued mentorship and friendship. I am at Rockefeller and in the Tri-Institutional MD-PhD program because Bob Darnell hired me as a research assistant, even as a fresh art school graduate with just a summer of lab experience. Your generosity and enthusiasm generated a lab environment that fostered creativity, collaboration and comradery. You gave the confidence and inspiration to pursue an MD/PhD.

Thank you to Zhongyan Gong, a research assistant, and Saher Rahiel, an undergraduate, for the time you put into collaborating with me on the projects outlined in this thesis. You taught me how to be a better mentor and a better scientist. I cannot wait to see how your careers unfold.

Leslie has created an unapparelled environment to do science, and I am grateful to members of the Vosshall Lab past and present for pushing me, inspiring me, and creating a scientific home that is a safe place to fail and a wonderful place to succeed. To Libby Mejia, Gloria Gordon, and Barbara Ghelardi, thank you for being the bedrock

of our lab and making mosquito work possible. To Nipun Basrur, my baymate, thank you for being a constant source of support, love, and laughter. I'll never forget the realization that our cackling can be heard at the far corners of the lab. Thank you to Veronica Jove for your wisdom and tenaciousness when approaching scientific problems, I learned so much from you. But more importantly, our friendship is one of the most important tangibles I will carry with me after graduating. I am so grateful to call you friend. To Krithika Venkataraman, thank you for your unwavering support and positivity. Being your friend and collaborating with you has been one of the great joys of my PhD. To Trevor Sorrells, thank you for your curiosity and friendship. Talking science with you is one of my favorite parts of the day, and I will miss that mischievous look in your eye when you glance over to me wondering if I'm available to chat (I always am). To Meg Younger, thank you for the energy and dedication you've brought to our collaboration. Having a teammate like you to tackle the questions presented in this thesis has been an amazing experience. To postdocs Takeshi Morita, Ellen de Obaldia, Nadav Shai, and Leah Houri-Ze'evi, thank you for all your support and positive feedback. Your expertise and kindness as I navigated these final days of grad school have been invaluable. To Emily Dennis and Ben Matthews, thank you for leading the way with your vision and excitement. I learned so much from you both in my early days in the lab. Thank you to newer students in the lab, Olivia Goldman, Yael Tsitohay, Adriana Rosas, and Priyanka Lakhiani, thank you for your energy – your enthusiasm is pushing this old, jaded grad student to the finish line.

Thank you to my family: my dad, mom, and sister Caroline, who have supported me through all my disparate career ambitions. You remind me what is most important, and I would not be here without your love, dedication, and your passion for learning. Finally, thank you to my partner, Shawna Altdorf. Your curiosity, irreverence, and unwavering love have sustained me. I love you.

TABLE OF CONTENTS

LIST OF FIGURES

CHAPTER 1. Introduction

1.1 Mosquito host-seeking drive is a multimodal chemosensory behavior

The deadliest animal in the world is not a shark, snake, or even a human, it is the tiny mosquito. Blood-feeding female mosquitoes transmit disease pathogens that kill over 700,000 people per year (WHO, 2020). Of the over 3500 known mosquito species, most are not interested in humans, many do not transmit diseases to any animal host, and some do not blood-feed at all (Rattanarithikul et al., 2007; Reeves et al., 2018). However, a handful of species, including *Anopheles gambiae* and *Aedes aegypti*, have evolved to specifically prefer to bite people (McBride, 2016). This preference for human odor evolved as a consequence of an ability to breed in human habitats (McBride, 2016; McBride et al., 2014; Rose et al., 2020; Takken and Verhulst, 2013). These human-preferring mosquitoes pose a lethal threat because they require a blood meal in order to reproduce, are carriers for viruses and parasites such as Zika (*Ae. aegypti)* and malaria (*An. gambiae)*, and take multiple blood meals throughout their lives thus spreading these diseases from human to human (Allan et al., 1987).

Human-preferring mosquitoes therefore offer a fascinating system to study olfaction, as female mosquitoes utilize their keen sense of smell to locate a human host. To identify a suitable meal, female *Ae. aegypti* use a combination of cues including CO_2 emitted from breath, human body odor, and body heat (Acree et al., 1968; Bernier et al., 2000; Davis and Bowen, 1994; Gallagher et al., 2008; Geier et al., 1999; Smallegange et al., 2005; Smith et al., 1970). Carbon dioxide is one of the most potent stimulants,

causing mosquitoes to engage in flight behavior in laboratory settings and to augment the attractiveness of other cues, such as components of human body odor and heat (McMeniman et al., 2014). Mosquitoes are also strongly attracted to warm objects as a feature of their host-seeking drive, and this behavior is further potentiated by addition of carbon dioxide (Majeed et al., 2014; McMeniman *et al.*, 2014). However, carbon dioxide and heat are ultimately non-specific cues and do not account for the selectivity of *Ae. aegypti* mosquitoes for their attraction to humans.

Human body odor, on the other hand, is a mixture of hundreds of different volatile chemicals and contains compounds that play a critical role in attracting specialists (Bernier *et al.*, 2000) Several compounds secreted by human sweat glands or released by the metabolism of commensal skin bacteria have proven to be attractive to mosquitoes, including lactic acid, 1-octen-3-ol, and ammonia (Acree *et al.*, 1968; Geier *et al.*, 1999; Takken and Kline, 1989; Verhulst et al., 2010). Lactic acid, in particular, is highly abundant on human skin and several studies have demonstrated that exposing female mosquitoes to only lactic acid and carbon dioxide in combination can recapitulate human host-seeking behaviors (Acree *et al.*, 1968). Even though human body odor contains other attractive compounds, remarkably, enzymatic removal of lactic acid renders human odor unattractive (Geier et al., 1996). Further, addition of lactic acid to the previously unattractive odor extras from cows and goats generates host-seeking behaviors at the levels of attractive humans (Steib et al., 2001). Although our understanding of the molecular makeup of the human odor space is still evolving, these

results demonstrate how monomolecular odorants can be utilized to manipulate mosquito attraction to their preferred human hosts.

While these compelling studies have elucidated important concepts of the roles of individual compounds driving host-seeking behaviors, mosquitoes encounter blends of odors in the wild. The sensory context in which an odor is encountered is critical to how it is perceived. An odor that is neutral or aversive alone may be attractive when presented with other compounds (Cao et al., 2017; Turner and Ray, 2009). For example, ammonia enhances the attractiveness of the host cue lactic acid in *Ae. aegypti* (Geier *et al.*, 1999). Additionally, many odors are attractive at a narrow range of concentrations, and neutral or aversive at higher or lower doses (Giang et al., 2017; Li and Liberles, 2015). Much work has been dedicated to producing blends of odorants that attract mosquitoes and understanding how these blends are encoded in the brain (Okumu et al., 2010; Smallegange et al., 2010; Zhao et al., 2020), but it is largely unknown how mosquitoes detect critical human odors or how human odor, heat, and carbon dioxide are integrated in mosquito brains to drive host-seeking behaviors. It is also not known how the mosquito's olfactory circuitry is organized to enable her robust host-seeking capabilities.

1.2 Convergent evolution of complex olfactory principles in vertebrates and insects

How might the mosquito olfactory system be organized? We can examine the organizational principles in other organisms for hints. An essential function of any

nervous system is to convert external cues into neuronal signals that communicate environmental information to the brain. Volatile chemicals, including odorants and pheromones, contain vital information about food sources, potential mates, predators, and danger. Chemosensory behaviors are observed in bacteria, nematodes, mollusks, insects, and vertebrates, but the genes involved in olfaction in these organisms show little to no sequence similarity. It is hypothesized that chemoreception evolved independently in each lineage (Brand et al., 2018; Hansson and Stensmyr, 2011; Niimura, 2009). Despite these independent evolutionary events, there are striking similarities between the organizational and functional principles of olfactory systems, particularly in the model systems of the fly *Drosophila melanogaster* and the mouse *Mus musculus.*

The molecular basis for the ability to detect odor in every species examined is the olfactory receptor. Olfactory receptors are membrane-bound proteins expressed in olfactory receptor neurons that are required for the detection of odorants. Olfactory receptor neurons then relay this information to the brain. Olfactory receptors make up one of the largest if not the largest gene family in insect and vertebrate genomes, often comprising hundreds to thousands of genes: in two incredible cases, olfactory receptors comprise approximately 6% of all functional genes in rats, and a staggering 10% in elephants (Ache and Young, 2005; Brand and Ramirez, 2017; Buck and Axel, 1991a; Niimura et al., 2014). The number of genes dedicated to olfactory receptors underscores the highly specialized nature of these receptors, and this specialization

extends to the cellular organization of olfactory systems in flies and mice. With notable exceptions, only one or occasionally two olfactory receptors are expressed in each olfactory neuron, and axons from olfactory neurons expressing the same receptors synapse onto dedicated glomeruli in the first olfactory processing centers of the brain: the olfactory bulb in vertebrates, and the antennal lobe in insects (Price and Powell, 1970; Stocker et al., 1990b; Vosshall et al., 2000).

The similarities in these olfactory systems extend to how individual odorants and blends of odors are detected by receptors and encoded in the brain. Many olfactory receptors are broadly tuned, meaning they are able to detect multiple odorants (in both flies and mice, however, social cues such as pheromones are often detected by a dedicated receptor (Ha and Smith, 2006; Haga-Yamanaka et al., 2015; Hagino-Yamagishi et al., 2001). Odor identity therefore is often encoded by activation of subpopulations of olfactory neurons in a combinatorial manner (Hallem and Carlson, 2004; 2006; Malnic et al., 1999). Combinatorial coding is thus thought to equip olfactory systems with the ability to detect and distinguish an astonishingly large number of stimuli by expanding an organism's potential coding capacity from the number of expressed receptors to the number of combinations among them. This system of combinatorial coding and segregation of olfactory information in the fly and mouse brain is what enables olfactory system's remarkable sensitivity and specificity. Finally, olfactory information in both mice and flies is processed in higher brain regions responsible both for innate and adaptive behaviors, underscoring the importance of

olfaction in a plethora of behaviors (Illig and Haberly, 2003; Li et al., 2008; Seki et al., 2017; Tanaka et al., 2004).

The differences between mouse and fly olfactory systems for the most part pertain to developmental patterning and receptor family type. Mouse odorant receptors not only engage in odorant detection, but also participate in axon guidance to olfactory bulb glomeruli as well as driving transcriptional feedback that enforces single olfactory receptor gene expression (Lomvardas et al., 2006; Mombaerts, 1996; Wang et al., 1998). Olfactory receptors in Drosophila direct neither axon targeting nor gene choice. Rather, flies utilize multiple, complex mechanisms to enforce appropriate gene expression and connectivity: certain transcription factors regulate both gene choice and wiring specificity, others regulate gene choice in some neurons and wiring specificity in other neurons (Li et al., 2020). Additionally, flies use Hedgehog, Toll, and Teneurin signaling to establish wiring specificity and achieve proper synaptic partner matching between olfactory receptor neurons and projection neurons in antennal lobe glomeruli (Chou et al., 2010; Hong et al., 2012; Ward et al., 2015). Finally, vertebrate olfactory receptors are G-protein coupled receptors, whereas insect receptors are ligand-gated ion channels, allowing insects faster processing speed (Benton et al., 2006; Butterwick et al., 2018; Kaupp, 2010). The speed achieved through ionotropic signaling is thought to be critical especially for winged insects that utilize olfaction to navigate dynamic odor plumes in flight.

It is notable that the differences between the mouse and fly olfactory systems are related to developmental architecture and signaling mechanisms while the similarities pertain to the overall functional logic, suggesting these systems arose via convergent evolution. The remarkable conservation of olfactory organizational principles between flies and mice – in particular, restricted expression of one or few olfactory receptors in each olfactory neuron, axonal projections to dedicated olfactory glomeruli, and utilization of combinatorial coding – might encourage us to hypothesize that all species in between follow these principles. Why would the mosquito be any different? One driver for a possible divergent organization is that while both mice and flies are generalist species, *Ae. aegypti* is a specialist and must find and bite humans for blood-meals, potentially requiring an olfactory system more suited to its needs. Another possibility is over-reliance on organizational principles discovered in "model" species, and that there is more diversity in olfactory circuitry in non-model organisms that can only be appreciated upon developing the tools to investigate them. In this work, we generate the genetic reagents necessary to begin to understand how the olfactory system in our non-model-organism is organized.

1.3 The *Drosophila melanogaster* olfactory system is highly stereotyped

Detecting an odor in insects begins when a volatile odorant diffuses into porous hair-like structures called sensilla housed on the main olfactory organs: antennae and maxillary palps. Olfactory sensory neurons send dendritic projections to the tips of these hair-like sensilla, where olfactory receptors encounter diffused odorants and transmit

this information to the brain, thus converting a chemical signal into an electrical one. Sensilla can be distinguished from each other based on the number of neurons innervating the hair as well as the width, height, and density of pores (Keil and Steinbrecht, 1964). Scientists in the 18th and 19th centuries hypothesized that the antennae are responsible for insect olfaction, but it was Karl von Frisch in 1923 who demonstrated that lose behavioral responses to odor following antennal amputation (Schneider, 1964; von Frisch, 1923). Indeed, the critical importance of olfaction in the life of insects is reflected in the elaborate nature of the main olfactory structure, the antenna (Figure 1.1A-F).

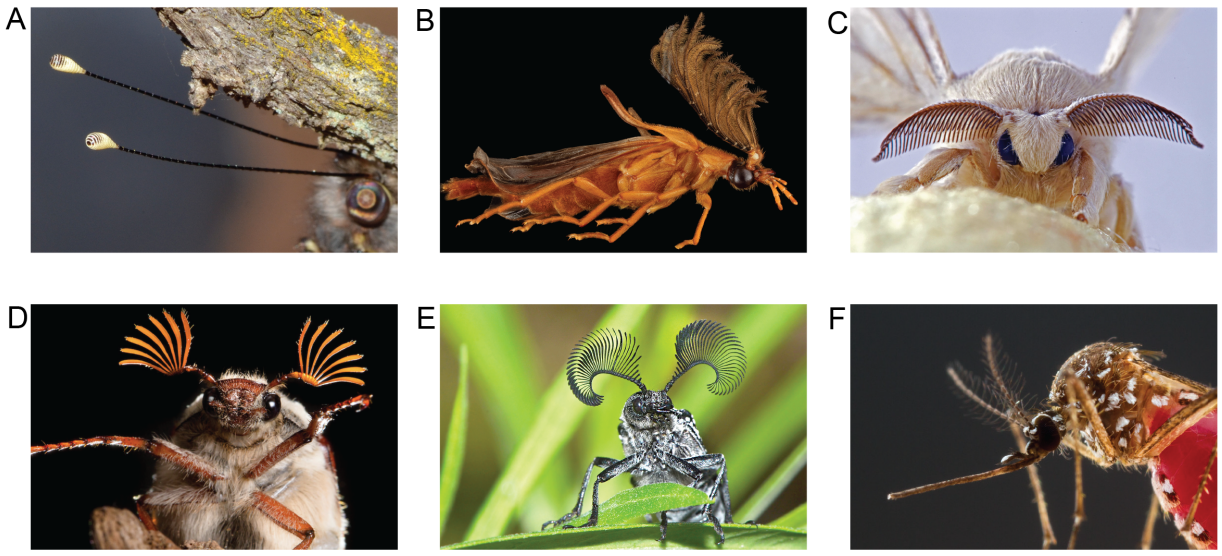

Figure 1.1 Diversity and beauty of antennal structures across insects.

(A) *Megacmonotus magnus.* Photo credit: Mark Vuaran.
(B) *Phengodes arizonensis*. Photo credit: Alex Hyde.
(C) *Bombyx mori*. Photo credit: Mark Vuaran.
(D) *Melolontha melolontha.* Photo credit: Alex Hyde.
(E) *Rhipicera femorata.* Photo credit: Fred Hort.
(F) *Aedes aegypti.* Photo credit: Alex Wild.

In *Drosophila melanogaster*, olfactory sensilla are located in stereotyped regions of the third antennal segment and maxillary palps (de Bruyne et al., 2001; Laissue and Vosshall, 2008). Through detailed dissection of olfactory receptor expression initially by RNA *in situ* hybridization and then later from transgenic reporter lines, it has been demonstrated that the position and number of olfactory sensory neurons expressing distinct olfactory receptors is bilaterally symmetric and highly stereotyped between individuals (Couto et al., 2005; Fishilevich and Vosshall, 2005; Kreher et al., 2005; Vosshall et al., 1999). Additionally, there is astounding correlation between olfactory neuron gene expression and sensilla type, suggesting that developmental programs that dictate sensillar morphology also determine olfactory neuron gene expression (Couto *et al.*, 2005).

Following detection of an odorant by an olfactory sensory neuron, axonal projections carry this information to the main olfactory processing center in the insect brain, the antennal lobe. This information is then carried by projection neurons to higher-order brain regions important for learned and innate behaviors, the mushroom body and lateral horn (Jeanne et al., 2018). The ease of generating genetic tools in *Drosophila* has led to a nearly complete yet evolving map of projections from olfactory organs to antennal lobe glomeruli (Couto et al., 2005; Fishilevich and Vosshall, 2005; Task et al., 2020; Vosshall et al., 2000). Each olfactory neuron expresses one or sometimes two olfactory receptors, and studies that expressed a membrane-bound GFP from the promoter of each olfactory receptor demonstrate that all olfactory neurons expressing the same receptor project to a single glomerulus in the antennal lobe (the one-receptor,

one-neuron, one-glomerulus hypothesis, discussed later). And just like the distribution of sensilla in the antenna, this organization is symmetrical and stereotyped between individuals (Couto et al., 2005; Fishilevich and Vosshall, 2005).

Is the mosquito olfactory system as stereotyped as *Drosophila melanogaster?* A lack of genetic reporter lines for each olfactory receptor currently precludes the ability to replicate detailed analysis performed in *Drosophila,* but several studies provide hints that while the mosquito may play by some of the same rules as the vinegar fly, its system may not be as stereotyped. The *Ae. aegypti* antenna is a long, flagellar structure made up of 13 segments which are believed to be repeating units (Afify et al., 2019) (Figure 1.1F). Although the antenna is covered in the same types of chemosensory sensilla found on *Drosophila* antennae, unlike the fly, different types of olfactory sensilla are not found in differential topographical distribution (Ghaninia et al., 2007b). Anterograde dye-filling of single functionally defined sensilla to determine antennal lobe axonal targeting in some cases revealed single glomeruli targeted by stimulated neurons, which is consistent with the one-neuron-one-glomerulus organization observed in *Drosophila*. However, as this study was able to only label a single sensillum at a time and the molecular identities of the labeled neurons were not determined, it is not known if glomeruli are innervated by multiple populations of neurons. Lack of extensive genetic tools in mosquitoes and other non-model insects like ants and honeybees leaves open the possibility that the extreme stereotypy observed in *Drosophila* may be an exception, rather than a rule.

1.4 Three chemosensory receptor families mediate olfactory behaviors

Which chemosensory receptors are required for the detection of human cues? Insects utilize three main receptor families to distinguish cues critical for feeding, mating, oviposition, and navigation. These large gene families, Odorant Receptors (ORs), Ionotropic Receptors (IRs), and Gustatory Receptors (GRs) encode ionotropic ligand-gated ion channels. Studies performed in *Drosophila* demonstrated that although there is overlap in the chemical repertoires these receptors detect, ORs, IRs, and GRs are generally tuned to different classes of volatile and non-volatile stimuli. ORs are activated by floral odors including aldehydes, alcohols, esters, and ketones, as well as pheromones (Benton et al., 2007; Gomez-Diaz et al., 2018; Hallem and Carlson, 2006; Hallem et al., 2004). IRs detect amines, acids, temperature, humidity, and have been implicated in taste circuits for polyamines, amino acids, salt, and carbonation (Abuin et al., 2011; Benton et al., 2009; Hussain et al., 2016; Zhang et al., 2013). GRs detect non-volatile compounds responsible for sweet and bitter taste, as well as pheromone and carbon dioxide detection and thermotaxis (Jones et al., 2007; Moon et al., 2009; Ni et al., 2013; Thorne et al., 2004; Wang et al., 2004). While the exact repertoire of chemosensory receptors required to locate humans for blood-meals is unknown, female mosquitoes likely utilize members of all three gene families to detect carbon dioxide, body heat, and human odor.

1.4.1 Odorant receptors

Odorant receptors (ORs) are odorant-gated ion channels (Butterwick *et al.*, 2018; Sato et al., 2008; Wicher et al., 2008) that are formed by a heteromultimeric complex of the conserved co-receptor Orco and a ligand-sensitive OR (Benton *et al.*, 2006; Larsson et al., 2004; Neuhaus et al., 2005; Sato *et al.*, 2008). Odorant receptors are insect-specific, are among the largest gene families in insect genomes, and are hypothesized to have evolved from gustatory receptors as an adaptation to terrestrial life (Brand *et al.*, 2018; Robertson et al., 2003). Most species encode just one Orco and a range of complementary ORs, from only three in the dragon fly to approximately 500 in some ant species (Brand *et al.*, 2018; McKenzie and Kronauer, 2018). While Orco is highly conserved, incredible sequence diversity exists between ORs both within and across species (Wicher and Miazzi, 2021). One-to-one orthologous ORs are relatively rare between insect taxonomic orders, indicating that different species have evolved distinct repertoires that enable them to be optimally suited to their environments (Butterwick *et al.*, 2018; Soffan et al., 2018; Zhao and McBride, 2020). Indeed, rapid evolution of ORs is thought to play a critical role in driving adaptive behaviors in new ecological niches, thereby allowing the hundreds of thousands of different insect species to coevolve with groups from plants to humans, display complex social behaviors, and occupy nearly every corner of terrestrial earth (Misof et al., 2014; Zhao and McBride, 2020).

Consistent with the critical role ORs play in evolution and survival, mutagenesis of *Orco* has produced fascinating effects in several insects examined, particularly in

specialist species. In fact, *Orco* has been amongst the first genes mutated in several non-model invertebrates, underscoring the critical role of Orco and ORs in feeding, social, and reproductive behaviors. In the hawkmoth *Manduca sexta*, *Orco* mutagenesis inhibited the moth's foraging abilities to perform odor-direct flight orientation to its preferred nectar source plant, *Datura wrightii* (Fandino et al., 2019). Loss of *Orco* in two ant species, *Harpegnathos saltator* and *Ooceraea biroi* caused defects in social behavior, reproduction, and dramatically impaired development of the main olfactory processing center, the antennal lobe (Trible et al., 2017; Yan et al., 2017). *Drosophila sechellia,* a species that specializes on toxic noni fruit, do not exhibit defects in feeding on noni when *Orco* or I*r8a*, an ionotropic receptor co-receptor, are mutated alone, but double mutants exhibit a total loss of preference for noni, indicating redundancy in the requirements of OR and IR pathways in this Drosophilid specialist (Auer et al., 2020).

While *Aedes aegypti* mosquitoes lacking *Orco* are still able to find and bite humans, these mutants lose strong preference for human odor over animal odor (DeGennaro et al., 2013). Indeed, when 'domestic' *Ae. aegypti,* who prefer humans over animals, were compared to 'forest' *Ae. aegypti,* who prefer animals over humans, transcript expression and ligand sensitivity of one odorant receptor, *Or4*, was tightly linked to human odor preference (McBride et al., 2014). Further, while human odor blends activate several antennal lobe glomeruli that are also activated by guinea pig, rat, sheep, and dog odor, human odor also activates a glomerulus not activated by any of the tested animals, suggesting a dedicated olfactory circuit for this human-specialized mosquito (Zhao et al., 2020). Together, these data suggest a critical role for ORs in the evolution of

human-preference behaviors of disease-carrying mosquitoes. However, since mosquitoes lacking Orco are still able to find and bite humans, other sensory modalities mediated by IRs and GRs are likely required to work in concert with ORs to drive this deadly behavior.

1.4.2 Ionotropic receptors

Ionotropic receptors are variant ionotropic glutamate receptors that are formed by one or more of three conserved co-receptors and ligand-sensitive subunits that determine the selectivity of the receptor complex (Abuin et al., 2011; Benton et al., 2009; Silbering et al., 2011). While odorant receptors are primarily expressed in olfactory organs and mediate detection of volatile odorants, ionotropic receptors are expressed far more broadly and in addition to olfaction mediate temperature sensation as well as contact food and oviposition site evaluation (Chen and Amrein, 2017; Hussain et al., 2016; Ni et al., 2016; Rimal and Lee, 2018). Also in contrast to odorant receptors, which are insect-specific, ionotropic receptors are far more evolutionarily ancient and can be found in chemosensory organs across Protostomia: in arthropods, nematodes, and mollusks (Croset et al., 2010). Interestingly, IRs that are expressed in olfactory organs such as the antenna are much more highly conserved than IRs expressed in gustatory receptor neurons and other neurons in non-olfactory organs (Rimal and Lee, 2018). While ORs use a single co-receptor, the IR family employs at least 3 to mediate a diverse array of chemosensory tasks: *Ir25a*, *Ir8a*, and *Ir76b* (Benton et al., 2009). These co-receptors are expressed in multiple neuronal populations and

are required in various combinations to mediate ligand detection with ligand-selective IRs (Abuin et al., 2011; Knecht et al., 2016; Sanchez-Alcaniz et al., 2018). In *Drosophila, Ir25a* and *Ir76b* are broadly expressed throughout the body and mediate multiple sensory modalities in addition to olfaction such as taste, hygrosensation, and thermosensation (Abuin et al., 2011; Ahn et al., 2017; Hussain *et al.*, 2016; Knecht et al., 2017; Zhang et al., 2013). *Ir8a* meanwhile is selectively expressed in the antenna and is required for volatile acid detection (Abuin *et al.*, 2011; Task *et al.*, 2020).

What roles do IRs play in mediating mosquito sensory behaviors? Since there are at least 3 IR co-receptors, knocking out all IR signaling is not as simple as eliminating all OR signaling through *Orco* mutagenesis. However, mutations in single IR co-receptors as well as ligand-sensitive IRs shed light on how this family may be operating in mosquitoes. As in *Drosophila*, *Ir8a* is selectively expressed in the antenna (Matthews et al., 2016). Mutagenesis of *Ir8a* shows it is required for detection of an important component of human odor, lactic acid (Raji et al., 2019). *Ir25a* and *Ir76b* transcripts have been identified in mosquito olfactory organs, feeding appendages, and legs, and likely mediate a broad range of sensory modalities as they do in *Drosophila* (Matthews et al., 2016). Mutagenesis of *Ir25a* and *Ir76b* suggest potential roles for these co-receptors in the detection of heat and human odor, although these mutants still retain some host-seeking capabilities (Takeshi Morita, Ellen de Obaldia, pers. comm.). Similarly, through knocking out a cooling receptor in *Anopheles gambiae, Ir21a*, reduces this mosquito's attraction to heat at host temperatures, these mutants show no deficits in their abilities to locate a human arm (Greppi et al., 2020). The roles for IRs in lactic

acid and heat detection demonstrate that this family likely plays a critical part in human host-seeking, eliminating all IR activity may not be sufficient to eliminate a mosquito's ability to find her host.

1.4.3 Gustatory receptors

The insect gustatory system shares many properties with the olfactory system in that both detect chemical stimuli, however, in both vertebrates and invertebrates, these systems are for the most part anatomically and functionally separated and operate by different organizational principles (Yarmolinsky et al., 2009). Unlike olfactory systems, wherein neurons express a single or few receptors per cell, single odorants often activate multiple receptors, and thousands of distinct odorants are decoded by combinatorial coding, taste coding is generally categorized into a small palette of qualities (including sweet and bitter) and loosely follow a labeled-line organization (Chandrashekar et al., 2006; Liman et al., 2014). The separation of olfactory and taste stimuli may reflect a requirement to distinguish long-range chemical signals and short-range contact cues. Further, the elegant, simplified organization of the taste system may be the result of an evolutionary need to quickly evaluate food qualities before ingesting, as bitter taste is often associated with the potential for toxicity and are innately aversive (Ventura and Worobey, 2013). For example, *Drosophila* express as many as 28 bitter receptors in a single taste neuron, suggesting that the identity of individual bitter tastants is not as critical as the ability to quickly signal to taste

processing centers in the brain that a food may contain toxic compounds (French et al., 2015).

Although insect gustatory receptors are primarily taste receptors (Clyne et al., 2000; Montell, 2009; Scott et al., 2001), insects utilize these receptors for purposes beyond taste and food evaluation. Cuticular hydrocarbons are compounds essential for both initiation and inhibition of courtship behaviors, and three such inhibitory hydrocarbons activate Gr32a (which is also a bitter taste receptor) (Kohl et al., 2013). Additionally, GRs form a complex that detects carbon dioxide (Jones et al., 2007; Kwon et al., 2007). CO_2 is an important volatile human host cue that activates and attracts mosquitoes (Gillies, 1980). In *Ae. aegypti*, *Gustatory Receptor 3* (*Gr3*) encodes an essential subunit of the CO_2 receptor, and *Gr3* mutant mosquitoes lose all sensitivity to CO_2 (McMeniman et al., 2014). However, lacking sensitivity to CO_2, while an important volatile cue, is not sufficient to eliminate host-seeking behavior when mosquitoes are presented with other cues such as heat and human odor.

1.5 Mutations in large chemosensory families fail to eliminate host-seeking drive

A theme is emerging: mutation of chemosensory co-receptors thought to be essential for olfaction does not eliminate host-seeking behaviors. Why? The drive to find humans is strong and innate, and likely utilizes multiple families of chemosensory receptors acting in concert with each other. Previous studies demonstrated that mosquitoes engage in host-seeking behaviors when exposed to heat, CO_2, and human

odor, or any combination of 2 of these stimuli, implying that there is redundancy in the way human cues are encoded in the mosquito brain (McMeniman et al., 2014). Thus, knocking out a family of receptors required for a single modality has not been sufficient to suppress host-seeking behaviors. As stated above, animals lacking the olfactory receptor co-receptor (Malaspina), the obligate co-receptor required for the function of the entire family of ORs, show strong attraction to humans (DeGennaro *et al.*, 2013). Independently deleting the *Ir8a, Ir76b,* or *Ir25a* co-receptors reduce but do not eliminate attraction to humans (Raji et al., 2019). Finally, mosquitoes lacking the obligate CO_2 receptor subunit, *Gr3* are still highly effective in finding humans in a more naturalistic semi-field setting (McMeniman et al., 2014).

A reasonable assumption, therefore, that knocking out multiple chemosensory receptor families would eliminate host-seeking capabilities, but this is not yet the case. However, we still gain important insights about the redundancy of sensory modalities from the generation of co-receptor double mutants. In the absence of CO_2, animals lacking *Ir8a* (required for lactic acid detection) and *Orco* (required for human-animal discrimination) are more impaired than animals lacking *Ir8a* alone, suggesting these families are acting in a non-redundant manner. *Ir8a* and *Gr3* double mutants, on the other hand, are just as impaired as *Gr3* mutants and none of the *Ir8a* mutant phenotypes can be rescued by the addition of CO_2 (Raji et al., 2019), implying that although these cues may be integrated in the same circuit, CO_2 activation is not sufficient to rescue the *Ir8a* mutant phenotypes. This finding also builds on previous studies that show that activation by CO_2 is necessary to promote host-seeking

behaviors in concert with host odors such as lactic acid, but is not attractive on its own (Acree et al., 1968). How does heat, an important host cue, interact with CO_2 and human odor? Mosquitoes unable to respond to a presentation of heat and CO_2 are still able to locate a human arm at the rate of wild-type animals, but it is not yet known if double mutants lacking the ability to sense CO_2 and heat or lactic acid and heat would lose all host-seeking capabilities (Greppi et al., 2020). Gaining further understanding of how the olfactory system is organized may enable us to identify the right combination of mutations that would eliminate host-seeking drive.

1.6 The one-receptor, one-neuron, one-glomerulus organization in insects

The cloning of the first odorant receptors by Buck and Axel in 1991 (Buck and Axel, 1991b) led to the subsequent discovery that each olfactory sensory neuron expresses a unique odorant receptor that specifies its functional properties. With few exceptions, the well-studied olfactory systems of *Drosophila melanogaster* flies (Clyne et al., 1999; Gao and Chess, 1999; Vosshall et al., 1999) and *Mus musculus* mice (Bashkirova and Lomvardas, 2019; Chess et al., 1994) feature olfactory sensory neurons that are thought to express a single olfactory receptor. In both species, neurons expressing a given receptor project axons to dedicated olfactory glomeruli in the first sensory processing center in the brain, the antennal lobe in insects (Couto et al., 2005; Fishilevich and Vosshall, 2005; Vosshall et al., 2000) and the olfactory bulb in vertebrates (Mombaerts et al., 1996; Ressler et al., 1994; Vassar et al., 1994). This “one-receptor-to-one-neuron-to-one-glomerulus” organization is believed to be a

widespread motif in insect olfactory systems, and the convergence onto discrete glomeruli is hypothesized to permit the brain to utilize combinatorial coding and parse which subpopulation of olfactory neurons is activated by a given odor (Bisch-Knaden et al., 2018; Semmelhack and Wang, 2009; Wang et al., 2003).

Consistent with this “one-receptor-to-one-neuron-to-one-glomerulus” organization in insects, the number of expressed chemosensory receptors in the OR and IR gene families roughly correlates to the number of olfactory glomeruli. This holds true in *Drosophila melanogaster* flies (~60 receptors/~55 glomeruli) (Benton et al., 2009; Laissue et al., 1999; Robertson et al., 2003), the honey bee *Apis mellifera* (~180 receptors/~160 glomeruli) (Flanagan and Mercer, 1989; Robertson et al., 2010), and the tobacco hornworm *Manduca sexta* (~60 receptors/~70 glomeruli) (Grosse-Wilde et al., 2011). Based on these studies, it is widely thought that merely counting the number of antennal lobe glomeruli in a new species would be reasonably predictive of the number of chemosensory receptors found in its genome. In *Ae. aegypti*, however, there is a striking mismatch between the number of expressed chemosensory receptors and the number of antennal lobe glomeruli, with at least twice as many receptors as available glomeruli (Bohbot et al., 2007; Ignell et al., 2005; Matthews et al., 2018; Shankar and McMeniman, 2020; Zhao et al., 2020). How is the mosquito olfactory system organized to accommodate so many receptors and does this departure from rules established in other species explain their exquisite ability to locate human hosts?

1.7 Concluding remarks

Here we show that the olfactory systems of *Ae. aegypti* mosquitoes encode redundancy in their olfactory systems by utilizing novel olfactory organizational principles. To understand how human odor is encoded in the mosquito olfactory system, we developed a CRISPR-Cas9-based genetic knock-in strategy in *Aedes aegypti* and generated a suite of transgenic mosquito strains that label populations of olfactory sensory neurons. We found that the olfactory system of *Aedes aegypti* does not have the expected “one-receptor-to-one-neuron-to-one-glomerulus” organization seen in other organisms. Instead, we found that many mosquito neurons profiled express multiple members of at least two chemosensory receptor families. We frequently observed co-expression of multiple chemosensory receptors within individual olfactory sensory neurons and individual glomeruli are commonly innervated by olfactory sensory neurons expressing different receptors. Some chemosensory receptors belonging to different families are consistently co-expressed together, indicating transcriptional coordination. We also found evidence of co-convergence of neurons expressing different receptors to the same glomerulus. This unexpected co-expression is functional, as assessed by GCaMP imaging in the antennal lobe showing that a given glomerulus is activated by multiple ligands specific to different gene families. Finally, we demonstrate that this dogma-disrupting co-expression has direct functional consequences for mosquito host-seeking behavior.

To gain insight into how this unconventional organization relates to human odor detection by mosquitoes, we examined a minimal mixture that drives host seeking behavior. Mosquitoes are attracted to the combination of the cues CO_2 and lactic acid. We found that the same neurons that sense CO_2 also sense volatile amines, including triethyl amine. These amines are detected by separate chemosensory receptor proteins and we discovered that these cues can be interchanged to drive attraction in the presence of lactic acid. Thus, the behavioral deficits of CO_2-insensitive mutant mosquitoes can be rescued by activating additional receptors expressed in CO_2 neurons with their cognate ligand. This sensory organization, in which multiple receptors that respond to very different types of chemicals are co-expressed, suggests a redundancy in the odor code at the level of the olfactory sensory neurons for cues that signal the presence of a human to bite. We speculate that this non-canonical olfactory system organization featuring overlapping gene expression and co-convergence of molecular distinct neurons to the same glomerulus affords the female mosquito redundant and robust attraction to humans.

CHAPTER 2. Mismatch in chemosensory receptor and olfactory glomerulus number suggests a novel olfactory organization

To understand how an organism's olfactory system is organized, we need to know the identity of the olfactory genes expressed, the spatial distribution of genes expressed in olfactory sensory neurons, and how these neurons are wired to the brain. To enable these studies in the mosquito, prior work from our lab re-sequenced the mosquito genome, generated a library of chemosensory transcriptomes, and established methods for CRISPR-Cas9 mutagenesis (Kistler et al., 2015; Matthews et al., 2018; Matthews et al., 2016). Further, work in *Anopheles gambiae* established the QF-QUAS binary expression system as a potential method to label and manipulate neuronal subpopulations (Riabinina et al., 2016). The QF system is analogous to the Gal4-UAS system wherein a transcription factor (QF/Gal4) expressed from promoter sequences or endogenous loci from a gene of interest binds to its target sequence (QUAS/UAS) which drives expression of a desired gene to enable fluorescent labeling, activation or inactivation, or functional calcium imaging. Thus, the mosquito became a genetically tractable organism, and we were primed to make discoveries previously impossible without molecular, genetic and genomic advances. In this chapter, we get our first glimpses of a non-canonical olfactory organization in female *Ae. aegypti* mosquitoes.

2.1 Chemosensory gene expression exceeds number of antennal lobe glomeruli

In the mosquito, olfactory cues are sensed by olfactory sensory neurons in the antenna and the maxillary palp, whose axons project to the ipsilateral antennal lobe of

the brain (Distler and Boeckh, 1997; Ignell et al., 2005) (Figure 2.1A-B). The antennal lobe, the insect equivalent of the vertebrate olfactory bulb, is organized into discrete olfactory glomeruli in which axons from peripheral olfactory sensory neurons terminate and synapse with local interneurons and projection neurons that relay olfactory information to the higher brain (Stocker, 1994). Previous studies used morphological criteria to define 50 (Ignell *et al.*, 2005), 60 (Zhao et al., 2020), or 81 (Shankar and McMeniman, 2020) discrete olfactory glomeruli in the female *Ae. aegypti* antennal lobe.

The canonical “one-receptor-to-one-neuron-to-one glomerulus” organization posits that the number of chemosensory receptors should roughly match the number of glomeruli in the antennal lobe. While there is not yet a clear consensus on the number of olfactory glomeruli in *Ae. aegypti*, it ranges from 50 to 81. How does this relate to the number of chemosensory receptors expressed? In the updated *Ae. aegypti* genome (Matthews et al., 2018), there are 117 OR, 135 IR, and 72 GR genes for a total of 324 structural genes that could function in the olfactory system (Figure 2.1C,D). We have reanalyzed published RNA expression data (Matthews *et al.*, 2016) using multiple thresholds to estimate the number of receptors expressed in the antenna and maxillary palp. Even at the conservative threshold of 5 transcripts per million (TPM), the mosquito olfactory system expresses 102 chemosensory receptors, and moving the threshold to 2, 1, or 0.5 TPM increases the number of receptors plausibly expressed to 134, 156, and 178, respectively (Figure 2.1E,F).

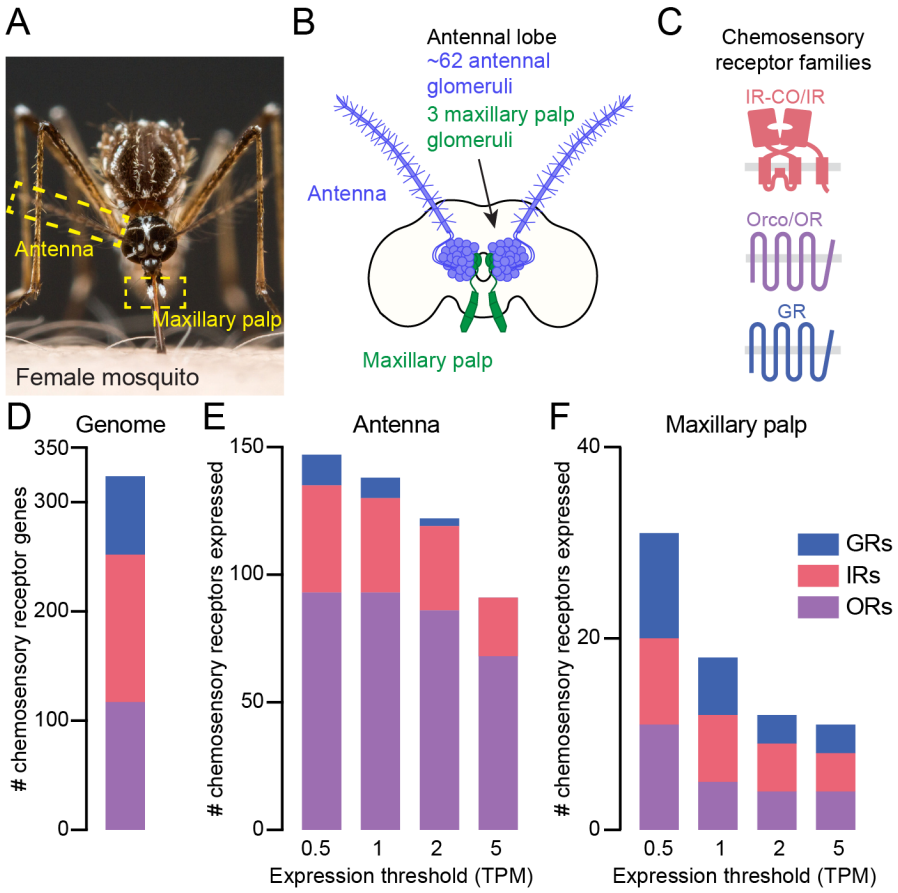

Figure 2.1 Chemosensory gene expression exceeds number of antennal lobe glomeruli

(A) Ae. aegypti female with sensory structures highlighted in yellow boxes.
(B) Approximate number of antennal lobe glomeruli per brain hemisphere innervated by the indicated sensory structure, derived from quantification of the left antennal lobe in 12 brains presented in Figure 2.3.
(C) Cartoons of insect chemosensory gene families.
(D-F) Stacked bar plots of the number of chemosensory genes in the Ae. aegypti genome (D), and the number expressed above the indicated TPM thresholds in the antenna (E) and maxillary palp (F)
Work performed by: Margo Herre, Meg Younger, Ben Matthews

In order to gain a clearer consensus on the number of antennal lobe glomeruli in female *Ae. aegypti* brains, we define approximately 65 olfactory glomeruli (64.9 ± 0.9,

mean ± SEM), obtained by counting antennal lobe glomeruli in the left hemisphere of 12 female *Ae. aegypti* brains stained to reveal synaptic neuropil (Figure 2.2A,B). The glomerulus count ranged from 60-72 glomeruli per antennal lobe, indicating a high level of variability in the organization of the antennal lobe(Figure 2.2C). We generated 3-D reconstructions of complete antennal lobes and saw considerable variability in the size and shape of the glomeruli (Figure 2.2D-K). We were able to consistently identify certain landmark glomeruli, most notably the three glomeruli that are innervated by the maxillary palp (Ignell *et al.*, 2005; Shankar and McMeniman, 2020) (Figure 2.2D-K).

Figure 2.2 Organization of *Ae. aegypti* antennal lobe glomeruli

(A-B) Maximum-intensity projections of confocal Z-stacks of a brain after anterograde dye fill of a single ipsilateral antenna (A) or ipsilateral maxillary palp (B) using a dextran-conjugated fluorophore (green) with immunofluorescent labeling of Brp (synaptic marker, magenta).
(C) Approximate number of antennal lobe glomeruli per brain hemisphere innervated by the indicated sensory structure, derived from quantification of the left antennal lobe in 12 brains presented in Figure 2.3.
(Meyer et al.) 3-D reconstruction of a single left antennal lobe with 61 (D-G) or 66 (Bisch-Knaden *et al.*) glomeruli shown at 4 different angles. Glomeruli are colored according to innervation by the indicated sensory appendage.
Scale bars: 50 μm (A-B), 20 μm (Meyer *et al.*). Orientation: d=dorsal, m=medial, p=posterior.
Work performed by: Meg Younger

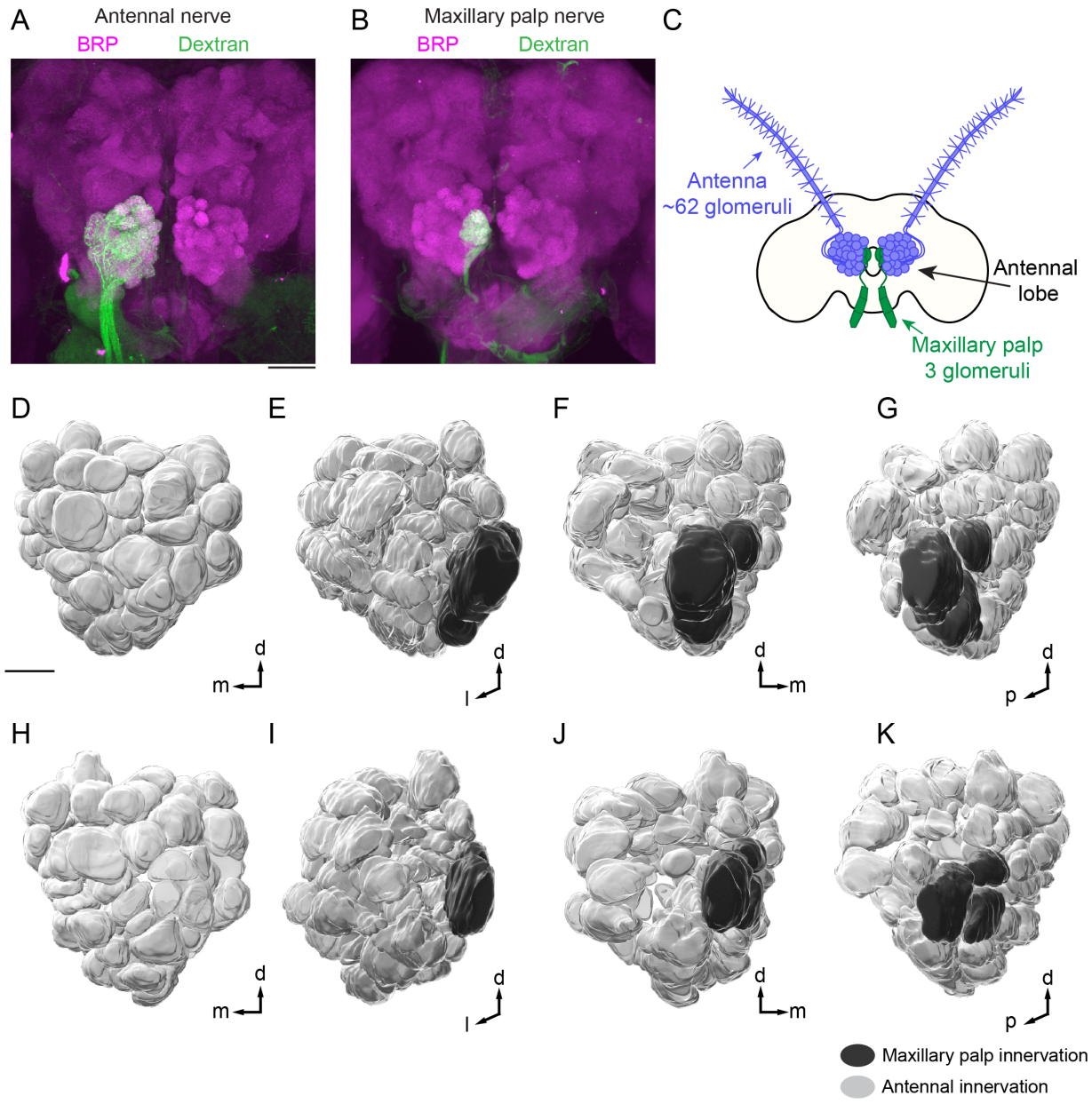
A
Antennal nerve
BRP
Dextran
B
Maxillary palp nerve
BRP
Dextran
C
Antenna
~62 glomeruli
Antennal
lobe
Maxillary palp
3 glomeruli
D
E
F
G
H
I
J
K
d
m
l
p
Maxillary palp innervation
Antennal innervation

Thus, there are many more chemosensory receptors expressed in the olfactory system than available antennal lobe glomeruli, suggesting that the organization of the *Ae. aegypti* olfactory system must differ from the canonical scheme (Figure 2.3A). We speculate that the mismatch can be resolved by expressing multiple receptors per neuron or having multiple different types of neurons co-converge on a single glomerulus or both (Figure 2.3B).

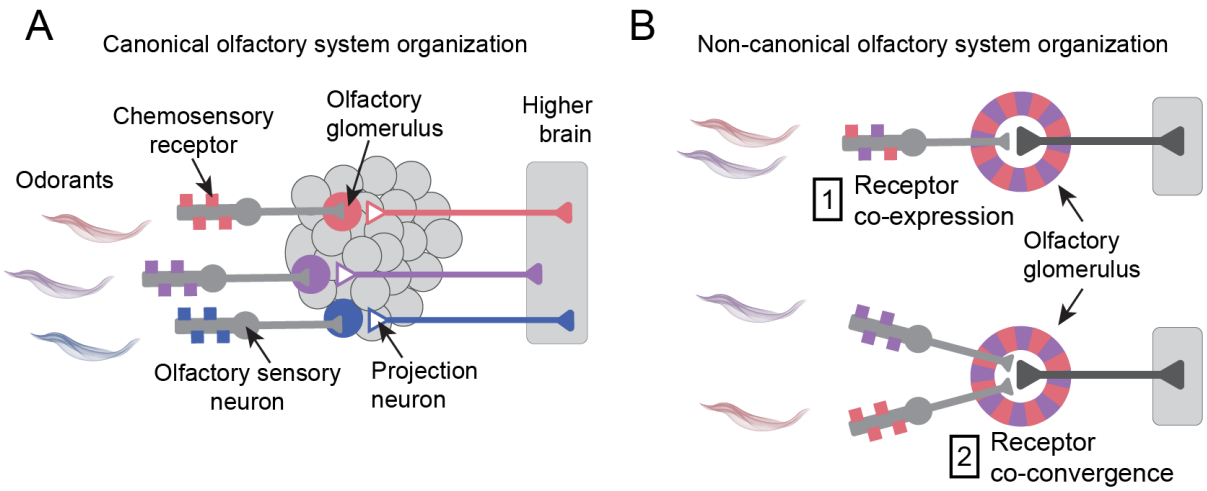

Figure 2.3 Models of canonical versus hypothesized mosquito non-canonical olfactory system organization

(A) Cartoon of canonical olfactory system organization.
(B) Two models of olfactory system organization that can account for the observation that there are far more chemosensory receptors than olfactory glomeruli in Ae. aegypti.
Work performed by: Margo Herre, Meg Younger

2.2 Extensive overlap of antennal lobe glomeruli targeted by neurons expressing distinct classes of chemosensory co-receptors

To begin to distinguish between these two organizational principles, we generated a collection of CRISPR-Cas9 gene-targeted strains that label subpopulations of olfactory neurons using the Q-system, a binary expression system similar to Gal4/UAS (Brand and Perrimon, 1993) that uses cell type-specific expression of the QF2 transcription factor to induce expression of an effector from the QF2 binding *QUAS* enhancer (Potter et al., 2010; Riabinina et al., 2015; Riabinina et al., 2016). We introduced an in-frame insertion that replaced the stop codon of each of the co-receptors *Orco*, *Ir25a*, *Ir8a*, and *Ir76b*, as well as the CO_2 receptor subunit *Gr3* with the transcription factor *QF2* (Figure 2.4A) (Matthews et al., 2019; Potter et al., 2010; Riabinina et al., 2016). These five new gene-sparing knock-in strains were designed to cause minimal disruption to the locus to increase the likelihood that they would faithfully report expression of the endogenous gene. We crossed these *QF2* driver lines individually to a *QUAS-CD8:GFP* reporter to label neuronal membranes and visualized axonal projection patterns in the antennal lobe.

Orco, *Ir25a*, *Ir8a*, and *Ir76b* co-receptor driver lines were expressed in olfactory sensory neurons with distinct projection patterns in the antennal lobe (Figure 2.4B-D). Unexpectedly, neurons that expressed *Ir25a* projected to almost all of the glomeruli in the antennal lobe (89.9 ± 1.4%, mean ± SEM, n = 3)(Figure 2.4B-D), and expression overlapped extensively with glomeruli labeled by *Orco* (Figure 2.4B-D). While these co-receptor driver lines labeled glomeruli in the same regions from brain to brain, the

interindividual expression patterns were not identical, consistent with the variability in glomerular anatomy that we have observed. Neurons that detect CO_2 are located in the maxillary palp (Grant et al., 1995; Lu et al., 2007; Omer and Gillies, 1971) and we saw that *Gr3*-expressing neurons projected to a large glomerulus in the posterior antennal lobe, Glomerulus 1 (Figure 2.4B-D) which is also innervated by *Ir25a*-expressing neurons. These initial findings point to the overlap of *OR*-, *IR*-, and *GR*-expressing neurons in the antennal lobe of *Ae. aegypti*, which are believed to remain segregated in *Drosophila melanogaster*.

Figure 2.4 Extensive overlap of antennal lobe glomeruli targeted by neurons expressing distinct classes of chemosensory co-receptors

(A) Generation of QF2 driver and effector lines to label chemosensory co-receptor populations by CRISPR-Cas9 mutagenesis and homologous recombination. CRISPR guides targeting the stop codon of *Orco, Ir25a, Ir8a, Ir76b,* and *Gr3* enable cutting at endogenous loci, and homologous recombination removes the stop codon and replaces it with a sequence encoding the ribosomal skipping sequence T2A and the QF2 transcription factor.
(B) Maximum-intensity projections of confocal Z-stacks of antennal lobes in the left-brain hemisphere of the indicated genotype with immunofluorescent labeling of GFP (green) and the nc82 monoclonal antibody, which recognizes Brp (magenta). Brp is used throughout this work as a synaptic marker. Scale Bar: 50 μm. Orientation: d=dorsal, m=medial.
(C) 2-D representation of the boundary of each glomerulus that is GFP positive and GFP negative.
(D) Cartoon schematic of the glomeruli receiving projections from olfactory sensory neurons expressing the indicated chemosensory receptor.
Work performed by: Meg Younger

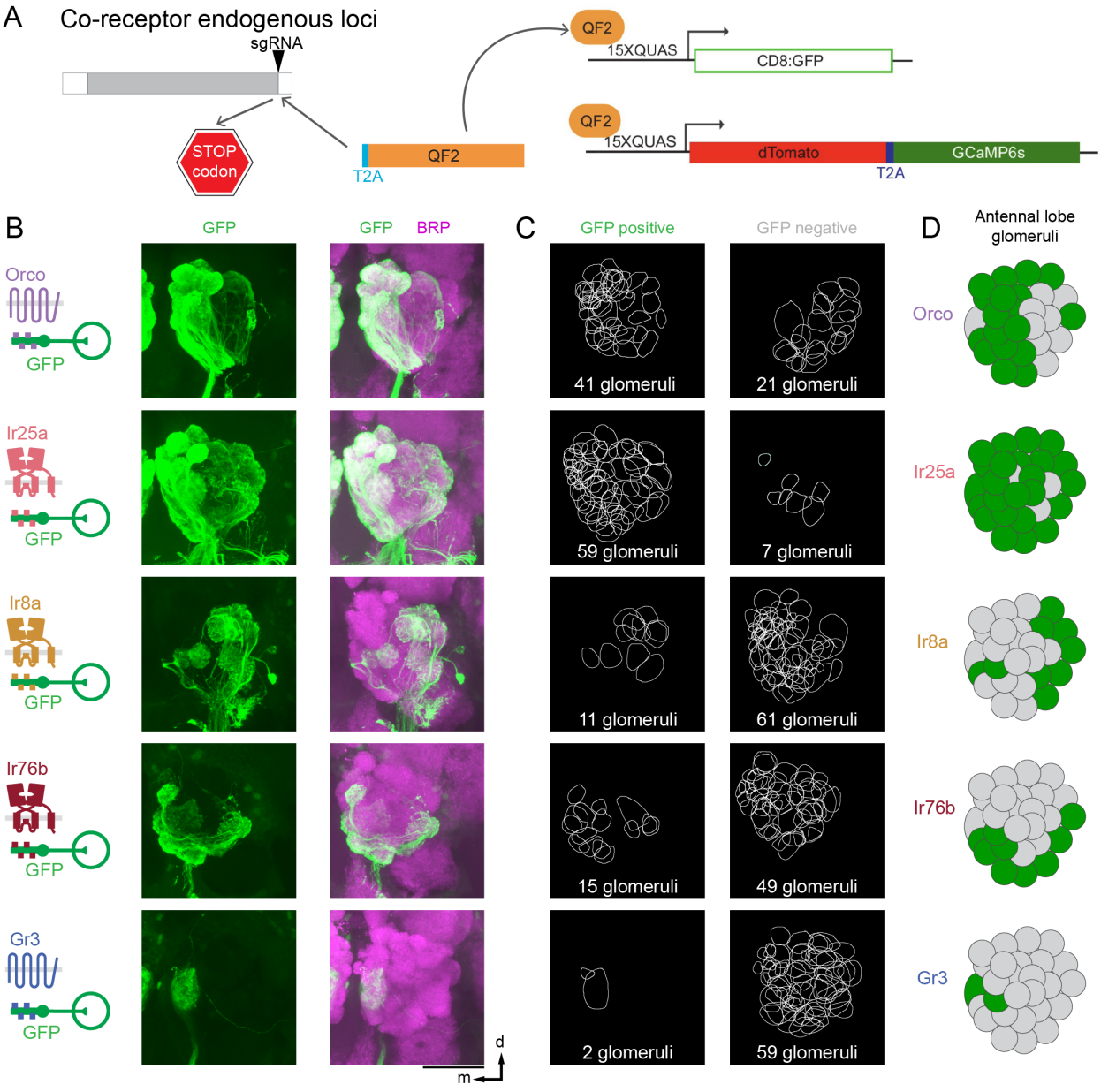
A
Co-receptor endogenous loci
sgRNA
STOP codon
QF2
T2A
QF2
15XQUAS
CD8:GFP
QF2
15XQUAS
dTomato
GCaMP6s
T2A
B
GFP
GFP BRP
C
GFP positive
GFP negative
D
Antennal lobe glomeruli
Orco
GFP
41 glomeruli
21 glomeruli
Ir25a
GFP
59 glomeruli
7 glomeruli
Ir8a
GFP
11 glomeruli
61 glomeruli
Ir76b
GFP
15 glomeruli
49 glomeruli
Gr3
GFP
2 glomeruli
59 glomeruli
d
m

2.3 Variability in antennal lobe glomerulus innervation by chemosensory co-receptor neuron populations

The antennal lobe glomerular organization observed in *Drosophila melanogaster* is highly stereotyped in that olfactory neurons expressing the same chemosensory receptors target the same glomerulus in every individual, and the number and anatomical positions of these glomeruli are fixed (Couto et al., 2005; Fishilevich et al., 2005; Stocker et al., 1990b). Upon generating QF2 driver lines for each chemosensory co-receptor, we observed striking variability in the number and location of innervated glomeruli, suggesting that the mosquito olfactory system is not nearly as stereotyped as that of *Drosophila.* Below I provide additional information regarding expression and projection patterns of our chemosensory co-receptor knock-in lines.

Gr3>GFP

Gr3 is a gustatory receptor that forms part of a complex with two other gustatory receptors, Gr1 and Gr2, to mediate carbon dioxide sensing in *Ae. aegypti* (McMeniman et al., 2014). All antennal lobes in this line show innervation of a single glomerulus (also referred to as ”MD1” and here referred to as “Glomerulus 1”; (Ignell et al., 2005; Shankar and McMeniman, 2020). In several brains, we saw a second small medial glomerulus that derives its innervation from the antenna and is in a small medial cluster of landmark glomeruli midway down the anterior-posterior axis closest to the center of the brain. Innervation appears to come from only a few axons.

This low and variable reporter expression is consistent with the low level of expression of Gr3 in the antennal transcriptome (Matthews *et al.*, 2016). We analyzed

both left and right antennal lobes from 4 brains and found that in 3 of the 4 brains there was a second glomerulus in one or both antennal lobes (Figure 2.5A). The presence of the second glomerulus was not specific within a single animal as we found all variations of presence and absence of this glomerulus across both antennal lobes in these 4 animals. In some Gr3>GFP animals, we detected a small number of processes that extended beyond the antennal lobe and into the higher brain, although the exact termination site varied. We never observed CO2-evoked activity in the variable second glomerulus or these projections outside the antennal lobe (data not shown).

Orco>GFP

We noted that the intensity of GFP varies between glomeruli in this driver line, with some bright and others comparably dim (Figure 2.5B). We speculate that this is due to a combination of the variability in *Orco* expression levels in individual neurons and variability in the density of innervation in individual glomeruli. A large region of the anterior ventral antennal lobe was previously referred to as the Johnston's organ center and was thought to comprise a single large glomerulus (Ignell et al., 2005). In other insect species, Johnston's organ mediates detection of auditory cues. Consistent with a recent study (Shankar and McMeniman, 2020), we segmented this region into multiple glomeruli based on anatomical boundaries revealed with Brp immunofluorescence. Glomeruli in this region are innervated by *Orco*-expressing neurons, calling into doubt the original report that these glomeruli process auditory stimuli and suggesting instead that they serve an olfactory function. In support of this hypothesis, the analogous area of the *Anopheles coluzzii* antennal lobe has been shown to receive projections from

Orco-expressing olfactory sensory neurons (Riabinina et al., 2016). We also observed GFP projections into the subesophageal zone in *Orco-QF2>QUAS-mCD8:GFP* animals, which appear to derive from expression in the proboscis, the primary taste organ in insects. This is consistent with similar expression in *Anopheles coluzzii* (Riabinina et al., 2016) and functional data in *Anopheles gambiae* showing that olfactory responses are detected in this gustatory organ (Kwon et al., 2006).

We also observed GFP projections into the subesophageal zone in Orco-QF2>QUAS-mCD8:GFP animals, which appear to derive from expression in the proboscis, the primary taste organ in insects. This is consistent with similar expression in *Anopheles coluzzii* (Riabinina et al., 2016) and functional data in *Anopheles gambiae* demonstrate that olfactory responses are detected in this gustatory organ (Kwon et al., 2006).

Ir25a>GFP

The intensity of GFP projections varies between glomeruli in this driver line, with some bright and other comparably dim, as noted for Orco-QF2 (Figure 2.5C). The brightest glomeruli are primarily medial and anterior. We see the dimmest innervation in the area previously described as Johnston's organ center as well as in the central antennal lobe. Labeling was also seen in other areas of the brain, most notably the subesophageal zone and anterior mechanosensory motor center.

Ir76b>GFP

In addition to projections to the antennal lobe, this line shows innervation of the subesophageal zone of the brain (Figure 2.5D).

Ir8a>GFP

Depending on the brain analyzed there were either 2 or 3 medial glomeruli labelled in this line. In the cases where there were 3 medial glomeruli, this third medial glomerulus was innervated by a few large-diameter axons (Figure 2.5E). These were larger and sparser than the smaller axons that densely innervated most other glomeruli in this line. We also note that there are 2-3 cell bodies that express GFP located in the cell body rind lateral to the antennal lobe (rALl). We are unable to definitively describe where these cells project without genetic reagents that selectively label these cells, but they appear to send bilateral processes that cross the midline within what appears to be the saddle to innervate the anterior mechanosensory motor center outside the antennal lobe.

Figure 2.5 Variability in innervation of antennal lobe glomeruli by olfactory sensory neurons

(A) Maximum-intensity projection confocal Z-stack through the medial antennal lobes of 4 brains with immunofluorescent labeling of GFP (green) and Brp (synaptic marker, magenta). Scale bar: 25 μm. Orientation: d=dorsal, m=medial.
(B-E) Maximum-intensity projections of confocal Z-stacks of left antennal lobes from two different brains of the indicated genotype with immunofluorescent labeling of GFP (green) and Brp (synaptic marker, magenta) (top) and 2-D representation of the boundary of each glomerulus that is GFP positive.
Scale bar (C-D): 50 μm. Orientation: d=dorsal, m=medial.
Work performed by: Meg Younger

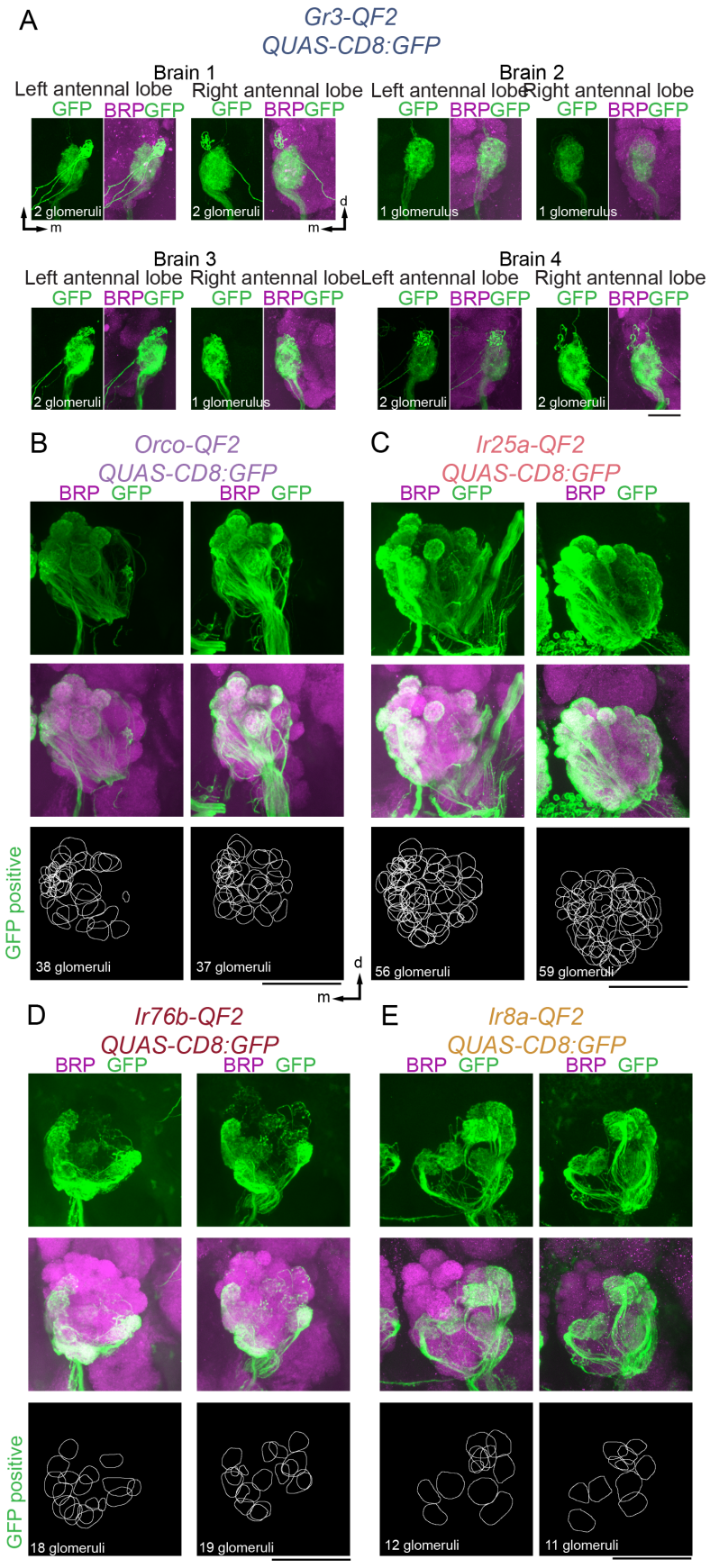
A
Gr3-QF2
QUAS-CD8:GFP
Brain 1
Left antennal lobe
Right antennal lobe
Brain 2
Left antennal lobe
Right antennal lobe
GFP BRPGFP
2 glomeruli
2 glomeruli
1 glomerulus
1 glomerulus
m
d
Brain 3
Left antennal lobe
Right antennal lobe
Brain 4
Left antennal lobe
Right antennal lobe
2 glomeruli
1 glomerulus
2 glomeruli
2 glomeruli
B
Orco-QF2
QUAS-CD8:GFP
C
Ir25a-QF2
QUAS-CD8:GFP
BRP GFP
GFP positive
38 glomeruli
37 glomeruli
56 glomeruli
59 glomeruli
D
Ir76b-QF2
QUAS-CD8:GFP
E
Ir8a-QF2
QUAS-CD8:GFP
18 glomeruli
19 glomeruli
12 glomeruli
11 glomeruli

In this chapter we begin to grapple with the puzzling observation that mosquitoes express far more olfactory receptors than they have antennal lobe glomeruli (Figure 2.1). To address how the mosquito olfactory system accommodates so many olfactory receptors, we generated knock-in driver lines that express the QF transcription factor from the endogenous loci of *Orco*, *Ir25a*, *Ir76b*, *Ir8a,* and *Gr3*, such that we were able to gain genetic access to much of the mosquito olfactory system (Figure 2.4). By examining axonal projections into the antennal lobe, we determined there is variability in the number and position of antennal lobe glomeruli, a feature not observed in *Drosophila* (Figure 2.5). Further, we observe extensive overlap in the projections of neurons expressing Ionotropic Receptors and neurons expressing Odorant Receptors into the antennal lobe, formally excluding the one-receptor, one-neuron, one-glomerulus organization previously observed in *Drosophila* as a potential motif for *Ae. aegypti* (Figure 2.3,2.4). These results suggest that olfactory neuron populations expressing single receptors are converging onto antennal lobe glomeruli or that the neurons themselves express multiple classes of chemosensory populations (Figure 2.3).

CHAPTER 3. Co-expression and co-convergence of *Orco* and *Ir25a* in the mosquito olfactory system

The high degree of overlap between glomeruli labeled by *Orco*- and *Ir25a*-expressing olfactory sensory neurons suggests that there is either widespread *Orco* and *Ir25a* co-expression within individual sensory neurons or that *Orco* and *Ir25a* are expressed in different neurons whose axons co-converge onto individual antennal lobe glomeruli or both (Figure 2.3B). The generation of genetic lines that label co-receptor families was a major step forward in understanding how the mosquito olfactory system is organized and gives us the ability to label and manipulate broad populations of olfactory neurons, but we were unable to use them to distinguish between co-expression in sensory neurons or co-convergence in the antennal lobe. In this chapter, we utilized an intersectional genetic strategy to label a subpopulation of olfactory neurons that co-expresses *Ir25a* and *Orco*. By doing so, we discovered broad *Ir25a* and *Orco* co-expression.

3.1 Generation of an intersectional genetic system to probe co-expression in *Ae. aegypti*

To distinguish between models of co-expression vs co-convergence, we adapted the Split-QF2 system (Riabinina et al., 2019) for use in the mosquito. This system “splits” the transcription factor QF2 into two components, the DNA binding domain (QF2-DBD)

and the activation domain (QF2-AD) each tagged with a synthetic leucine zipper (Figure 3.1A). When both the QF2-DBD and QF2-AD are co-expressed in the same cell, the two domains associate via the leucine zipper, reconstitute a functional QF2 protein, initiate transcription at the QUAS enhancer, and drive expression of a reporter gene (Figure 3.1B,C). Using the same stop-codon replacement approach that we used to generate the QF2-lines, we inserted the QF2-AD into the Ir25a locus (here referred to as *Ir25a-QF2-AD*) and the QF2-DBD into the *Orco* locus (here referred to as *Orco-QF2-DBD*). This is the first implementation of an intersectional genetic system in mosquitoes.

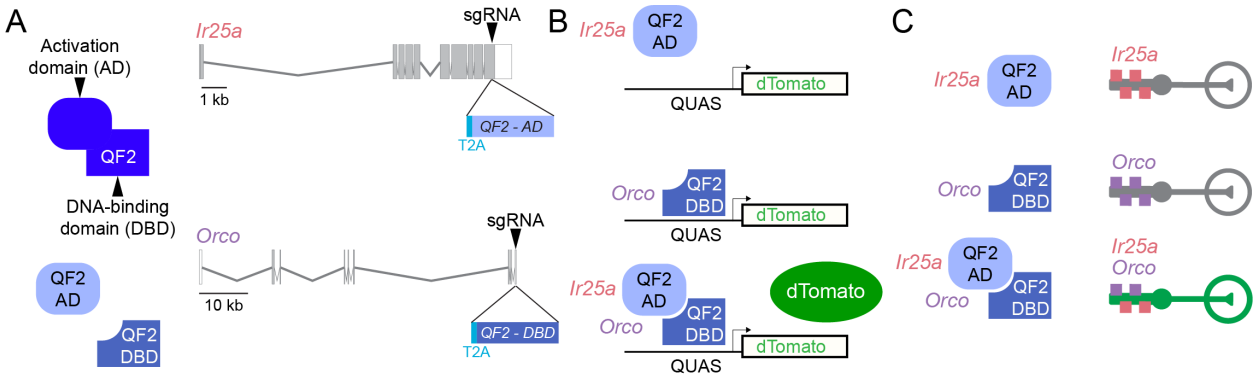

Figure 3.1 Generation of QF2-SPLIT lines

(A) Schematic of the Split-QF2 system (left) and diagrams of *Orco* and *Ir25a* gene loci with exons (grey boxes), introns (grey lines) and CRISPR-Cas9 gRNA site (arrowhead) used to insert T2A-QF2-AD (light blue) and T2A-QF2-DBD (medium blue). AD and DBD gene maps are not to scale.
(B-C) Schematic of the Split-QF2 system (B) and outcome of gene expression in olfactory sensory neurons of the indicated genotypes (C).
Work performed by: Margo Herre, Zhongyan Gong

3.2 QF2-SPLIT reagents reveal co-expression of *Orco* and *Ir25a* in chemosensory tissues

When either *Ir25a-QF2-AD* or *Orco-QF2-DBD* was used to drive expression of dTomato, we did not observe fluorescence in the antenna, maxillary palp, or the antennal lobe (Figure 3.2A-B). Therefore, neither QF2-DBD nor QF2-AD alone can activate expression from the QUAS enhancer. However, when *Orco-QF2-DBD* and *IR25a-QF2-AD* were crossed into the same animal, we observed expression of dTomato in antennal and maxillary palp neurons, as well as axonal projections in the antennal lobe (Figure 3.2A-C). Nearly half of the glomeruli in the antennal lobe were labelled with dTomato (Figure 3.2E,F). This points to widespread *Orco* and *Ir25a* co-expression within *Ae. aegypti* olfactory sensory neurons.

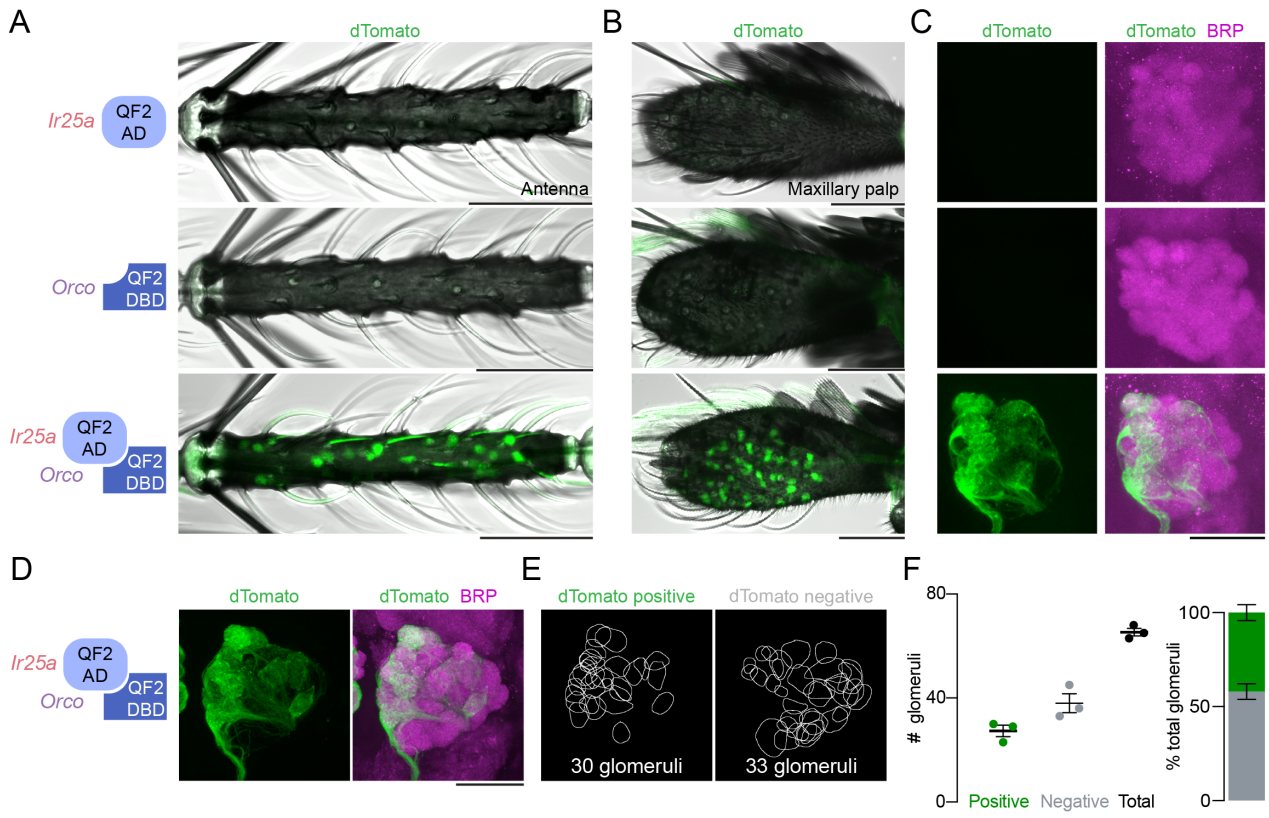

Figure 3.2 Expression of QF2-SPLIT in olfactory tissues
(A-B) Maximum-intensity projections of confocal Z-stacks of antennae (A) and maxillary palp (B) of the indicated genotypes showing intrinsic dTomato fluorescence, with transmitted light overlay.
(C-D) Maximum-intensity projections of confocal Z-stacks of antennal lobes from the left brain hemisphere of the indicated genotype with immunofluorescent labeling of dTomato (green) and Brp (synaptic marker, magenta).
(E-F) 2-D representation of the boundary of each glomerulus in (G) that is GFP positive and GFP negative (E) and quantification (F). n=3, mean ± SEM.
Scale bars: 50 μm.
Work performed by: Margo Herre, Zhongyan Gong, Meg Younger

Another source of olfactory information in *Ae. aegypti* may derive from olfactory neurons on the proboscis, the mouthpart of the mosquito that engages in taste and food ingestion. *Drosophila* expresses IRs and GRs in the proboscis, but does not express

ORs (Larsson et al., 2004). However, *Orco* neurons are widespread in both the *An. gambiae* and *Ae. aegypti* proboscises and RNA-sequencing data from *Ae. aegypti* has shown there are many ligand-specific ORs expressed in this taste tissue (Matthews et al., 2016; Riabinina et al., 2016) (Figure 3.3). Cells in the proboscis have been shown to respond to volatile odorants in *An. gambiae*, but projections from these neurons extend to the taste processing center of the brain (the sub-esophageal zone or SEZ) in *Anopheles* as well as *Aedes,* not the antennal lobe, leaving open the question of if the brain interprets these cues as olfactory or gustatory (Ghaninia et al., 2007a; Jové et al., 2020; Kwon et al., 2006; Riabinina et al., 2016). We identified extensive co-expression of *Orco* and *Ir25a* in the *Ae. aegypti* proboscis (Figure 3.3). Since *Ir25a* complexes mediate not only detection of volatile odorants but also gustatory cues, it therefore is possible that sensory neurons in the *Ae. aegypti* proboscis are able to detect olfactory as well as gustatory information within the same cell.

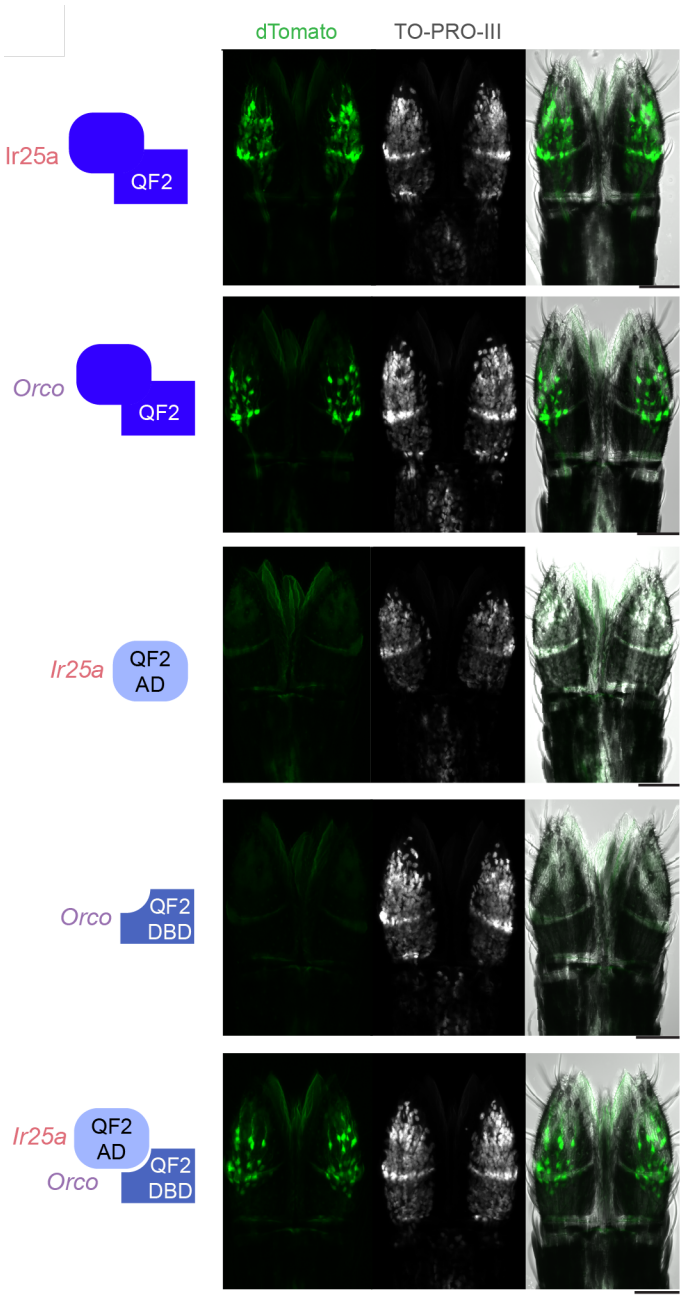

Figure 3.3 Co-expression of *Orco* and *Ir25a* in the proboscis

Maximum-intensity projections of confocal Z-stacks of proboscis of the indicated genotypes showing intrinsic dTomato fluorescence and stained with the nuclear dye TO-PRO-3, with transmitted light overlay.
Scale bars: 50 µm.
Work performed by: Margo Herre

3.3 Co-convergence of *Ir25a* and *Orco* neuronal populations in the antennal lobe

While examining these antennal lobes we consistently noticed that a cluster of anterior dorsal glomeruli was unlabeled when the Orco-QF2-DBD, IR25a-QF2-AD combination was used to drive expression in animals. However, these glomeruli were labelled when either Orco-QF2 or IR25a-QF2 were used to drive expression (Figure 3.4A-B).

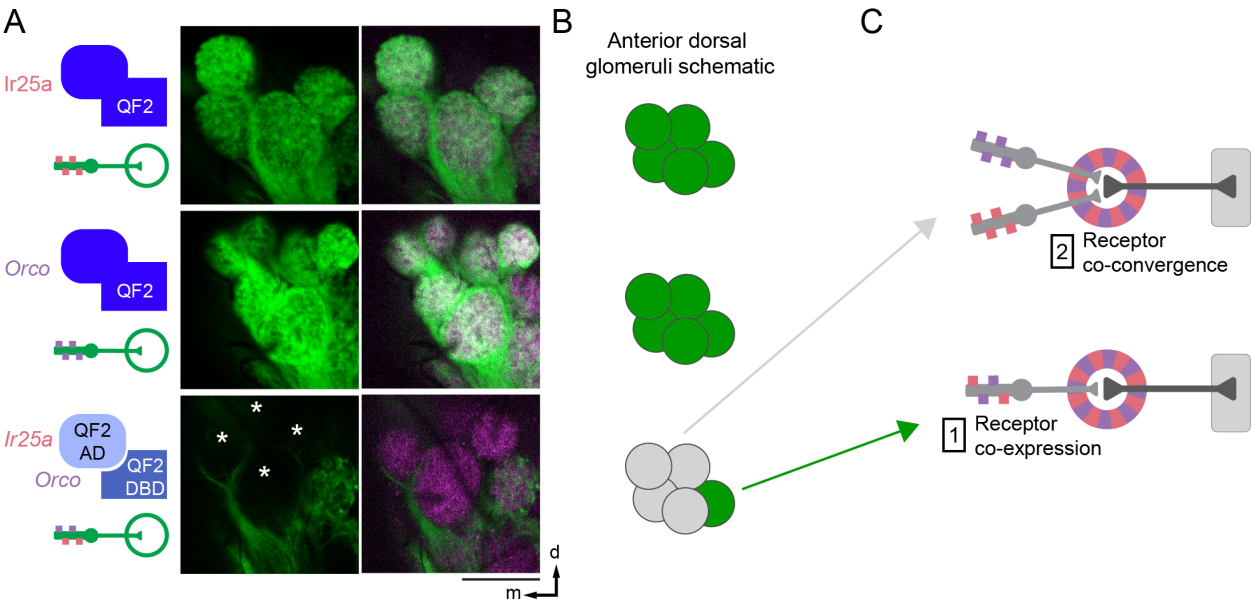

Figure 3.4 Co-convergence of Orco and Ir25a olfactory neurons in the antennal lobe

(A) Single confocal sections of the anterior dorsal region of the antennal lobe in the left-brain hemisphere of the indicated genotype with immunofluorescent labeling of dTomato (green) and Brp (synaptic marker, magenta).
(B) Schematic of the 5 glomeruli shown in (C) with GFP positive glomeruli (green).
(C) Two models of Ae. aegypti olfactory system organization supported by data in this figure.
Scale bar: 25 μm. Orientation: proximal left (D), distal left (E); (F,G,H,J): d=dorsal, m=medial.
Work performed by: Margo Herre, Meg Younger, Zhongyan Gong

This observation strongly suggests that separate populations of Orco-positive and Ir25a-positive neurons co-converge onto these glomeruli. Therefore, the mosquito olfactory system shows evidence of both co-expression and co-convergence, motifs that are not typically seen in the conventional model organisms *Drosophila melanogaster* flies or *Mus musculus* mice (Figure 3.4C). It is also possible that a given glomerulus shows co-convergence of molecularly distinct neurons while also receiving projections from neurons co-expressing multiple chemosensory co-receptors.

In this chapter, we generated the first intersectional genetic system (QF-SPLIT) employed in any mosquito and show that the chemosensory co-receptors *Ir25a* and *Orco* are widely co-expressed in the mosquito olfactory and gustatory systems (Figure 3.2). This co-expression appears to be extensive, as nearly 50% of antennal lobe glomeruli are innervated by neurons co-expressing *Orco* and *Ir25a,* however, additional reagents discussed in later chapters are required to determine the extent of co-expression at the cellular level. We also identify several antennal lobe glomeruli that are innervated by *Orco*-expressing neurons and *Ir25a*-expressing neurons, but not *Orco* and *Ir25a* co-expressing neurons, demonstrating that distinct populations of olfactory neurons can co-converge onto the same glomerulus (Figure 3.4).

CHAPTER 4. Extensive co-expression of chemosensory co-receptors in the antenna

The observation that *Orco* and *Ir25a* co-expressing neurons project to nearly 50% of antennal lobe nuclei was highly suggestive of widespread co-expression in olfactory tissues. Still, more than 50% of glomeruli are targeted by olfactory neurons that do not co-express *Orco* and *Ir25a* and we identified at least 4 glomeruli that are targeted by populations that express either *Orco* or *Ir25a* but not both. These observations about the olfactory system organization in the antennal lobe led to several possibilities for the organization at the cellular level: glomeruli not labeled by the *Orco/Ir25a* QF-SPLIT system could instead be co-expressing other families of chemosensory receptors (for example, *Orco* and *Ir76b*), thus all cells express multiple receptors. Another possibility is that some olfactory neurons express single receptors and others co-express multiple.

4.1 Quantification of co-receptor co-expression in QF lines

To distinguish between these possibilities, we needed to directly visualize olfactory neurons to evaluate co-expression on a cellular level. We optimized a whole-mount antenna immunostaining protocol that enabled us to visualize olfactory sensory neurons as well as their dendritic projections (Figure 4.1A,B). We utilized our co-receptor QF driver lines to express a membrane-bound GFP in target neurons and co-stained with an antibody that labels endogenous Orco protein. We then quantified cell numbers and

the degree of co-expression between Orco and the IR co-receptors (Figure 4.1C,D, 4.2).

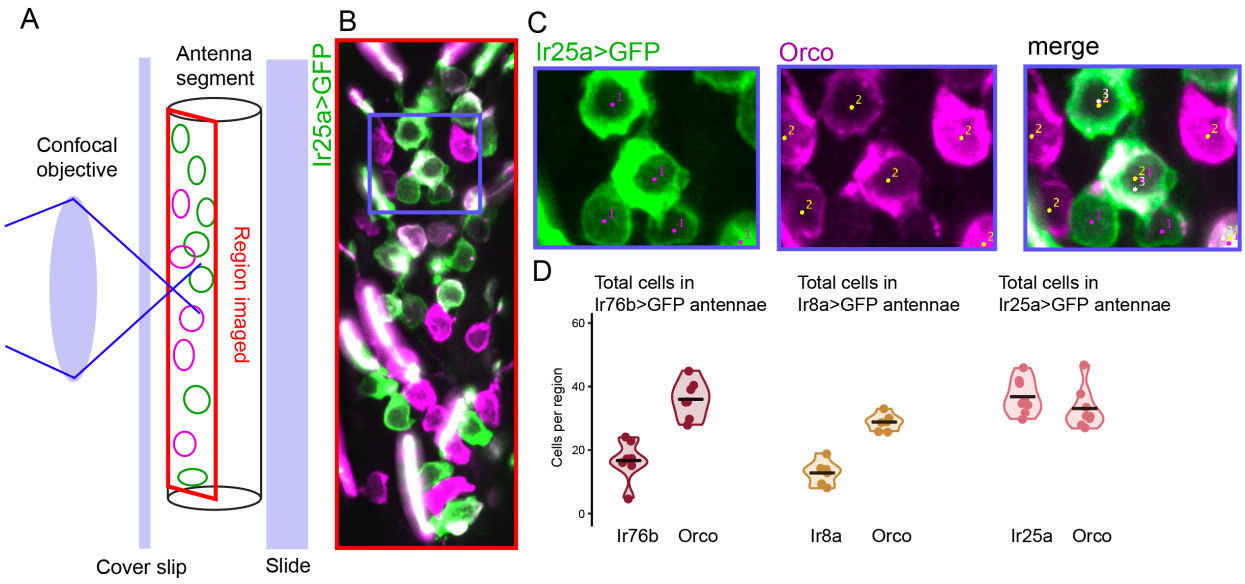

Figure 4.1 Quantification of antennal cell populations

(A-C) Workflow for cell quantification. Schematic of antennal region imaged on a confocal microscope (A) and image of an antenna with imaged area indicated with the red square (B). Whole-mount maxillary palp RNA in situ, blue region from (B). Cells are manually marked independently as Ir25a+ or Orco+ (blue inset from B) using FIJI Cell Counter and markers from each channel are merged. Cells with markers 1 and 2 are then scored as Orco+Ir25a+ with marker 3. Counts from each marker for each image are exported into Excel and R for further analysis.
(D) Total cell counts from whole mount antenna immunostaining in Figure 4.2. Mean with range, n=6-8.
Work performed by: Margo Herre

The observation that nearly half of antennal lobe glomeruli receive projections from neurons co-expressing *Ir25a* and *Orco* in gene-targeted strains suggested that there is extensive co-expression of the IR and OR chemoreceptor families, but what is the degree of co-expression? We carried out whole mount antennal immunostaining and observed extensive co-expression of Orco and *Ir25a*, with substantially fewer cells co-

expressing either Orco and *Ir8a* or Orco and *Ir76b* (Figure 4.2B-E), even after accounting for fewer total Ir76b and Ir8a cells (Figure 4.1D). This enrichment of co-expression between *Orco* and *Ir25a* may suggest co-expression of chemosensory receptors is non-random.

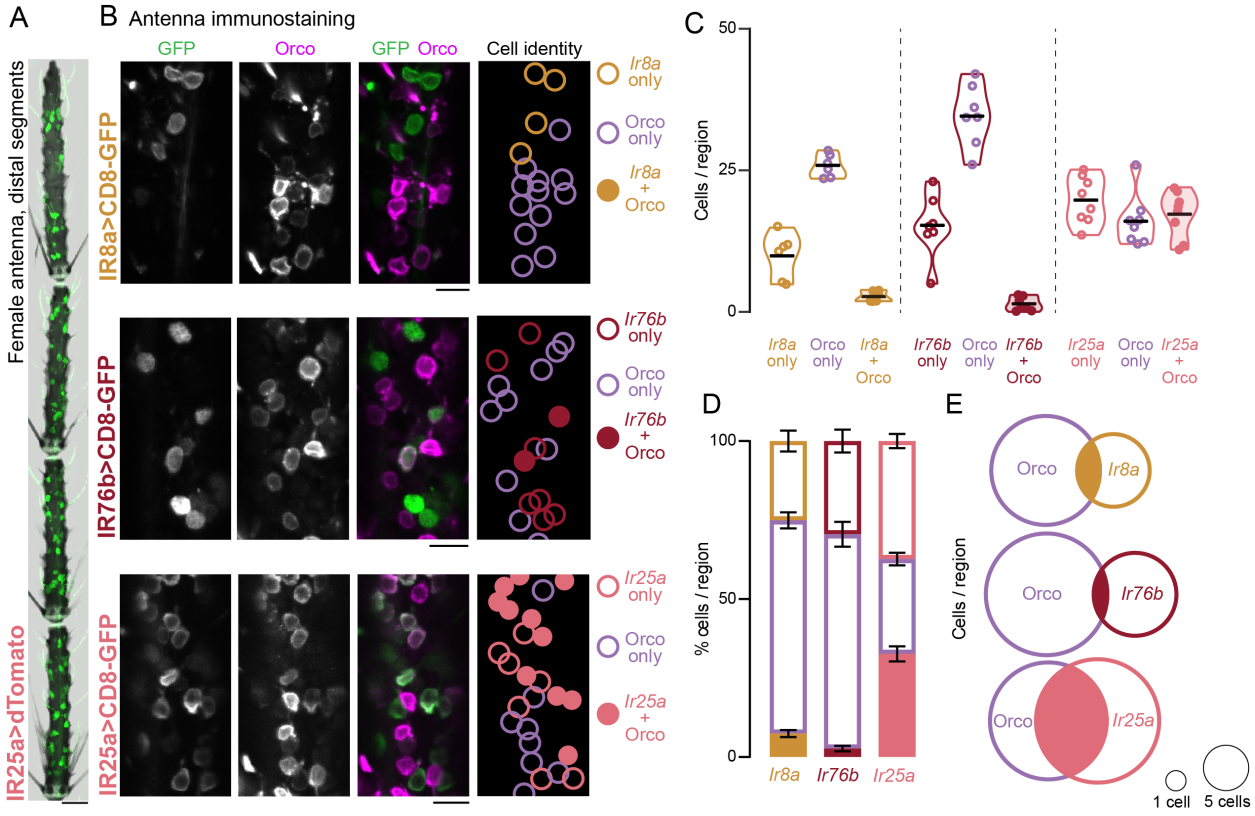

Figure 4.2 Antenna immunostaining demonstrates extensive co-expression in olfactory neurons

(A) Maximum projection of the 4 distal segments of the female antenna. dTomato expression (green) driven by Ir25a-QF2>QUAS-GCaMP6s-T2A-dTomato.
(B) Orco and GFP immunostaining in antennae of the indicated genotypes with cartoon schematic indicating cell identity.
(C-E) Quantification of antennal cells in the indicated genotypes co-expressing Orco protein and GFP presented as violin plots showing raw cell counts (C)(mean with range), stacked bar plots (D)(mean ± SEM), and Euler diagrams with area scaled to mean cells/region (E). n=6-8 antennal segments, 34-68 cells/region.
Scale bars: 25 μm (A) 10 μm (B).
Work performed by: Margo Herre

4.2 Co-expression of endogenous mRNA transcripts by RNA *in situ*

To confirm and extend these results, we performed RNA in situ hybridization in wild-type antennae with probes designed to target endogenous *Orco, Ir76b*, and *Ir25a* transcripts (Figure 4.2A). These experiments replicated patterns of co-expression observed in immunostained antennae (Figure 4.2B-E), with almost half of *Orco* cells co-expressing *Ir25a*, and few *Orco* cells co-expressing *Ir76b* (Figure 4.3A-D) indicating that widespread co-expression is not an artifact of the genetic reporter lines.

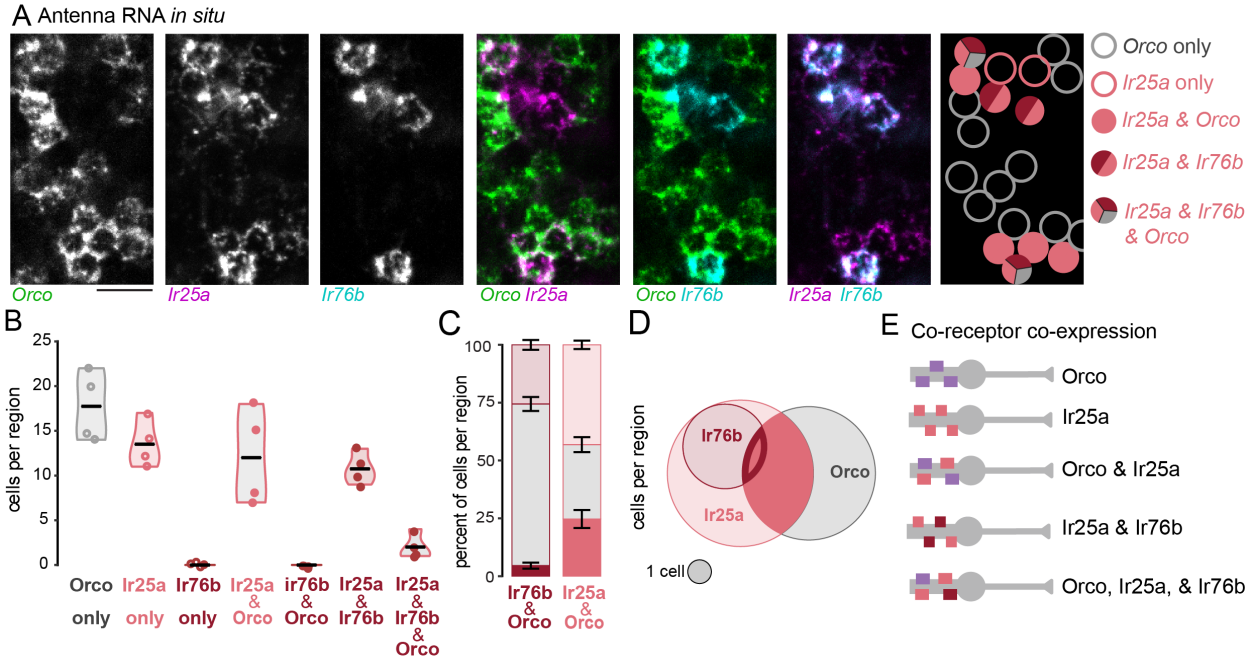

Figure 4.3 Co-expression by in situ

(A) RNA in situ hybridization in wild-type antennae with the indicated probes.
(B-D) Quantification of wild- type antennal cells expressing the indicated genes as violin plots showing raw cell counts (B)(mean with range), stacked bar plots (C)(mean ± SEM), and Euler diagrams with area scaled to mean cells/region (D). n=4 antennal segments, 45-63 cells/ region. (E) Cartoon schematic of olfactory neuron populations identified in this figure.
Scale bars: 10 μm.
Work performed by: Margo Herre, Saher Rahiel

By examining the expression pattern of these three transcripts simultaneously, we were also able to elucidate the relationship between *Ir25a* and *Ir76b* expression. In *Drosophila melanogaster*, *Ir76b* is co-expressed with *Ir25a* in olfactory sensory neurons in the antenna and in gustatory neurons in the labellum (Abuin et al., 2011; Lee et al., 2018). In *Ae. aegypti*, we found that 100% of *Ir76b*-expressing neurons in the antenna also express *Ir25a* (Figure 4.3A-E). We also observed that in addition to widespread co-receptor co- expression, some mosquito olfactory neurons express just one co-receptor (Figure 4.1E). Our data demonstrate not only extensive co-expression between Orco and IR co-receptors, but also complexity in the rules that govern receptor expression in antennal olfactory sensory neurons.

CHAPTER 5. Coordinated co-expression of chemosensory receptors in the maxillary palp

To further understand the extent of co-expression of not only co-receptors but also ligand-sensitive olfactory receptors, we next turned to the maxillary palp. The maxillary palp expresses many fewer chemosensory receptors genes than the antenna, with 18 receptors detected at the 1 TPM threshold in the maxillary palp compared to 138 in the antenna at the same threshold, simplifying the task of selecting genes for expression analysis (Figure 2.1E,F). Importantly, decades of scholarship point to the palps playing an important role during host-seeking behavior. The palps have been implicated in response to CO_2 (Acree et al., 1968; Gillies, 1980; Grant et al., 1995), thermosensation (Roth, 1951), mechanosensation (Bohbot et al., 2014), detection of attractive monomolecular odorants such as 1-octen-3-ol (Syed and Leal, 2007; Takken and Kline, 1989; Vythilingam et al., 1992), as well as blends of odorants extracted from human hosts (Tauxe et al., 2013). Maxillary palp transcriptomes offer insights into how these tiny sensory organs can sense a broad range of stimuli, as the palps express hundreds of genes, including chemosensory genes and their associated cellular machinery, that enable these sensory modalities (Bohbot et al., 2014; Matthews et al., 2018), Figure 2.1). Despite the transcriptional complexity of the palp, the basiconic sensilla responsible for the detection of volatile odorants have been described to be a repeating unit of only three neurons: one large CO_2-sensitive neuron that expresses *Gr3*, and two smaller neurons that express *Orco* (Lu et al., 2007; McIver and Hutchinson, 1972).

How do these identical repeating units of just three neurons enable the detection of so many stimuli and accommodate the expression of so many chemosensory genes? Our objective in this chapter was to generate a molecular map of the maxillary palp using QF reporter reagents, antibody staining, and RNA *in situ* to understand how a tissue that theoretically houses repeating units of 3 cells expresses 18 receptors. More importantly, we sought to determine if ligand-selective ORs are co-expressed with ligand-selective IRs, thus rendering the possibility that this co-expression is functional and enables palp neurons to detect distinct classes of chemosensory stimuli.

5.1 Maxillary palp neurons can be distinguished by size and molecular identity

We have documented extensive chemosensory co-receptor co-expression, but to form functional odorant-sensitive IR or OR complexes, olfactory sensory neurons must express both co-receptors and ligand-sensitive receptors (Abuin et al., 2011; Benton et al., 2009; Larsson et al., 2004; Neuhaus et al., 2005). To simultaneously monitor the extent of co-expression of both co-receptors and ligand-sensitive receptors, we carried out multiplexed whole mount RNA in situ hybridization (Choi et al., 2018) as well as antibody staining in the maxillary palp, the olfactory organ that detects the potent host cue CO_2 as well as other host odors (Grant et al., 1995; Lu et al., 2007; McMeniman et al., 2014; Omer and Gillies, 1971) (Figure 5.1, 5.2).

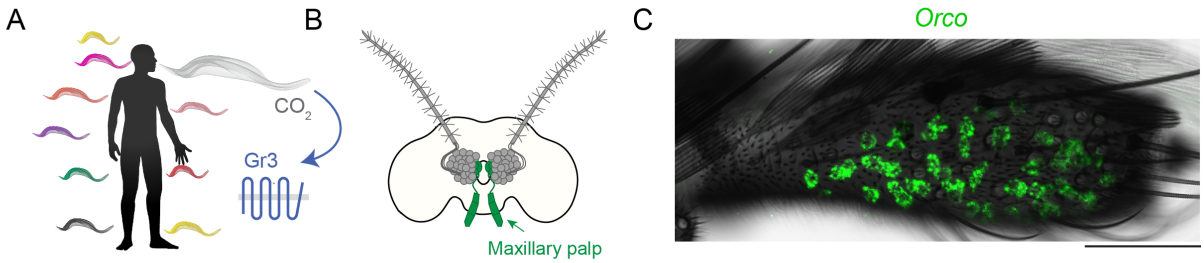

Figure 5.1 The maxillary palp detects carbon dioxide

(A) Schematic of human chemosensory cues: CO_2 detection requires Gr3.
(B) Cartoon indicating maxillary palp (green).
(C) Maxillary palp expression of *Orco* revealed by whole-mount RNA in situ hybridization. Orientation: fourth segment, distal right.
Scale bar: 50 μm.
Work performed by: Margo Herre

The maxillary palp is comprised of approximately 100 chemosensory neurons that innervate club-shaped olfactory basiconic sensilla on the dorso-lateral region of the fourth segment (Boo and McIver, 1975). Each chemosensory sensilla houses 3 neurons, which previous literature has termed “A”, “B”, and “C” largely based on the action potential spike amplitude during electrophysiology experiments. The spike amplitude for the “A” cell is larger than for the “B” and “C” cells because the size of the “A” neuron is much larger than the other two, and spike amplitude correlates with neuron size (Faller and Luttges, 1995; McIver, 1972). The “A” neuron strongly responds to CO_2 and produces the largest and easily distinguishable spike, while the “B” and “C” neurons produce much smaller spikes and are not easily distinguishable from each other (Boo and McIver, 1975; Grant et al., 1995; Kellogg, 1970; Syed and Leal, 2007). Depending on the study, either the “B” or the “C” cell responds to the mosquito attractant 1-octen-3-ol. This response is dependent on Or8, one of the few olfactory

receptors in mosquitoes with known ligand identity (Bohbot and Dickens, 2009; McIver, 1982; Xu et al., 2015). Previous studies in *Anopheles gambiae* predicted *Orco* to be expressed in the smaller "B" and "C" cells and therefore postulated that the palp is composed of repeating units of 3 cells per each basiconic sensilla: one larger CO_2-sensitive, *Gr3*-expressing neuron and two smaller *Orco*-expressing neurons, one of which detects 1-octen-3-ol (Lu et al., 2007). Going forward, we will refer to these neurons by their molecular identity and not their spiking characteristics, and thus will cease to use the "A", "B", and "C" neuron nomenclature.

We previously showed *Ir25a* and *Orco* co-expression in the palp through QF-SPLIT reagents (Figure 3.2) and transcriptomic data demonstrated that *Gr3* is expressed in the palp (Matthews et al., 2016). As *Gr3* is required for CO_2 detection, it would follow that we would observe Gr3-QF2 reporter expression in large cells and data from *Anopheles gambiae* demonstrates that the *Gr3* ortholog and *Orco* are expressed in non-overlapping cell populations in the palp (Lu et al., 2007). Thus, we set out to determine if large cells co-express *Gr3* and *Ir25a*. Upon examining *Ir25a>GFP* reporter expression in the palp, we immediately noticed that Ir25a could be observed in cells of two distinct sizes, which we predicted to correspond to large *Gr3* neurons and small *Orco* neurons (Fig 5.2A). Upon staining *Gr3>GFP* palps for endogenous Orco protein, we observed expected *Gr3* expression in larger cells, and Orco protein in smaller cells (Fig 5.2B). While these data together were highly suggestive of *Ir25a* and *Gr3* co-expression in large cells, we needed to generate additional tools to directly visualize *Ir25a* and *Gr3* co-expression.

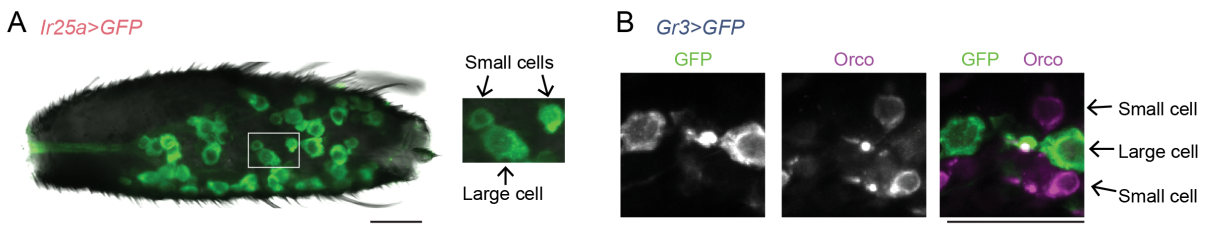

Figure 5.2 Maxillary palp neurons can be distinguished by size

(A-B) Whole-mount maxillary palp immunostaining showing Ir25a expression in “small” and “large” cells (A) and Gr3 expression in “large” cells and Orco protein in “small” cells (B).
Scale bar: 25 μm. Orientation (A): distal right.
Work performed by: Margo Herre

In order to determine the relationship of *Ir25a* and *Gr3* expression, as well as to understand the expression patterns of the remaining 16 ORs and IRs in the palp, we optimized the Hybridization Chain Reaction RNA *in situ* protocol to enable DNA probes to penetrate the chitin exoskeleton encasing palp chemosensory neurons (Choi et al., 2018). By multiplexing probes to chemosensory receptors in sets of 3, we were able to resolve spatial relationships for the co-receptors *Orco, Ir25a, Ir76b* as well as *Gr3* and the ligand-selective receptors *Or8, Or49, Or71, Ir93a, Ir100a,* and *Ir75g* (Figure 5.4, 5.5, 5.6, 5.7, 5.8). Further, we implemented a semi-blinded manual cell counting system to quantify cell numbers and degree of co-expression between chemosensory receptors (Figure 5.3). These innovations enabled us to generate a detailed molecular map of the maxillary palp.

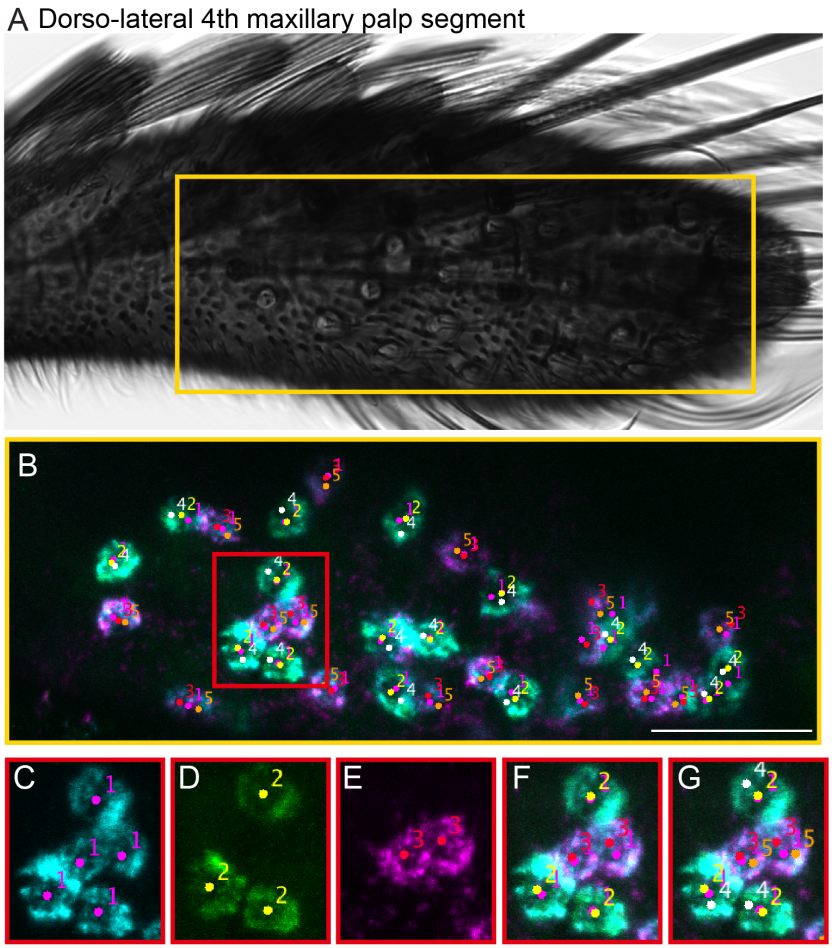

Figure 5.3 Quantification of chemosensory populations in the maxillary palp

(A-G) Workflow for cell quantification. Schematic of antennal region imaged on a confocal microscope (A) and image of maxillary palp with imaged area indicated with the yellow square (B). Whole-mount maxillary palp RNA in situ, yellow region from (C). Cells are manually marked independently as Orco+, Or49+, or Or8+ (red inset from B) using FIJI Cell Counter (C-E) and markers from each channel are merged (F). Cells with markers 1 and 2 are then scored as Orco+Or49+ with marker 4, and cells with markers 1 and 3 are then scored as Orco+Or8+ with marker 5 (G). Counts from each marker for each image are exported into Excel and R for further analysis.
Scale bar: 50 μm.
Work performed by: Margo Herre

5.2 Maxillary palp in situ demonstrates extensive, coordinated co-expression

In agreement with previous studies as well as hints from our QF reporter lines, we observed no overlap in expression of *Orco* and *Gr3* in the maxillary palp, but *Ir25a* was expressed in all *Orco* and all *Gr3* cells (Figure 5.1, 5.4). Previous work in *Anopheles gambiae* suggested that *Orco*-expressing neurons in the maxillary palp can be evenly divided into two non-overlapping groups: an *Or8* population and an *Or49* population (Lu et al., 2007). We show definitively that *Or8* and *Or49* are in segregated populations of *Orco*-expressing neurons in *Ae. aegypti* (Figure 5.5), and when combined with the results of the previous experiment (Figure 5.4), that these cells are also all *Ir25a*-positive.

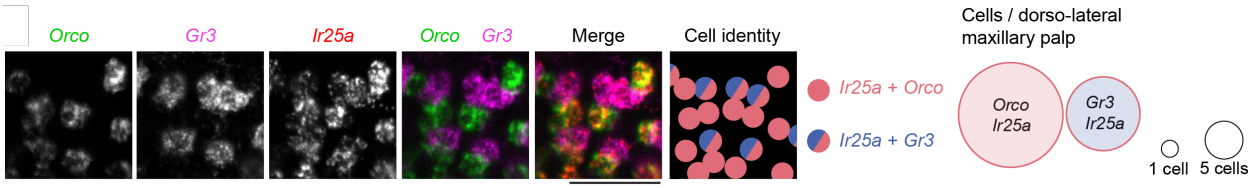

Figure 5.4 Co-expression of Orco and Ir25a in the maxillary palp

Whole-mount maxillary palp RNA in situ hybridization with the indicated probes, cartoon schematic indicating cell identity, and quantification of co-expression shown as Euler diagrams, area scaled to mean. n=5 maxillary palps, 26-65 cells/dorso-lateral maxillary palp.
Scale bar: 25 μm.
Work performed by: Margo Herre

Additional RNA *in situ* hybridization experiments revealed that *Or8*- and *Or49*-expressing cells also often express *Ir76b,* with a bias towards expression in *Or8*-expressing cells (Figure 5.6A). This unequal distribution of *Ir76b* between these two evenly distributed cell populations gave us our first clue that the palp basiconic sensilla

are unlikely to be perfectly repeating units of three identical neurons. Taken together these data show that olfactory sensory neurons express co-receptors *Orco*, *Ir25a*, *Ir76b* and either of the ligand-sensitive subunits *Or49* or *Or8.*

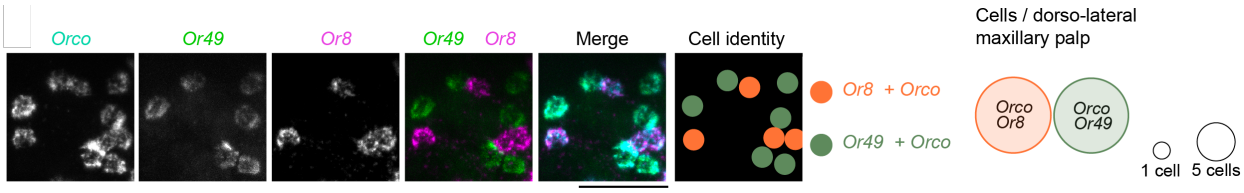

Figure 5.5 Or8 and Or49 expression is evenly segregated in Orco neurons

Whole-mount maxillary palp RNA in situ hybridization with the indicated probes, cartoon schematic indicating cell identity, and quantification of co-expression shown as Euler diagrams, area scaled to mean. n=5 maxillary palps, 26-65 cells/dorso-lateral maxillary palp.
Scale bar: 25 μm.
Work performed by: Margo Herre

When we analyzed IR ligand-sensitive subunit expression, we found that *Ir100a* and *Ir93a* are also expressed in a subset of *Or49*-expressing neurons (Figure 5.6B-C), suggesting that these cells can form functional OR and IR complexes with their respective co-receptors in the same neuron. It was fascinating to observe that *Ir100a* and *Ir93a* are expressed nearly exclusively in *Or49 cells*, raising the possibility that transcriptional machinery in these cells ensures these IRs are only expressed with *Or49*. How are these genes be selectively expressed together? In *Anopheles gambiae,* several ORs form polycistronic clusters and thus are consistently co-expressed in the same olfactory neurons (Karner et al., 2015). While chemosensory genes also form clusters in the *Ae. aegypti* genome, *Or49, Ir100a,* and *Ir93a* are each on separate chromosomes, ruling out the possibility that they may be co-expressed as a part of a gene cluster (Matthews et al., 2018). Further studies are warranted to understand the

gene regulatory mechanisms in palp neurons that may elucidate the transcriptional networks involved in coordinated co-expression.

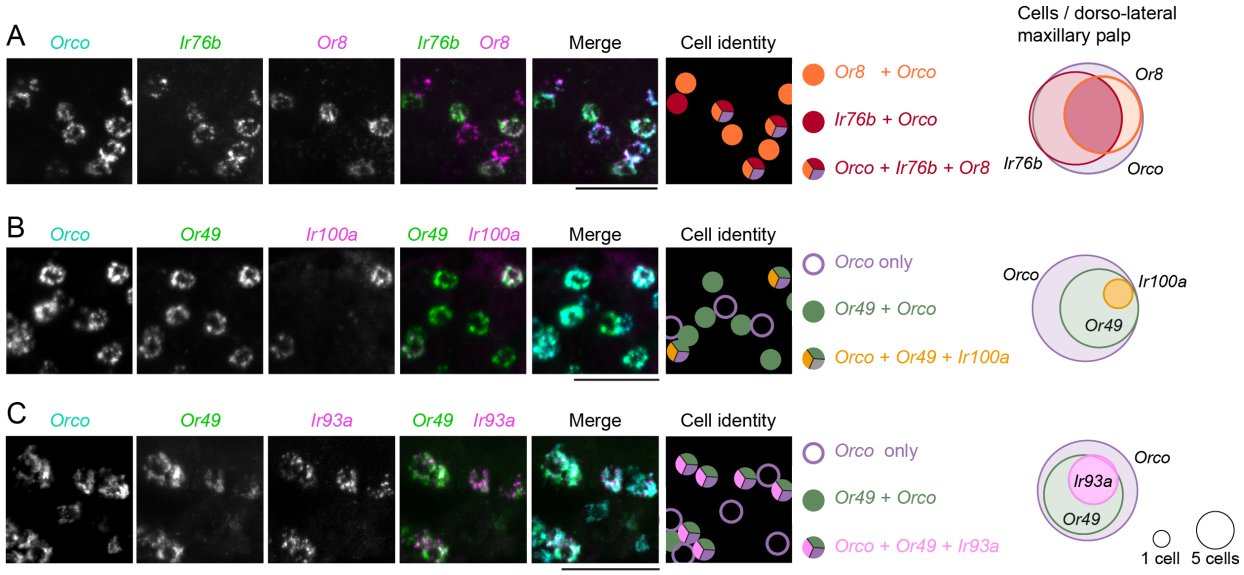

Figure 5.6 Ligand-selective IRs are expressed in select populations of Orco neurons

(A-C) Whole-mount maxillary palp RNA in situ hybridization with the indicated probes, cartoon schematic indicating cell identity, and quantification of co-expression shown as Euler diagrams, area scaled to mean. n=5 maxillary palps, 26-65 cells/dorso-lateral maxillary palp.
Scale bar: 25 μm.
Work performed by: Margo Herre

Additionally, we identified co-expression of *Or71* and *Or49*, demonstrating that more than one ligand-sensitive OR can also be expressed in an olfactory sensory neuron in *Ae. aegypti* (Figure 5.7). While these genes are both located on the same chromosome, they are not in a cluster. Thus, similar to the coordinated co-expression

observed between *Ir93a* and *Or49* and *Ir100a* and *Or49*, we do not yet understand the transcriptional milieu required to enforce this coordinated co-expression.

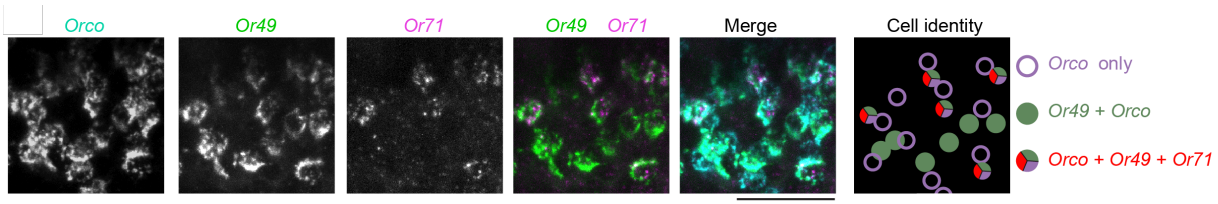

Figure 5.7 Multiple ORs are expressed in Orco neurons

Whole-mount maxillary palp RNA in situ hybridization with the indicated probes, cartoon schematic indicating cell identity, and quantification of co-expression shown as Euler diagrams, area scaled to mean. n=5 maxillary palps, 26-65 cells/dorso-lateral maxillary palp.
Scale bar: 25 μm.
Work performed by: Margo Herre

Lastly, we found that 65% of *Gr3*-expressing cells also express the ligand-selective IR subunit *Ir75g* (Figure 5.8). Taken together with the finding that *Gr3*-expressing cells express *Ir25a* (Figure 5.4) this raises the possibility that a functional IR complex can be found in CO_2-sensitive neurons.

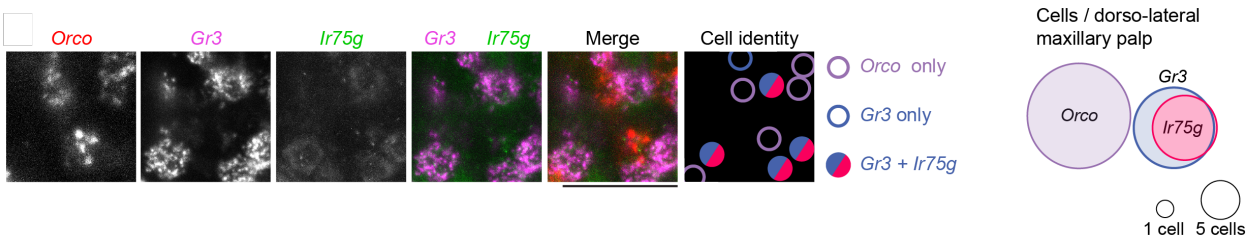

Figure 5.8 Ir75g is expressed in Gr3 neurons

Whole-mount maxillary palp RNA in situ hybridization with the indicated probes, cartoon schematic indicating cell identity, and quantification of co-expression shown as Euler diagrams, area scaled to mean. n=5 maxillary palps, 26-65 cells/dorso-lateral maxillary palp.
Scale bar: 25 μm.
Work performed by: Margo Herre

In this chapter, we demonstrate that the identity of neurons projecting their dendrites to basiconic sensilla is far more complex than previously understood. Through serial RNA *in situ* hybridization experiments, we discovered that the maxillary palps house many more than three cell types (Figure 5.4, 5.5, 5.6, 5.7, 5.8). As we did not evaluate the anatomic relationship of every combination of chemosensory genes expressed in the palp, we hypothesize that comprehensive RNA *in situs* or single-cell RNA-sequencing would reveal additional complexity of the palp chemosensory neuron population. Further, we show extensive co-expression of IRs, ORs, and GRs in the palp which may enable palp neurons, such as the CO_2-sensitive neuron, to detect volatile odorants belonging to multiple chemical classes. Moreover, the co-expression we observe sheds light on previous intriguing data: CO_2-sensitive neurons also respond to human foot odor, a blend of dozens of volatile odorants (Dormont et al., 2013; Tauxe *et al.*, 2013), and mosquitoes unable to detect CO_2 are still able to locate a human host (McMeniman et al., 2014). That CO_2 neurons respond to human foot odor (Tauxe et al., 2013). which likely consists of volatile ligands that bind to *Gr3* as well as IRs residing in CO_2 neurons, further underscores the importance of understanding the molecular identity of these neurons. Taken together, our data demonstrate how the palp, a

complex chemosensory organ, is able to play a critical role in the detection of human cues that enable mosquitoes' deadly host-seeking behavior.

The extensive co-expression of IRs, ORs, and GRs documented in this work likely enables maxillary palp neurons to detect volatile odorants belonging to multiple chemical classes and may explain how CO_2-sensitive neurons also respond to human skin odor (Dormont et al., 2013; Tauxe et al., 2013), and why mosquitoes unable to detect CO_2 can still locate a human host (McMeniman et al., 2014). I speculated earlier in this chapter about *how* certain ligand-selective receptors are co-expressed, but it is equally as intriguing to postulate *why* certain receptors are co-expressed. The observation that CO_2 neurons also respond to non-CO_2 human odors raises the interesting possibility that co-expression enables olfactory neurons to respond to more than one human cue, perhaps allowing for direct integration at the level of the sensory neuron instead of in the antennal lobe. Another possibility is since human odor is variable from person to person, recognizing multiple components in one cell may ensure that certain neuronal populations critical for host-seeking drive will always be activated by human cues.

These hypotheses underscore another critical gap in our understanding of the mosquito olfactory code: our field has currently defined the ligand tuning properties of very few olfactory receptors in *Ae. aegypti*. Not knowing the odorants that activate these receptors complicates our ability to understand why they may be co-expressed. For example, we know the ligand sensitivity of neither Or49 nor Ir100a, so as of now it's

difficult to postulate if or how they act in concert to detect a stimulus. In *Drosophila*, *Ir93a* is required for physiological and behavioral responses to cool temperatures (Knecht et al., 2017), but the function of Ir93a in *Ae. aegypti* is unknown. As *Ir93a* is always expressed in *Or49* cells, it would be interesting if cool temperatures modulated those neurons' response to Or49 ligands.

CHAPTER 6. Volatile amine sensing by CO2 neurons that lack the Gr3 CO2 sensor

The observation that multiple classes of co-receptors and their ligand-sensitive receptors are expressed in the same neurons in the maxillary palp led to the exciting possibility that *Ae. aegypti* olfactory neurons are able to detect multiple types of odorants. Although the ligand tuning properties very few olfactory receptors in *Ae. aegypti* have been defined, knowing the molecular identity of the receptors expressed in our neurons of interest gave us hints for which odorants to test in a functional imaging setup, as the tuning properties of their *Drosophila* orthologs have been well-explored. Thus, we set out to investigate the functional relationships of these extensive receptor co-expression patterns by focusing on the maxillary palp, which is both simpler in organization than the antenna and also uniquely important because it is the sensory appendage that detects CO_2.

6.1 Three antennal lobe glomeruli are innervated by maxillary palp neurons

To delineate the organization of maxillary palp projections in the brain, we used our QF2 and Split-QF2 driver lines to examine sensory innervation of antennal lobe glomeruli (Figure 6.1A-H). Glomerulus 2 and Glomerulus 3 received input from both *Orco*-expressing neurons and *Ir25a*- and *Ir76b*-expressing neurons (Figure 6.1A-G), consistent with data presented in Chapter 5. Co-expression of *Orco* and *Ir25a* in neurons that project to these two glomeruli was confirmed using the Split-QF2 system. In *Orco-QF2-DBD*, *IR25a-QF2-AD* animals, Glomerulus 2 and Glomerulus 3 were labeled, but Glomerulus 1 was not (Figure 6.1H). We also discovered that Glomerulus 1, which is the largest glomerulus in the antennal lobe (Shankar and McMeniman, 2020), received input from *Gr3*-expressing sensory afferents. Glomerulus 1 was also innervated by *Ir25a*-expressing sensory neurons (Figure 6.1A-I), consistent with the co-expression of *Gr3* and *Ir25a* in olfactory neurons. This finding raised the possibility that Glomerulus 1 may respond to additional odorant ligands independent of CO_2-sensitive *Gr3.*

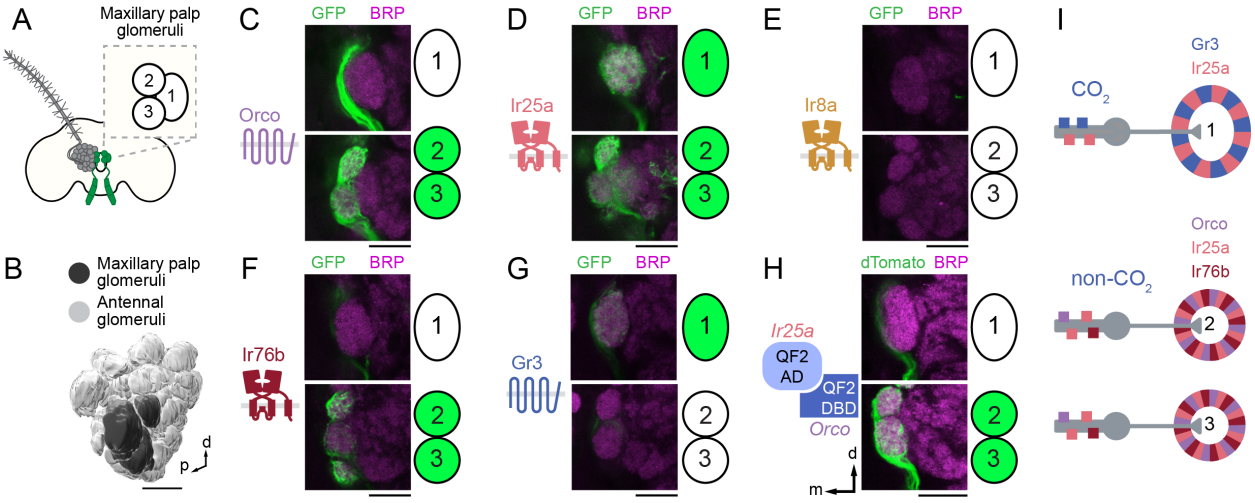

Figure 6.1 Three antennal lobe glomeruli are innervated by maxillary palp olfactory neurons

(A-B) Cartoon (A) and left 3-D antennal lobe reconstruction (B) showing 3 glomeruli that are innervated by the maxillary palp. Image in (B) is reprinted in Figure S1G.
(C-H) Single confocal sections through the center of Glomerulus 1 (top) or Glomerulus 2 and Glomerulus 3 (bottom) in left antennal lobes of the indicated genotypes. Sections are taken from Z-stacks presented in Figure 1I (C-G) and Figure 2G (H).
(I) Schematic of sensory neuron gene expression and glomerular convergence based on (C-H).
Scale bars: 25 μm.
Work performed by: Meg Younger, Margo Herre

6.2 Maxillary palp neurons respond to multiple classes of volatile odorants

Given the extensive receptor co-expression observed in the maxillary palp, we next explored the possibility that functional expression of multiple receptor types would allow maxillary palp CO_2-sensitive neurons to respond to additional odorants. We set out to examine odorants detected by maxillary palp neurons by developing an *in vivo* calcium imaging preparation with the genetically-encoded calcium sensor GCaMP6s (Chen et

al., 2013), allowing us to monitor stimulus-evoked activity in the antennal lobe of a mosquito as it was exposed to different odorants or to CO_2 (Figure 6.2A).

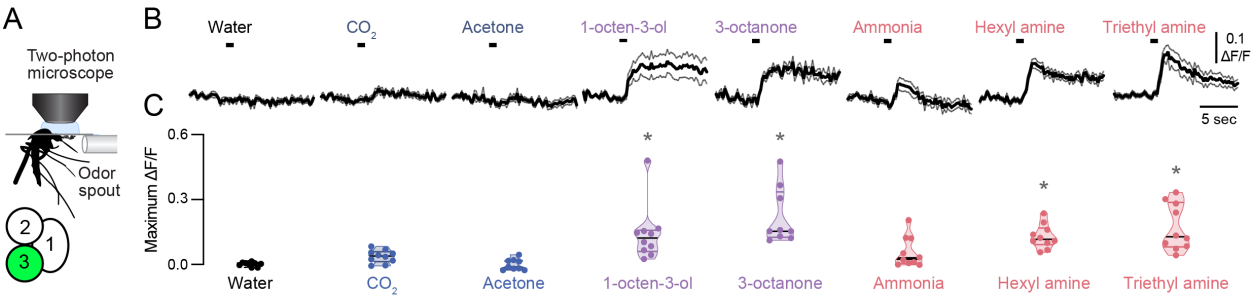

Figure 6.2 Orco neurons in the maxillary palp responds to alcohols and volatiles amines

(A) Side view schematic of live- imaging preparation of Glomerulus 3.
(B) GCaMP6s fluorescence traces from Glomerulus 3 presented with the indicated stimuli. Black bar indicates stimulus presentation, mean ± SEM, n=9-10 sweeps from 3 animals/stimulus.
(C) Summary of data in (B) indicating the maximum ΔF/F (arbitrary units). Lines denote median and quartiles, *p<0.05 one-way ANOVA with Bonferroni correction compared to water control.
Work performed by: Meg Younger

We imaged the axon terminals of maxillary palp sensory neurons in the antennal lobe with two-photon microscopy using a custom-built olfactometer to deliver odorants and CO_2 within a continuous airstream. We expected that Glomerulus 1 would respond to CO_2 because it receives projections from *Gr3*-expressing neurons. Indeed, in preliminary experiments when we imaged GCaMP6s responses in axonal termini of *Gr3*-expressing neurons in Glomerulus 1, we observed low fluorescence at baseline

and concentration-dependent responses to CO_2, with no apparent desensitization across trials (data not shown).

To image activity simultaneously in CO_2-sensitive Glomerulus 1 and the non-CO_2-sensitive Glomerulus 3, we used the *Ir25a*>GCaMP6s strain, which expresses GCaMP6s in all maxillary palp olfactory neurons. We saw consistent activation of Glomerulus 3 by 1-octen-3-ol and 3-octanone (Figure 6.2B-C), odorants that have been shown in *in vitro* heterologous expression experiments to activate Or8-Orco from both *Ae. aegypti* and *Anopheles gambiae* (Bohbot and Dickens, 2009; Lu *et al.*, 2007). Therefore Glomerulus 3 is likely to be innervated by *Or8*-expressing neurons. From a panel of candidate odorants, we found that Glomerulus 3 also responded to two volatile amines, hexyl amine and triethyl amine (Figure 6.2B-C). Volatile amines, including polyamines, have been proposed to be IR ligands in *Drosophila melanogaster* (Geier *et al.*, 1999; Hussain *et al.*, 2016; Min et al., 2013; Silbering *et al.*, 2011). These findings are consistent with the hypothesis that IRs and ORs are functionally co-expressed in maxillary palp neurons and that this co-expression enables these cells to respond to ligands that activate both classes of receptors.

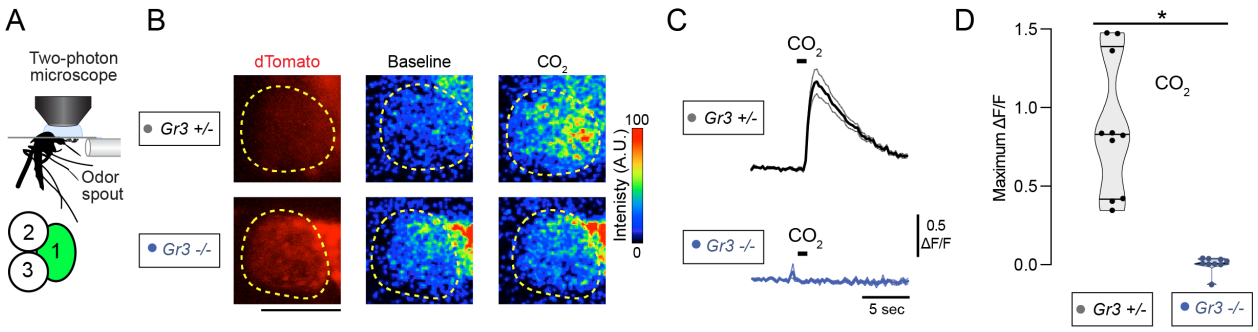

Figure 6.3 Gr3 mutant mosquitoes lose antennal lobe activity when exposed to CO_2

(A) Side view schematic of live-imaging preparation of Glomerulus 1.
(B) Two-photon image of Glomerulus 1 in the left antennal lobe of Ir25a>dTomato-T2A-GCaMP6s animals with dTomato (left), GCaMP6s fluorescence at baseline (middle), and after CO_2 presentation (right) with region of interest (yellow), in the indicated Gr3 genotypes.
(C) GCaMP6s traces from Glomerulus 1 from animals of the indicated genotype presented with CO_2 at the time indicated by the black bar, mean ± SEM, n=9-10 sweeps from 3 animals.
(D) Summary of data in (C) indicating the maximum ΔF/F (arbitrary units). Lines denote median and quartiles, *p<0.05 one-way ANOVA with Bonferroni correction.
Scale bar: 25 μm.
Work performed by: Meg Younger

We next turned to the CO_2-sensitive Glomerulus 1 (Figure 6.3A) and imaged stimulus-evoked activity in *Gr3* heterozygotes, which have no defects in CO_2 sensation, and in *Gr3* homozygous mutants, which lose all physiological and behavioral responses to CO_2 (McMeniman et al., 2014). We used *Gr3* heterozygotes as the control genotype in these experiments because this mutation was introduced in a different wild-type strain than our QF2/QUAS reagents and this genetic configuration better controls for genetic background. As expected, we saw robust activation of Glomerulus 1 by CO_2 in *Gr3* heterozygotes, and a complete loss of response to CO_2 in *Gr3* homozygous mutant animals (Figure 6.3B-D).

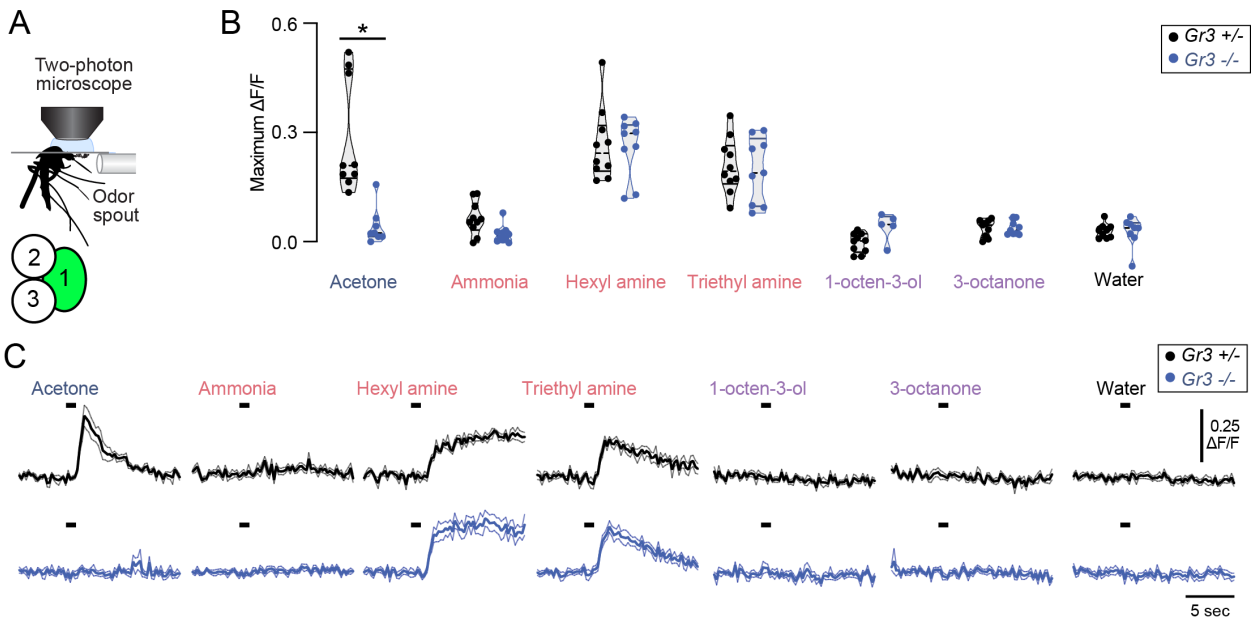

Figure 6.4 CO_2 neurons respond to volatile amines in the absence of the CO_2 receptor Gr3

(A) Side view schematic of live-imaging preparation of Glomerulus 1.
(B) Summary of data in (C) indicating the maximum ΔF/F (arbitrary units). Lines denote median and quartiles. *p<0.05 one-way ANOVA with Bonferroni correction.
(C) GCaMP6s fluorescence traces from Glomerulus 1 presented with the indicated stimuli. Black bar indicates stimulus presentation, mean ± SEM, n=5-10 sweeps from 3 animals/stimulus.
Work performed by: Meg Younger

CO_2-sensing neurons in the maxillary palp respond to multiple odorants in *Aedes*, *Culex*, and *Anopheles* mosquitoes (Lu et al., 2007; Tauxe et al., 2013; Turner et al., 2011) and it has been proposed that *Gr3* is a broadly-tuned receptor that responds to many odorants. We examined the response to a recently identified CO_2-neuron activator, acetone (Ghaninia et al., 2019) (Figure 6.4A). This odorant activated Glomerulus 1 in the *Gr3* heterozygote but the response to acetone was abolished in the homozygous *Gr3* mutant (Figure 6.4B,C). This suggests that the CO_2 receptor can interact with non-CO_2 ligands. We examined the response to volatile amines, and saw

consistent responses to hexyl amine and triethyl amine (Figure 6.4B,C). The response to both of these volatile amines was unaffected in *Gr3* homozygous mutant animals (Figure 6.4B,C). We speculate that hexyl amine and triethyl amine are activating the CO_2-sensitive neuron by stimulating IRs expressed in this neuron, which we have shown include at least *Ir25a* and *Ir75g* (Figure 6.5).

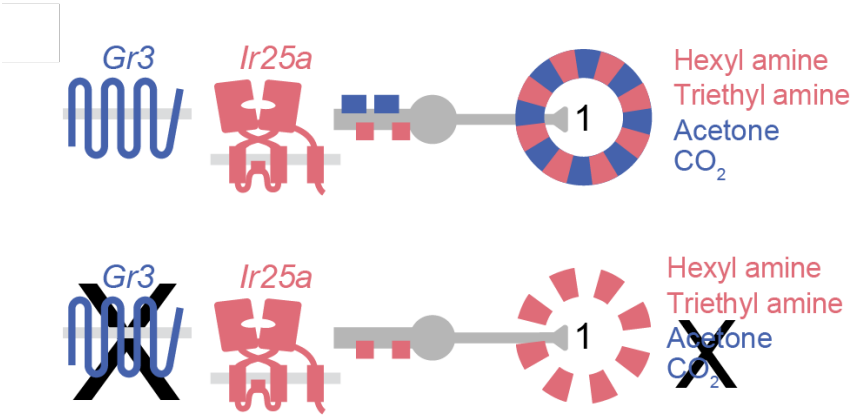

Figure 6.5 Model for volatile amine detection in CO2 neurons

Summary of Glomerulus 1 responses with and without Gr3 function.
Work performed by: Margo Herre, Meg Younger

CHAPTER 7. Volatile amines partially substitute for CO_2 in activating mosquito attraction to humans

Female mosquitoes integrate multiple sensory cues to drive strong attraction to humans. Human odor is a blend of hundreds of volatile odorants, including lactic acid and volatile amines (Acree et al., 1968; Bernier et al., 2000; Dormont et al., 2013). While body heat, CO_2 emitted in the breath, and individual odorants produced by human skin individually elicit weak to no mosquito attraction, the combination of multiple sensory cues leads to robust attraction in laboratory behavioral assays (Corfas and Vosshall, 2015; Dekker et al., 2005; McMeniman et al., 2014). Among these cues, CO_2 heat and odorants (Dekker et al., 2005; McMeniman et al., 2014). The discovery that triethyl amine and hexyl amine activate Glomerulus 1 in *Gr3* homozygous mutants that are unable to detect CO_2 led us to hypothesize that volatile amines could substitute for CO_2 in sensitizing *Gr3* mutant mosquitoes to human body odor (Figure 7.1A).

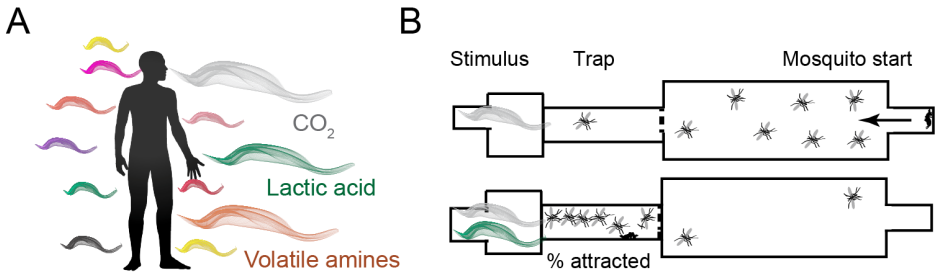

Figure 7.1 Host-seeking behavior is recapitulated in the quattroport olfactometer assay

(A) Humans emit a complex blend of volatile odorants, including CO_2, lactic acid, and volatile amines.
(B) Schematic of behavioral assay and percent wild-type mosquitoes of the indicated blood-feeding status attracted to the indicated stimuli in the assay.
Work performed by: Margo Herre, Meg Younger

To test this, we used the quattroport, a behavioral assay that measures activation and attraction of mosquitoes to various stimuli (Basrur et al., 2020) (Figure 7.1B). In control experiments, we baited the assay with either CO_2 or lactic acid, a human host volatile, or both CO_2 and lactic acid combined, and monitored how many mosquitoes accumulated in the trap. As previously shown, either CO_2 or lactic acid alone only weakly attracted mosquitoes, but the combination of lactic acid with CO_2 caused potent dose-dependent attraction in two different wild-type strains of *Ae. aegypti* (Figure 7.2A-C) (Acree et al., 1968; Bernier et al., 2000; Davis, 1984; Geier et al., 1999; Majeed et al., 2014; McMeniman et al., 2014; Smith et al., 1970).

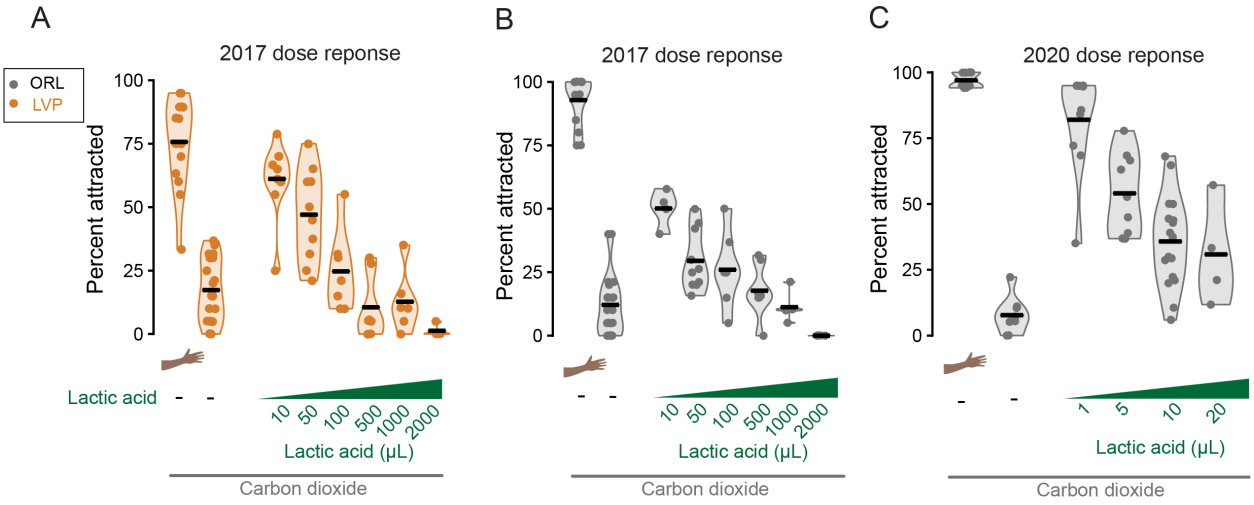

Figure 7.2 Dose-dependent effect of lactic acid and CO2 on attraction behavior

(A-C) Attraction of mosquitoes of the indicated genotype to the indicated stimuli. Lot number and batch of Lactic acid changed between trials conducted in 2017 (A-B), and trials conducted in 2020 (C) (see methods for additional details). Lactic acid was supplied at the indicated volume with CO_2 present throughout all trials. Mean with range, n=5-23 trials, 15-21 mosquitoes/trial.
Work performed by: Margo Herre, Meg Younger, Ali Ehrlich

Although lactic acid has been identified as a component of human odor and presentation of lactic acid and CO_2 has been described to drive attraction behavior at levels similar to that when presented with a human host (Acree *et al.*, 1968), it was not known if mosquito attraction to lactic acid and CO_2 is subject to the same internal state regulation that modulates attraction to human hosts. For example, female mosquito attraction to humans is suppressed for 72-96 hours after ingestion of a blood-meal (Davis, 1984; Duvall et al., 2019; Klowden, 1981). Thus, if presentation of lactic acid and CO_2 signals the presence of a human to female mosquitoes, this attraction behavior should be similarly suppressed following a blood-meal. We tested non-fed and blood-fed mosquitoes in our host-seeking behavior assay and observed the same state-dependent suppression of attraction to CO_2 and lactic acid by blood-fed mosquitoes, confirming that these stimuli serve as a proxy for the attraction to human host odor (Figure 7.3).

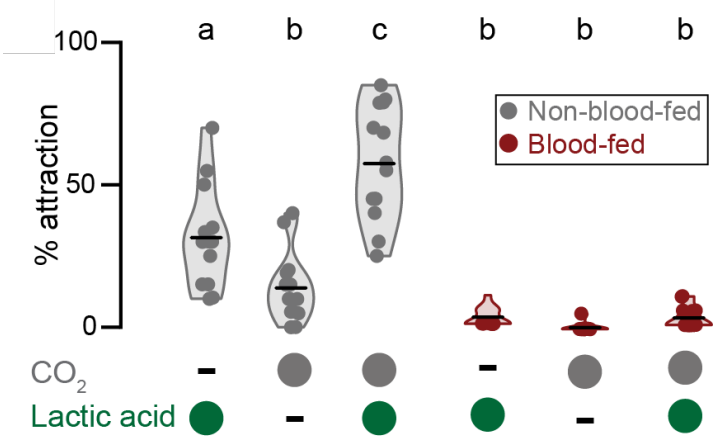

Figure 7.3 Blood-feeding suppresses mosquito attraction to lactic acid and CO2

Attraction of mosquitoes of the indicated genotype to the indicated stimuli. Lactic acid was supplied at 10 µl. Mean with range, n=11-15 trials, 19-21 mosquitoes/trial, *p<0.05, two-way ANOVA followed by Tukey's HSD.
Work performed by: Meg Younger, Ali Ehrlich

We next tested the hypothesis that activating Glomerulus 1 with volatile amines in CO_2-insensitive *Gr3* mutants could sensitize these animals to respond to lactic acid. In control experiments, we observed that neither wild-type nor *Gr3* mutants were attracted to CO_2 alone, and that only wild-type animals and not *Gr3* mutants showed synergistic attraction to CO_2 and lactic acid (Figure 7.4A). As previously observed, both wild-type and *Gr3* mutants showed strong attraction to a live human host in the presence of CO_2 (McMeniman et al., 2014) (Figure 7.4A). Live human hosts emit many sensory cues, effectively compensating for the inability of *Gr3* mutant mosquitoes to detect CO_2 (McMeniman et al., 2014).

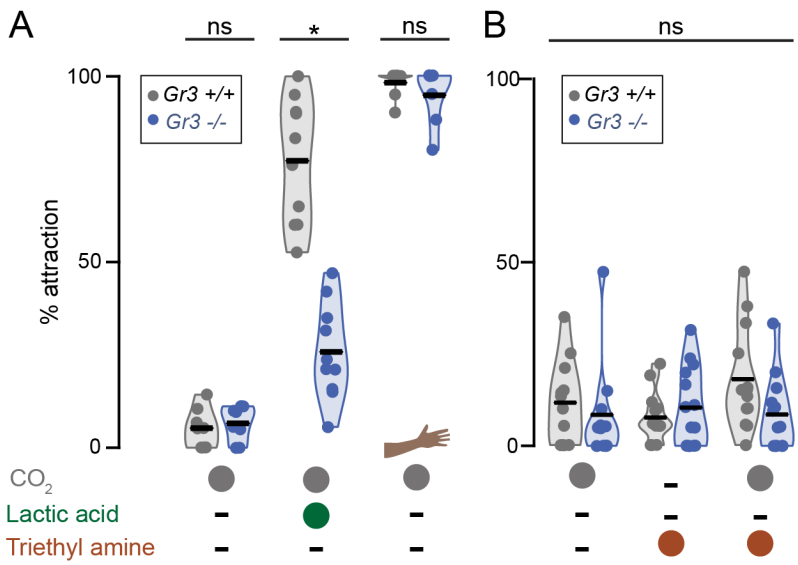

Figure 7.4 Triethyl amine is not attractive alone or when administered with CO2

(A-B) Attraction of mosquitoes of the indicated genotype to the indicated stimuli. Lactic acid was supplied at 1 µl in A. Triethyl amine was presented at 50 µl in B. Mean with range, n=7-16 trials, 15-22 mosquitoes/trial. *p<0.05, ns=not significant (*p>0.05), two-way ANOVA followed by Tukey's HSD.
Work performed by: Margo Herre, Meg Younger

Both CO_2 and triethyl amine activate Glomerulus 1 in wild-type animals but in *Gr3* mutants only triethyl amine and not CO_2 activates this glomerulus. We asked if triethyl amine alone or in combination with CO_2 was attractive to wild type or *Gr3* mutant mosquitoes. Neither wild type nor *Gr3* mutant mosquitoes showed any attraction to CO_2 alone, triethyl amine alone, or the combination of both (Figure 7.4B). This was expected because CO_2 alone—and by extension the activation of Glomerulus 1—is insufficient to mediate attraction in this assay. We next asked if triethyl amine can substitute for CO_2 in synergizing with lactic acid to attract *Gr3* mutant mosquitoes. We tested a range of concentrations of triethyl amine with a single concentration of lactic acid and quantified the number of attracted mosquitoes. Lactic acid alone, and both low and high concentrations of triethyl amine were not attractive to *Gr3* mutants. However, moderate concentrations of triethyl amine stimulated strong attraction when supplied together with lactic acid (Figure 7.4A-B). This sensitization to lactic acid triggered by triethyl amine was not further enhanced by the addition of CO_2, a stimulus that *Gr3* mutants do not detect (Figure 7.4B). We speculate that CO_2-insensitive *Gr3* mutants rely on a compensatory pathway that uses Ir25a and unknown ligand-sensitive IRs to activate Glomerulus 1 with volatile amines.

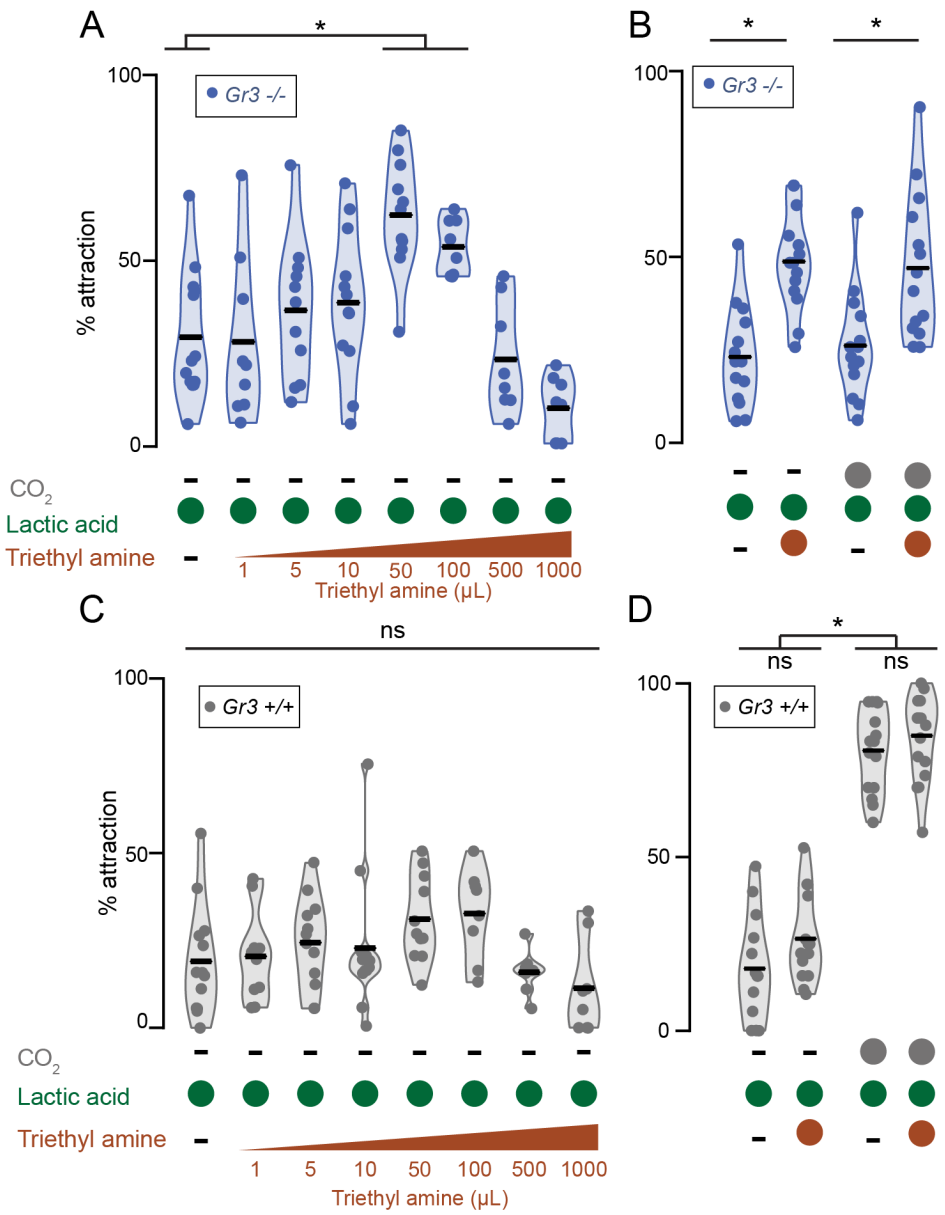

Figure 7.5 Triethyl amine partially substitutes for CO2 in activating mosquito attraction in Gr3 mutants but not in WT animals

(Costa-da-Silva et al.) Attraction of mosquitoes of the indicated genotype to the indicated stimuli. Lactic acid was supplied at 1 µl. Triethyl amine was presented at the indicated concentration in A, C and at 50 µl in B,D. Mean with range, n=7-16 trials, 15-22 mosquitoes/trial. *p<0.05, ns=not significant (*p>0.05), two-way ANOVA followed by Tukey's HSD.
Work performed by: Margo Herre, Meg Younger

To ask if this compensatory pathway is active in wild-type mosquitoes, we repeated these experiments and were surprised to discover that the concentrations of triethyl amine that stimulated Gr3 mutant attraction to lactic acid had no effect on wild-type animals (Figure 7.5B,D, 7.6A). These results suggest that when mosquitoes lack receptors for potent host cues such as CO_2, they rely more heavily on redundant cues detected by the same neurons via the expression of a diverse array of chemosensory receptors to ensure that host-seeking behavior is not compromised (Figure 7.6B).

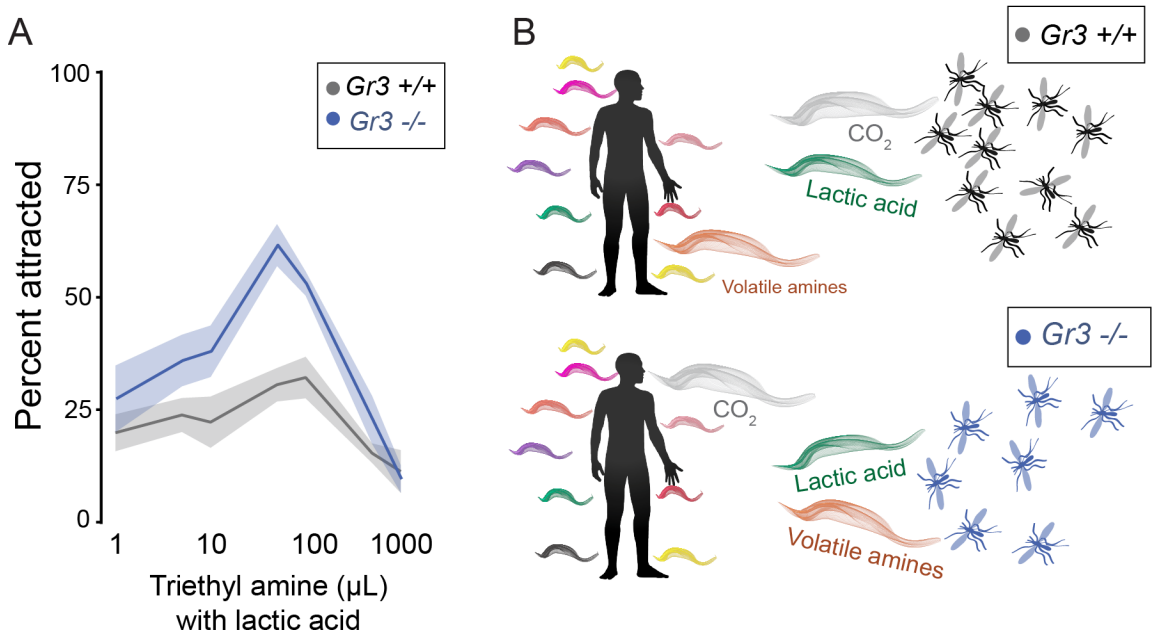

Figure 7.6 Gr3 mutant mosquitoes compensate for loss of CO_2 sensitivity with increased attraction to triethyl amine

(A) Summary of data presented in Figure 7.5. Dose dependency of attraction of WT and Gr3 mutant mosquitoes to triethyl amine presented with lactic acid. Lactic acid was supplied at 1ul. Solid lines = mean, shaded regions = SEM.
(B) Model of the compensatory pathway where volatile amines substitute for CO_2 to enable attraction to humans by CO_2-insensitive Gr3 mutants.
Work performed by: Margo Herre, Meg Younger

In this chapter, we show that we can substitute a volatile amine for CO_2 to drive attraction behavior to the human odor component, lactic acid (Figure 7.5,7.6). Using RNA *in situ* in the CO_2-detecting olfactory appendage, the maxillary palp, we identified ionotropic receptor expression in CO_2 neurons, suggesting the possibility that these neurons contain multiple chemosensory pathways to detect volatile cues (Figure 5.8). To confirm that these receptors are functional, we performed 2-photon calcium imaging in antennal lobe glomeruli innervated by *Gr3*-expressing CO_2 neurons in wild-type and *Gr3* mutant mosquitoes and discovered that these neurons respond to triethyl amine and hexyl amine in addition to CO_2, and that these responses are independent of *Gr3* (Figure 6.4). Thus, since CO_2 neurons respond to both CO_2 as well as triethyl amine, we set out to determine if we could replace CO_2 with triethyl amine to drive attraction behavior. We utilized the minimal mixture of lactic acid and CO_2 to drive human host-seeking behavior to allow us to examine the effects of each monomolecular compound affects mosquito attraction. Since *Gr3* mutants are unable to perform human host-seeking behavior when exposed to lactic acid and CO_2 due to their inability to sense CO_2, we were able to assess whether we could rescue this phenotype by replacing CO_2 with triethyl amine. Remarkably, triethyl amine and lactic acid partially rescued the *Gr3* phenotype. This partial rescue is consistent with the degree of activation *Gr3* neurons exhibit when exposed to CO_2 versus triethyl amine, in that these neurons are much more strongly activated by CO_2 than triethyl amine (Figure 5.8). That *Gr3* neurons are able to be activated by Gr3-independent volatiles may explain why *Gr3* mutant mosquitoes retain strong host-seeking drive even without the ability to detect the potent host cue CO_2 (McMeniman et al., 2014), Figure 7.4).

It was very surprising to us that wild-type animals showed attenuated behavioral responses to triethyl amine and lactic acid even though triethyl amine activates CO_2 neurons in the palp at similar levels in WT and *Gr3* mutants (Figure 5.8). This suggests that loss of *Gr3* may affect the activity and sensitivity of downstream neurons in the olfactory circuit, such as local interneurons or projection neurons. Future studies are warranted to determine how loss of one sensory modality alters olfactory circuits in cell-autonomous and non-cell-autonomous manners. Additionally, it will be fascinating to learn how co-expression of multiple chemosensory receptors enables redundancy in olfactory circuits and allows for compensation when key sensory modalities are lost or compromised.

CHAPTER 8. DISCUSSION

Our study reveals unexpected complexity in the gene expression and functional organization of the mosquito olfactory system. We show extensive co-expression of multiple classes of chemosensory receptors and using calcium imaging and host-seeking behavior assays demonstrate this co-expression to be functional and behaviorally relevant. The potential redundancy afforded by a system in which many neurons express receptors that respond to non-overlapping sets of odorant ligands may greatly increase the sensitivity and robustness of the mosquito olfactory system. Future attempts to refine the design of repellents to ward off mosquitoes or attractant traps to lure them will have to have to reckon with the complexity of this system.

8.1 A compensatory pathway promotes attraction behavior in the CO_2 receptor mutant

It has only recently become possible to generate targeted mutations in chemosensory genes in *Ae. aegypti*, and a striking finding from studying these mutants is how difficult it is to disrupt human host-seeking. Mutations in the co-receptor *Orco* (DeGennaro et al., 2013) and the co-receptor *Ir8a* (Raji et al., 2019) both eliminate entire classes of ligand-specific receptors. In spite of this, *Orco* mutants show normal attraction to humans and mutations in *Ir8a* reduce but do not abolish mosquito attraction to humans. *Gr3* mutants are completely unable to sense CO_2 yet they can also find human hosts, even when released into a large semi-field environment (McMeniman et

al., 2014). These findings raise the question: Why is it so difficult to break the mosquito olfactory system and prevent mosquitoes from finding humans? We propose that this is due to redundancy in receptor expression at the periphery. A recent paper examined *Ae. aegypti* antennal lobe responses of *Orco*-expressing neurons to physiological concentrations of odor collected from several individual humans, a variety of non-human animals, and floral odors (Zhao et al., 2020). They identified a glomerulus that responded to odor blends from all human individuals, animals, as well as honey and milkweed. It is tempting to speculate that this glomerulus is innervated by olfactory sensory neurons that co-express multiple receptors.

We have probed IR and GR redundancy in the CO_2 system and found that *Gr3* mutant mosquitoes that do not detect CO_2 can still detect triethyl amine and have demonstrated that triethyl amine can act as a behavioral substitute for CO_2 in driving attraction to lactic acid in *Gr3* mutants. This activation was strongly dependent on the dose of triethyl amine. Although human skin releases a large number of odorants, including volatile amines, we do not know how the concentrations used in our laboratory behavioral assays relate to those produced by human skin.

Surprisingly, this substitution of triethyl amine for CO_2 does not drive attraction in wild-type animals that are able to detect CO_2. One possible mechanism to explain this finding might be that in the absence of *Gr3*, the sensitivity of the circuit shifts to enhance the behavioral effect of compounds that activate the IRs co-expressed in the CO_2-sensitive neuron. If this were the case, it remains to be seen how the CO_2-sensing

circuitry is altered, whether it is the sensory neuron or downstream neurons involved in host-seeking, and if changes occur at the level of the receptor, synapse, or the intrinsic firing properties of the sensory neurons themselves (Marder and Goaillard, 2006). CO_2-sensing neurons in the maxillary palp rapidly reset their intrinsic firing to adjust to changes in background levels of CO_2 (Majeed et al., 2014) and perhaps the absence of background CO_2 sensation in the *Gr3* mutant enhances the signal to noise ratio of other odorants.

8.2 Receptor co-expression as a mechanism for redundancy or blend integration

We hypothesize that receptor co-expression is used broadly to detect redundant cues that are present in human odor, a blend that can vary from individual to individual and contains hundreds of different chemicals (Bernier et al., 1999; Bernier et al., 2000). We have not yet explored the role of co-expression of OR and IRs in single olfactory neurons. It is possible that receptor co-expression is always used to form a highly redundant detection system for different cues that represent the same ecological target: human hosts. This motif has the benefit of limiting the number of neurons needed to detect varied odorants with the same meaning, however, in exchange it may sacrifice the ability to distinguish between cues detected by receptors expressed in the same sensory neurons. In *Drosophila melanogaster* there are cases of co-expression of two ORs and even co-expression of ORs and IRs in the same neuron, but these are the exception rather than the rule. *Or35a* is co-expressed with *Ir76b* (Silbering et al., 2011), and while these neurons respond to many odorants (Silbering et al., 2011; Yao et al.,

2005), the role of co-expression remains unknown. In addition, *Or49a* and *Or85f* are co-expressed in a specific olfactory sensory neuron population where they play redundant roles in predator avoidance (Ebrahim et al., 2015). Intriguingly, recent data from *Drosophila melanogaster* also show *Orco* and *Ir25a* co-expression in the antenna and maxillary palp (McLaughlin et al., 2020; Task et al., 2020), suggesting that broad co-receptor co-expression may be a conserved motif in insects and upending previous data that suggested strict segregation of OR and IR sensory neuron populations in flies.

While extensive co-expression of different classes of olfactory receptors within olfactory neurons documented in this study is a novel organizational principle, there are counterexamples of receptor co-expression within a single class of chemosensory receptor. Karner et al. have documented polycistronic expression of multiple odorant receptors in *Anopheles gambiae* sensory neurons (Karner et al., 2015). The nematode *C. elegans* copes with a very large number of chemosensory receptor genes and a very small number of sensory neurons by extensive co-expression (Troemel et al., 1995; Vidal et al., 2018). Receptor co-expression to encode redundancy is reminiscent of the taste system in *Drosophila melanogaster,* as many as 28 receptors that detect bitter compounds are expressed in bitter taste neurons (Weiss et al., 2011). Further, in mice, necklace olfactory neurons express multiple MS4a chemoreceptors in each cell (Greer et al., 2016).

We demonstrate that *Ae. aegypti* mosquitoes employ receptor co-expression in primary sensory neurons as well as co-convergence of neurons that express distinct

classes of chemosensory receptors onto the same glomerulus. Consistent with these data, we also identified olfactory neurons in the antenna that express ORs without IRs, IRs without ORs, and neurons that express both ORs and IRs. What is the functional difference between integrating odorant information in the primary sensory neuron versus at the first synapse in the antennal lobe? Co-convergence of olfactory sensory neurons onto the antennal lobe could allow for the early integration of olfactory cues while still retaining discrete input channels that could be selectively modulated during changes in behavioral state, such as the suppression of host-seeking after a blood meal. By identifying distinct glomeruli that are innervated by co-expressing neurons and co-converging neurons, we gain an entry point to understanding how the brain may respond to odorant information integrated in co-expressing neurons versus information integrated in the glomerulus.

8.3 Co-expression is used to encode redundancy in the CO_2 system but co-expression in other olfactory sensory neurons may have different roles in *Ae. aegypti*

We hypothesize that co-expression is used broadly to detect redundant cues that are present in human odor, a blend that can vary from individual to individual and contains hundreds of different chemicals (Bernier et al., 1999; Bernier et al., 2000). This motif has the benefit of limiting the number of neurons needed to detect varied odorants

with the same meaning, however, in exchange it may sacrifice the ability to distinguish between cues detected by receptors expressed in the same sensory neurons.

Alternatively, it is possible that co-expression is exploited differently by different sensory neurons and could be used, for example, to integrate the detection of multiple odors in the sensory neuron itself. In *Drosophila* IRs that form functional complexes can depolarize resting membrane potential *Xenopus* frog oocytes (Ai et al., 2013). Should the same phenomenon be occurring in *Ae. aegypti* neurons that express both IR and OR complexes, it is possible that an IR complex could render a neuron more sensitive to OR ligands. Along this line, certain odors repress OR activity relative to baseline in *D. melanogaster* (Hallem and Carlson, 2006; Yao et al., 2005) and it is possible that multiple receptors housed in a single neuron could be a source of blend-specific repression. In the Ae. aegypti stylet, the needle-like blood-feeding appendage, a population of neurons only responds when multiple distinct ligands are presented simultaneously (Jové et al., 2020). Human odor is a blend of dozens of volatile odorants, engineering an olfactory neuron population that only responds when multiple ligands are presented would prove to be an elegant mechanism for detecting important host cues. Individual odor molecules found in human odor exist in many blends and this might be a way to limit the attraction to monomolecular components of human odor that are found in aversive blends or are produced by other animals. These ideas remain to be tested in the mosquito, but it is tempting to speculate that this could be used as a method to detect ratios of odors present in a blend, because this is a key determinant in

how attractive many monomolecular compounds are to mosquitoes (Bernier et al., 2007).

8.4 Coordinated co-expression between *IR, OR,* and *GR* ligand-sensitive receptors

We identified co-expression of co-receptors and ligand-sensitive receptors belonging to distinct chemosensory families in single neurons in the maxillary palp. This co-expression poses a gene regulatory problem for an olfactory neuron. For ORs and IRs to form functional chemoreceptors, at least one co-receptor and one ligand-sensitive receptor must be expressed in a cell. We have demonstrated that two IRs, *Ir93a* and *Ir100a*, are expressed nearly exclusively with *Or49* and the co-receptors *Orco* and *Ir25a*, whereas *Ir75g* is co-expressed with the coreceptor *Ir25a* and the CO_2 receptor subunit *Gr3*. Thus, the transcriptional landscape in *Ae. aegypti* maxillary palp olfactory neurons is not only permissive to co-expression, but ensures certain receptors are only expressed with others.

How might this complex code of chemosensory receptor co-expression be regulated? In vertebrates, an elaborate epigenetic silencing mechanism ensures that each olfactory neuron expresses only a single allele of a single odorant receptor (Bashkirova and Lomvardas, 2019). In contrast, *Drosophila* is thought to use a more conventional transcription factor code in which the specification of a neuron and the expression of its chemosensory receptor is tightly regulated (Jafari and Alenius, 2015; Li

et al., 2016; Ray et al., 2008). Single-cell sequencing data generated from developing *Drosophila melanogaster* olfactory neurons demonstrates a complex regulatory landscape wherein dependent on cell type, a set of transcription factors govern receptor expression, axon targeting, or both (Li et al., 2020). Two recent studies (McLaughlin et al., 2020; Task et al., 2020) also document extensive co-expression of receptors in *Drosophila melanogaster*, calling into question the rules that regulate olfactory organization in this insect. It is yet to be determined if mosquito orthologues of these transcription factors have been co-opted to regulate the co-expression we observe or if this novel olfactory organization demands a distinct transcriptional mechanism.

8.5 Intraspecies variability in glomerulus position and size

We found that the size, shape and number of antennal lobe glomeruli in *Ae. aegypti* was variable from animal to animal. It is possible that the boundaries between glomeruli are not easily distinguished by synaptic staining and that specific glomeruli will become identifiable once there are genetic tools available that label smaller populations of OSNs. The anatomical variability we see is consistent with both the original map that identified 50 glomeruli (Ignell et al., 2005), which divided glomeruli into 3 classes based on their variability in location, as well as a recent study that looked specifically at the size and shape of glomeruli across animals (Shankar and McMeniman, 2020) and revises the original map to a count of ~80 glomeruli. In this case, glomeruli were named and numbered across animals, but they note that they were only able to consistently identify 63 glomeruli. While we count ~65 glomeruli in total, the exact number of

glomeruli presented in any of these studies, or in ours, is far less than the number of chemosensory receptors in *Ae. aegypti*.

The variability in antennal lobe structure appears at first in contrast to *D. melanogaster*, where each glomerulus can be clearly identified and named, however, we note that the antennal lobe map in *D. melanogaster* has been refined with the advent of new genetic techniques, starting with 35 glomeruli in the original atlas (Stocker et al., 1990a), then modified to 40 glomeruli (Laissue et al., 1999), and further refined in numerous studies (Couto et al., 2005; Fishilevich and Vosshall, 2005; Tanaka et al., 2012) including a recent count of 54 glomeruli in an *in vivo* atlas (Grabe et al., 2015). We have refrained from naming glomeruli in *Ae. aegypti* at this time, however, it is possible that a more stereotyped anatomy will emerge as new genetic lines are generated in this insect that has only recently become amenable to cell-type-specific labelling.

A recent study in the mosquito *Anopheles coluzzii,* in which transgenic mosquitoes that label *Orco*-positive neurons were generated also noted that the antennal lobe was variable between animals relative to *D. melanogaster* (Riabinina *et al.*, 2016). It is possible that mosquito antennal lobes are more variable than Drosophilids (Grabe et al., 2015; Prieto-Godino et al., 2017). We also noted that the general regions of *Orco*-expressing OSN innervation are similar in both mosquito species and *D. melanogaster*, with the greatest density in the anterior medial antennal lobe. We saw *Orco* OSN innervation in a region that was previously identified as Johnston's Organ Center and

we have included this as part of the antennal lobe and segmented it, consistent with what was done in *Anopheles coluzzii* (Ghaninia et al., 2007a; Ignell et al., 2005; Riabinina et al., 2016).

Variability in antennal lobe structure is seen even in the mouse, *Mus musculus,* where the principles of olfactory organization were first established (Schaefer et al., 2001; Strotmann et al., 2000; Zou et al., 2009). A single type of OSN projects to either one or two glomeruli in the olfactory bulb. The exact size and location of glomeruli can vary between animals more than initially appreciated and appears to be determined by both genetic factors and activity in OSNs during the early life of the animal. In *D. melanogaster*, glomerulus size is highly genetically determined and correlates strongly with the number of OSNs that innervates each glomerulus (Grabe et al., 2015). Whether the variability in glomerulus size in the mosquito is due to activity-dependent changes in structure of other factors remains to be seen. Lastly, it remains to be determined how stereotyped the antennal lobe is in primates, including humans, which have a one receptor to 16 glomerulus organization (Maresh et al., 2008).

8.6 Future directions

How do olfactory systems compensate when one sensory modality is lost?

Our puzzling observation that triethyl amine is able to partially replace CO_2 to drive attraction behavior in the presence of lactic acid in *Gr3* mutants but not in wild-type

animals has led us to wonder how the loss of one sensory modality affect other sensory modalities in a cell-autonomous or non-cell-autonomous fashion. It is tempting to hypothesize that mutation of *Gr3* causes CO_2-sensitive neurons to become more sensitive to triethyl amine, but our calcium imaging data suggests that loss of *Gr3* has no effect on the activity of these neurons when exposed to triethyl amine. Thus, it is likely that loss of CO_2-evoked activity from these neurons has altered downstream olfactory processing circuits. One possibility is that projection neurons in *Gr3* mutants are more sensitive to activation by triethyl amine, as it is known that while *Gr3* neurons do not habituate to repeated presentations of CO_2 or high background CO_2, activity in projection neurons does habituate (Majeed et al., 2014). This suggests that in the opposite scenario with a lack of activity from CO_2, these neurons may be more sensitive.

It has been demonstrated that loss of one sensory modality can affect sensitivity of a completely different modality. In one recent study, silencing of all Orco neurons increased taste preference for sucrose (Junca et al., 2021), indicating that manipulating the olfactory system can alter sensitization in another chemosensory system. Where in the olfactory and taste circuit is this effect occurring? Silencing olfactory projection neurons produced sweet sensitization that was similar to the results obtained from silencing all Orco neurons, suggesting that this modulation may occur downstream of olfactory projection neurons. While it is not fully understood where the mechanistic connection between the olfactory and gustatory circuits is in the brain, it is likely that higher brain regions such as the mushroom body or lateral protocerebrum, which are

known to integrate olfactory and taste cues, could be implicated in gain control (Shyu et al., 2017; Talay et al., 2017; Yamagata et al., 2015).

These possibilities underscore the need for the generation of additional genetic tools in *Ae. aegypti* to gain access to second and third order neurons in the olfactory circuit. By doing so, we may not only be able to understand how the circuit is affected by loss of olfactory inputs, but also where in the brain information from distinct sensory modalities are integrated, such as CO_2 and heat. By understanding how olfactory information is processed in multiple brain regions, we gain entry points into determining how the detection of human cues lead to deadly host-seeking behaviors.

Do co-expressed olfactory receptors interact with each other within an olfactory sensory neuron?

Both ORs and IRs form ionotropic receptor complexes, but their firing properties are differentially regulated. Olfactory sensory neurons that express ORs display adaptation to repeated odor presentation in electrophysiological recordings of single sensilla or single neurons (Cao et al., 2016; Martelli et al., 2013; Nagel and Wilson, 2011), while IR-expressing neurons show no adaptation in single sensilla recordings or whole-cell patch clamp experiments (Abuin et al., 2019; Cao et al., 2016).

In neurons that express IRs and ORs, do the firing properties of one receptor affect the properties of another? The mosquito olfactory system offers an ideal model to study

this question. We can get hints, however, from previous work in *Drosophila* that involved ectopically expressing a second OR in an olfactory sensory neuron and examining if responses mediated by the two receptors, which detect two different stimuli, cross-adapt After stimulating one receptor for an extended period, the second receptor showed smaller responses to its stimulus, indicating that activation of one OR in a neuron could affect activation of the second OR. How might this phenomenon work in a cell that expresses ORs and IRs? Since IRs are not known to adapt in single IR-expressing neurons, repeated stimulation of an OR may not affect the responses of an IR. Vice versa, repeated stimulation of an IR may affect responses of an OR. For example, we discovered *Ir93a* expression in *Or49* neurons in the maxillary palp. *Ir93a* is a putative cooling receptor (Knecht et al., 2017): would exposure to cool temperatures inhibit the ability of *Or49* to properly respond to its ligand?

One hypothesis for how co-expression may affect mosquito olfactory behaviors is that it enables blend integration at the level of the individual sensory neuron. Neurons that do not respond when individual ligands are presented individually but do respond when these ligands are presented as a blend were discovered in the mosquito stylet (Jové et al., 2020), but it is yet to be determined if such blend integration occurs in the mosquito olfactory system. Gaining an understanding for how firing properties of chemosensory receptors are affected in co-expressing neurons could lead to discoveries regarding how complex blends of odors are detected. The maxillary palp, an olfactory organ with extensive co-expression of a limited number of chemosensory

receptors with a spatial distribution defined in this work, may be an ideal tissue to begin this dissection.

Roles for volatile odorant detection in the *Ae. aegypti* taste system

Insects engage in contact chemosensation for taste and mate selection with their legs and proboscis, the insect mouthpart. *Drosophila* express IRs and GRs in their proboscis, but not ORs (Larsson *et al.*, 2004). We identified Orco expression in the proboscis of *Ae. aegypti,* and previous studies in *An.* gambiae, which also express *Orco* in their proboscis, have shown that proboscis neurons respond to volatile odorants (Kwon *et al.*, 2006). We also observe extensive co-expression of *Ir25a* and *Orco* in the *Ae. aegypti* proboscis. Co-expression of these co-receptors in the antenna and maxillary palps could indicate that an olfactory neuron can respond to multiple classes of odorants, but what is the function of this co-expression in the context of a taste organ? In *Drosophila,* Ir25a mediates gustatory detection of several taste qualities including polyamines, amino acids, and salt detection (Abuin et al., 2011; Benton et al., 2009; Hussain et al., 2016; Zhang et al., 2013). Co-expression of *Ir25a* and *Orco* in the proboscis therefore could potentially mean that this population of neurons may respond to both tastants through contact as well as volatile odorants. Can the brain distinguish between volatile and gustatory cues encountered on the proboscis?

Although *Drosophila* do not express ORs in their proboscis, they can respond to at least one volatile cue through gustatory neurons: CO_2. Work from Kristin Scott's lab has

demonstrated that while CO_2 detection through the olfactory system can trigger avoidance behavior, activation of neurons that detect CO_2 by way of yeast, beer or volatile CO_2 is appetitive, demonstrating that the chemosensory context this volatile ligand is encountered matters for behavior output (Fischler et al., 2007). Many ORs expressed in the proboscis are also expressed in the antenna (Matthews et al., 2016). How does the mosquito brain process these olfactory and gustatory cues from the same ligand simultaneously?

It is tempting to hypothesize that mosquitoes utilize olfactory cues on their proboscis to evaluate shorter-range volatiles on human skin prior just to piercing to feed on blood. However, recent work has demonstrated that cues on skin are not necessary for blood-feeding, as mosquitoes exposed to CO_2 and heat will engorge on a blood-meal when presented in an artificial membrane feeding system (Jové et al., 2020). In this assay, the CO_2 and heat mimic volatile host cues but the parafilm covering the warmed blood-meal is devoid of any tastants or volatiles from skin. Thus, it is currently not known how or if volatile information detected by the proboscis is implicated in host-seeking behavior. It will be fascinating to determine how *Orco* neurons are functioning in the proboscis and how odorants that engage both the taste and olfactory systems are interpreted by the mosquito brain.

An olfactory sensory map of *Ae. aegypti*

Gaining a handle on the logic of olfactory coding in an organism requires knowledge of not only the number and identity of olfactory receptors expressed, but also the pattern of expression in sensory neurons and how these neurons are wired into the brain (Vosshall et al., 2000). By generating QF driver lines that enable fluorescent labeling and activity recordings of cells that express chemosensory co-receptors and optimizing whole mount immunostaining and RNA *in situ* protocols to visualize olfactory neurons, we have taken the first steps to generate an olfactory sensory map for *Ae. aegypti*. Further, we identified the maxillary palp as ideal tissue to begin detailed dissections of the *Ae. aegpti* olfactory system, as fewer than 20 chemosensory genes are expressed in olfactory neurons that send axonal projections to only 3 antennal lobe glomeruli, and it is a relevant organ for studying host-seeking behavior. Still, important questions remain that likely necessitate expansion of our genetic toolset. Which receptors are responsible for the detection of human odor? Does co-expression of multiple receptors enable blend detection? How and where is human odor integrated in the brain with other human cues such as CO_2 and heat?

Significant technological hurdles currently prevent the mosquito field from generating an olfactory map of similar scope to that of *Drosophila*. Creation of a genetic toolset was critical to generate a nearly complete anatomic and functional map of the fly olfactory system. Additionally, these regents allow for selective silencing and activation of olfactory neurons that allow for detailed dissection of an individual receptor's role in

olfactory behaviors. Decades of work from many labs and organized, centralized efforts have generated a library of *Gal4* driver lines in *Drosophila* that tile not only the peripheral olfactory system but also antennal lobe interneurons and projection neurons that carry olfactory information form the antennal lobe to higher brain regions.

What is necessary to generate this kind of library in *Ae. aegypti?* Mosquitoes not only express far more olfactory receptor genes than *Drosophila* but generating driver lines complementary of those in *Drosophila* will be difficult and time-consuming to generate unless current genetic methods are improved. Many *Drosophila* driver lines are transgenes composed of enhancer or promoter elements fused with the driver transcription factor sequence and inserted either randomly in the genome or at site-specific integrations by integrases. Unfortunately, utilization of cis regulatory elements to drive reporter expression in mosquitoes has been far less successful, necessitating the use of CRISPR knock-ins at endogenous loci. This this an inefficient technique in mosquitoes and combined with longer generation times and a more labor-intensive screening and rearing processes means generation of a new *Ae. aegypti* driver line currently requires approximately 6-9 months of labor. Using this method, how long would it take to generate a driver line library containing each of the approximately 150 expressed chemosensory genes in *Ae. aegypti*? This PhD candidate shudders at the thought.

Thus, improving methods for generation of driver lines in *Ae. aegypti* has the potential to rapidly speed progress in our understanding of the organization of the

olfactory system. Harnessing cis regulatory elements to replace CRISPR knock-in strategies may allow for much faster generation of genetic toolsets. Further, additional knowledge about how to efficiently generate driver lines in *Ae. aegypti* could then allow genetic access to other mosquito species, facilitating comparative analyses of mosquito olfactory behaviors.

We have developed genetic, immunofluorescence, functional imaging, and behavior techniques that provide a foundation to study the olfactory system and host-seeking behavior in *Ae. aegypti*. Extending the genetic toolkit and transgenic methods we established to cover the rest of the *Ae. aegypti* olfactory system will further our understanding of the organization of this system and how it may be optimized for human host-seeking. Ultimately, an understanding of mosquito olfaction is fundamental to prevent mosquito biting and blood-feeding behavior, which is responsible for transmission of vector-borne diseases to hundreds of millions of people world-wide each year.

METHODS

Human and animal ethics statement

Blood-feeding procedures and behavioral experiments with live hosts were approved and monitored by The Rockefeller University Institutional Animal Care and Use Committee (IACUC protocol 17018) and Institutional Review Board (IRB protocol LV-0652), respectively. Human volunteers gave their written informed consent to participate.

Mosquito rearing and maintenance

Aedes aegypti wild-type laboratory strains (Liverpool and Orlando), CRISPR-Cas9 knock-in, and piggyBAC *QUAS* transgenic strains were maintained and reared at 25 – 28^{o}C, 70-80% relative humidity with a photoperiod of 14 hr light: 10 hr dark as previously described (DeGennaro *et al.*, 2013). Adult mosquitoes were provided constant access to 10% sucrose. For routine strain maintenance, animals were primarily blood-fed on live mice and occasionally on live human volunteers. Newly generated strains were blood-fed on human volunteers until they were established. All experiments were conducted on female mosquitoes.

Generation of chemosensory receptor *QF2* and Split-*QF2* knock-in strains

T2A-QF2 gene-sparing stop codon replacement lines were generated using the strategy outlined in Matthews et al. (Matthews *et al.*, 2019). sgRNAs were placed as close to the stop codon as possible and donor constructs were designed to remove the stop codon

and replace it with an in-frame cassette containing the *T2A* ribosomal skipping sequence and the *QF2* transcription factor or Split-*QF2* domains, comprising the *QF2* activation domain *QF2-AD*, or the *QF2* DNA-binding domain *QF2-DBD*. This strategy spares the function of the gene at the locus being targeted, expresses *QF2* or Split-*QF2* domains in the cells specified by enhancers at the locus. Insertions were marked by the *3xP3* enhancer expressing a fluorescent protein. To identify effective sgRNAs, 5 candidate sgRNAs per gene were first injected into separate pools of 500 Liverpool embryos and CRISPR-Cas9-mediated cut rate was evaluated as previously described (Kistler *et al.*, 2015). Either a single sgRNA or 2 sgRNAs with the highest cut rates were then chosen to be injected with donor plasmids to target chemosensory gene loci using homology-directed repair. sgRNAs targeted the respective gene near the stop codon, target sequence with protospacer adjacent motif (PAM) underlined:

Ir25a: GTTTGTGTGCGTGTCCGTA TGG

Ir76b: GTATTACACTTATCTAAATA TGG

Ir8a: GTCACGCTTGTTGTACAGGG CGG, GAACAATTTGAACAAGGTCG TGG

Gr3: GTTAGTGATGCATAATATGA CGG

Orco: GTCACCTACTTCATGGTGT TGG

sgRNA DNA template was prepared by annealing oligonucleotides as described (Kistler *et al.*, 2015). *In vitro* transcription was performed using HiScribe Quick T7 kit (NEB E2050S) following the manufacturer's directions. Following transcription and DNAse treatment for 15 min at 37°C, sgRNA was purified using RNAse-free SPRI beads (Ampure RNAclean, Beckman-Coulter A63987), and eluted in Ultrapure water (Invitrogen, 10977–015).

Donor plasmids were constructed by Gibson assembly using the following fragments for QF2 lines:

1) *pUC19* digested with XbaI and BamHI

2) Left and right homology arms: *Gr3* (left: 1.9 kb, right: 1.6 kb), *Ir25a* (left: 1.8 kb, right: 1.6 kb), *Ir76b* (left: 1.2 kb, right: 2.2 kb), *Ir8a* (left: 1.7 kb, right: 1.7 kb), *Orco* (left: 1.2 kb, right: 1.3 kb) generated by polymerase chain reaction (PCR) using Liverpool genomic DNA as a template

3) A 2.6 kb fragment containing *T2A-QF2-SV40, 3xP3-dsRed*, PCR-amplified from a previously assembled vector (*ppk10779-T2A-QF2-SV40, 3xP3-dsRed*, Addgene accession #130667)

For Split-QF2 lines, donor plasmids were constructed by generating fragments using PCR from the indicated template with indicated primers below and assembled using NEBuilder HiFi DNA Assembly (NEB E5520S):

Primer sequences for generation of Split-QF constructs

Ir25a-T2A-QFAD::Zip+-SV40-3xP3-eYFP-SV40

1. Plasmid backbone with Ir25 homology arms from Ir25a-T2A-QF2 plasmid

Forward primer: 5'- tcttaaagcttatcGATACTGAAGTTCATTTTTTGAGTAG -3'

Reverse primer 5'- ctctgccctctcc AAAACGAGATTTAAAGTTGTTGG -3'

2. T2A-QFAD::Zip+-SV40 sequence from (Riabinina et al., 2019), fragment synthesized by Genewiz

Forward primer: 5'- taaatctcgttttGGAGAGGGCAGAGGAA -3'

Reverse primer: 5’-tagatccccgggcgCAGACATGATAAGATACATTGATGAG -3’

3. 3xP3-EYFP from pDSAY (Addgene, #62291)

Forward primer: 5’- tatcttatcatgtctgCGCCCGGGGATCTAATTCAATTAG -3’

Reverse primer: 5’- agtatcGATAAGCTTTAAGATACATTGATGAGTTTGG -3’

Orco-T2A-Zip−::QFDBD-SV40-3xP3-dsRED-SV40

1. Plasmid backbone with Orco homology arms and 3xP3-dsRED-SV40 from Orco-T2A-QF2 plasmid

Forward primer: 5’- aatgtatcttatcatgtctgAATTCGAGCTCGCCCG -3’

Reverse primer: 5’- tcctctgccctctccTTTCAACTGCACGAGCACC -3’

2. T2A-Zip−::QFDBD-SV40 synthesized by Genewiz

Forward primer: 5’- catggtgctcgtgcagttgaaaGGAGAGGGCAGAGGAA -3’

Reverse primer: 5’- gagctcgaattCAGACATGATAAGATACATTGATGAG -3’

T2A-Zip-::QFDBD-SV40 synthesized by Genewiz:

GGAGAGGGCAGAGGAAGTCTTCTAACATGCGGTGACGTGGAGGAGAATCCCGGC
CCTATGCTGGAGATCCGCGCCGCCTTCCTGCGCCAGCGCAACACCGCCCTGCGC
ACCGAGGTGGCCGAGCTGGAGCAGGAGGTGCAGCGCCTGGAGAACGAGGTGAG
CCAGTACGAGACCCGCTACGGCCCCCTGGGCGGCGGCAAGGCTAGCGGAGGAG
GTGGTGGAGGTGGAGGTGGAGGTGACGTCATGCCACCCAAGCGCAAAACGCTTA
ACGCTGCGGCTGAGGCTAACGCTCATGCCGACGGACACGCCGACGGAAACGCCG
ACGGACACGTGGCCAATACGGCCGCGTCCTCGAATAATGCGAGGTTCGCTGATCT
CACTAACATCGATACTCCGGGTCTGGGACCCACAACTACGACCCTGCTCGTGGAA
CCAGCACGCTCAAAGCGTCAACGAGTGTCCCGCGCATGCGACCAGTGCCGTGCA
GCCCGAGAGAAATGCGACGGAATACAGCCTGCGTGTTTCCCGTGCGTTTCCCAGG
GAAGGTCCTGCACTTATCAGGCTTCGCCGAAAAAGAGGGGAGTTCAAACCGGTTA
TATTCGTACGCTGGAGCTCGCCCTCGCCTGGATGTTTGAAAATGTCGCGCGTTCC

GAAGATGCCTTGCATAACCTCCTCGTCCGTGACGCCGGACAAGGATCAGCTCTGC
TCGTTGGTAAAGATTCGCCGGCTGCCGAGCGACTCCATGCCCGTTGGGCTACTAG
CCGTGTCAATAAGAGCATTACCCGCCTCCTCTAAGGCCGGCCGATCTTTGTGAAG
GAACCTTACTTCTGTGGTGTGACATAATTGGACAAACTACCTACAGAGATTTAAAGC
TCTAAGGTAAATATAAAATTTTTAAGTGTATAATGTGTTAAACTACTGATTCTAATTG
TTTGTGTATTTTAGATTCCAACCTATGGAACTGATGAATGGGAGCAGTGGTGGAAT
GCCTTTAATGAGGAAAACCTGTTTTGCTCAGAAGAAATGCCATCTAGTGATGATGA
GGCTACTGCTGACTCTCAACATTCTACTCCTCCAAAAAAGAAGAGAAAGGTAGAAG
ACCCCAAGGACTTTCCTTCAGAATTGCTAAGTTTTTTGAGTCATGCTGTGTTTAGTA
ATAGAACTCTTGCTTGCTTTGCTATTTACACCACAAAGGAAAAAGCTGCACTGCTAT
ACAAGAAAATTATGGAAAAATATTTGATGTATAGTGCCTTGACTAGAGATCATAATC
AGCCATACCACATTTGTAGAGGTTTTACTTGCTTTAAAAAACCTCCCACACCTCCCC
CTGAACCTGAAACATAAAATGAATGCAATTGTTGTTGTTAACTTGTTTATTGCAGCTT
ATAATGGTTACAAATAAAGCAATAGCATCACAAATTTCACAAATAAAGCATTTTTTTC
ACTGCATTCTAGTTGTGGTTTGTCCAAACTCATCAATGTATCTTATCATGTCTG

T2A-QFAD::Zip+-SV40 synthesized by Genewiz:

GGAGAGGGCAGAGGAAGTCTTCTAACATGCGGTGACGTGGAGGAGAATCCCGGC
CCTATGGATAAAGCGGAATTAATTCCCGAGCCTCCAAAAAAGAAGAGAAAGGTCGA
ATTGGACGTCCGTCAGTTGGAGCTCCCTCCTACCGCCACGGCTACGGCCTCGATA
ATGCCGCACGTGATGGAGCAGCCTCTCAGTACCAGCATTAACCCCGTCAACGACC
GCTTCAACGGTATTCCCAACCCCACTCCGTATAACTCCGATGCAGCTCTCGATGCT
ATCACTCAGACCAACGATTATGGAAGCGTAAATACACATGGTATCCTCTCTACTTAC
CCGCCACCGGCTACGCACCTTAATGAAGCTTCCGTCGCTCTCGCTCCCGGTGGCG
CCCCCCCCCGACCGCCTCCTCCGTATGTTGACAGCACGACCAATCACCCGCCGTA
CCACTCGAATCTGGTTCCAATGGCGAACTTTGGTTACTCGACCGTTGATTACGATG
CCATGGTTGACGATTTGGCTAGCATTGAATACACGGACGCTGTGGATGTCGACCC
ACAGTTTATGACCAATCTGGGATTCGTTCCTGGATGTAACTTCTCCGACATTAATAC
ATACGAACAGAGATCTGGAGGAGGTGGTGGAGGTGGAGGTGGAGGTACTAGTCT
GGAGATCGAGGCCGCCTTCCTGGAGCGCGAGAACACCGCCCTGGAGACCCGCGT
GGCCGAGCTGCGCCAGCGCGTGCAGCGCCTGCGCAACCGCGTGAGCCAGTACC
GCACCCGCTACGGCCCCCTGGGCGGCGGCAAGTAAGGCCGGCCGATCTTTGTGA
AGGAACCTTACTTCTGTGGTGTGACATAATTGGACAAACTACCTACAGAGATTTAAA
GCTCTAAGGTAAATATAAAATTTTTAAGTGTATAATGTGTTAAACTACTGATTCTAAT
TGTTTGTGTATTTTAGATTCCAACCTATGGAACTGATGAATGGGAGCAGTGGTGGA
ATGCCTTTAATGAGGAAAACCTGTTTTGCTCAGAAGAAATGCCATCTAGTGATGAT
GAGGCTACTGCTGACTCTCAACATTCTACTCCTCCAAAAAAGAAGAGAAAGGTAGA
AGACCCCAAGGACTTTCCTTCAGAATTGCTAAGTTTTTTGAGTCATGCTGTGTTTAG
TAATAGAACTCTTGCTTGCTTTGCTATTTACACCACAAAGGAAAAAGCTGCACTGCT
ATACAAGAAAATTATGGAAAAATATTTGATGTATAGTGCCTTGACTAGAGATCATAA
TCAGCCATACCACATTTGTAGAGGTTTTACTTGCTTTAAAAAACCTCCCACACCTCC
CCCTGAACCTGAAACATAAAATGAATGCAATTGTTGTTGTTAACTTGTTTATTGCAG
CTTATAATGGTTACAAATAAAGCAATAGCATCACAAATTTCACAAATAAAGCATTTTT
TTCACTGCATTCTAGTTGTGGTTTGTCCAAACTCATCAATGTATCTTATCATGTCTG

Ir25a-T2A-QFAD::Zip+-SV40-3xP3-eYFP-SV40 was composed of:

1. Plasmid backbone with *Ir25* homology arms from *Ir25a-T2A-QF2* plasmid (6 kb)

2. *T2A-QFAD::Zip+-SV40* sequence from (Riabinina *et al.*, 2019), fragment synthesized by Genewiz, sequence in Data File 1 (1.5 kb)

3. *3xP3-EYFP-SV40* from *pDSAY* (Addgene, #62291) (1.2 kb)

Orco-T2A-Zip−::QFDBD-SV40-3xP3-dsRED-SV40 was composed of:

1. Plasmid backbone with *Orco* homology arms and *3xP3-dsRED-SV40* from *Orco-T2A-QF2* plasmid (6.3 kb)

2. *T2A-Zip−::QFDBD-SV40* synthesized by Genewiz (1.5 kb)

For all *QF2* and Split-*QF2* constructs, the stop codon of the endogenous gene was removed and the PAM sequences corresponding to the sgRNAs used for injection were modified by PCR mutagenesis during Gibson assembly by introducing synonymous codon substitutions to protect the sequence from Cas9 cleavage while retaining the amino acid identity. Plasmids were isolated using an endotoxin-free plasmid midiprep kit (Macherey-Nagel) for QF2 lines and NucleoBond Xtra Midi Endotoxin-Free plasmid kit (Clontech 740420.50) for Split-QF2 lines and eluted in ultrapure water prior to injection. Donor plasmids are available at Addgene (accession numbers #162520-162526). Approximately 2000 wild-type Liverpool strain *Ae. aegypti* embryos were injected with a mix containing recombinant Cas9 protein (PNA Bio, CP01) at 300 ng/μL, sgRNAs at 40 ng/μL and donor DNA plasmid (300 ng/μL for QF2 lines, 600 ng/μL for Split-QF2 lines) at the Insect Transformation Facility at the University of Maryland Institute for Bioscience & Biotechnology Research. Embryos were hatched and surviving G0 males and females were crossed to wild-type Liverpool mosquitoes and their G1 offspring

were screened for fluorescence indicating positive stable germ line transformants. For QF2 lines, the fidelity of insertion was verified by PCR and Sanger sequencing. One representative line for each chemosensory receptor QF2 knock-in was selected for further study. QF2-driven expression patterns were examined by crossing to *QUAS-CD8:GFP-3xP3-ECFP* and/or *QUAS-dTomato-T2A-GCaMP6s-3xP3-ECFP*. All lines were outcrossed to wild-type Liverpool mosquitoes for at least 3 generations prior to being used in experiments. For Split-QF2 lines, a single family with the correct insertion was confirmed by PCR and Sanger sequencing for *Ir25a-QF2-AD* and *Orco-QF2-DBD*. To propagate these lines, a male founder was chosen to cross to wild-type Liverpool females. Animals were then back-crossed to Liverpool for at least 2 additional generations. To evaluate if the Split-QF2 system was functional in *Ae. aegypti*, *Ir25a-QF2-AD was crossed to QUAS-dTomato-T2A-GCaMP6s.* The resulting *Ir25a-QF2-AD, QUAS-dTomato-T2A-GCaMP6s* animals were then crossed to *Orco-QF2-AD*. Expression of the dTomato reporter was observed in larval antennae and subsequently confirmed in adult antennae and brains. dTomato is a dimer (Shaner et al., 2004).

QUAS **transgenic strains**

QUAS-CD8:GFP-3xP3-ECFP and *QUAS-dTomato-T2A-GCaMP6s-3xP3-ECFP* transgenic strains were described previously (Matthews *et al.*, 2019). Two independent insertions of the *QUAS-dTomato-T2A-GCaMP6s-3xP3-ECFP* reporter line (Jové *et al.*, 2020; Matthews *et al.*, 2019) were used in this study. These are located on different chromosomes and were used according to the crossing scheme needed for a given experiment.

Transcript abundance estimates of *Ae. aegypti* OR, IR, and GR genes

Expression values for adult sugar-fed, non-blood-fed female sensory tissues were retrieved from the *Ae. aegypti* L5 genome GitHub repository (https://github.com/VosshallLab/AGWG-AaegL5) at this link: https://github.com/VosshallLab/AGWG-AaegL5/raw/master/AGWG%20AaegL5%20Chemoreceptor%20TPM.xlsx. These expression values reflect libraries from a previous transcriptome study (Matthews *et al.*, 2016) that had been aligned to the *Ae. aegypti* genome (AaegL5) and chemoreceptor geneset annotation reported in units of Transcripts Per Million (TPM) (Matthews *et al.*, 2018). The number of genes from each of three gene families (ORs, IRs, and GRs) with expression values above the indicated threshold were plotted in Figure 2.1E,F.

Whole brain fixation and immunostaining

Dissection of adult brains and immunostaining was done as previously described (Matthews *et al.*, 2019). 6-14 day-old mosquitoes were anesthetized on ice. Heads were carefully removed from the body by pinching at the neck with sharp forceps. Heads were placed in a 1.5 mL tube for fixation with 4% paraformaldehyde, 0.1 M Millonig's Phosphate Buffer (pH 7.4), 0.25% Triton X-100, and nutated for 3 hr. Brains were then dissected out of the head capsule in ice-cold Ca^{+2}-, Mg^{+2}-free phosphate buffered saline (PBS, Lonza 17-517Q) and transferred to a 24-well plate. All subsequent steps were done on a low-speed orbital shaker. Brains were washed in PBS containing 0.25% Triton X-100 (PBT) at room temperature 6 times for 15 min. Brains were permeabilized

with PBS, 4% Triton X-100, 2% normal goat serum (Jackson ImmunoResearch #005-000-121) for ~48 hr (2 nights) at 4°C. Brains were rinsed once and then washed with PBT at room temperature 6 times for 15 min. Primary antibodies were diluted in PBS, 0.25% Triton X-100, 2% normal goat serum for ~48 hr (2 nights) at 4°C. Brains were rinsed once then washed in PBT at room temperature 6 times for 15 min. Secondary antibodies were diluted in PBS, 0.25% Triton X-100, 2% normal goat serum for ~48 hr (2 nights) at 4°C. Brains were rinsed once then washed in PBT at room temperature 6 times for 15 min. Brains were equilibrated overnight in Vectashield (Vector Laboratories H-1000) and were mounted in Vectashield. The following primary antibodies were used: anti-Brp/nc82 (mouse; 1:50, Developmental Studies Hybridoma Bank – see below) and/or anti-GFP (rabbit: 1:10,000; Life Technologies A-11122). The secondary antibodies used in all experiments were anti-mouse-Cy5 (1:250; Life Technologies A-10524) and anti-rabbit-Alexa Fluor 488 (1:500; Life Technologies A-11034).

Purification of nc82/Brp monoclonal antibody

Hybridoma cells expressing monoclonal antibody nc82 (Antibody Registry ID: AB_2314866), which recognizes the *Drosophila melanogaster* Brp protein (Wagh et al., 2006) developed by Erich Buchner were obtained from the Developmental Studies Hybridoma Bank, created by the NICHD of the NIH and maintained at The University of Iowa, Department of Biology, Iowa City, IA 52242. Frances Weis-Garcia and the members of the MSKCC Antibody and Bioresource Core Facility subsequently used these hybridoma cells to purify this monoclonal antibody. The hybridoma was adapted to Gibco™ Hybridoma-SFM (Cat # 12045084) and 1% fetal bovine serum prescreened

for ultra-low levels of bovine Ig. Antibody expression was confirmed and the adapted hybridoma was inoculated into the cell compartment of the Corning™ CELLine Disposable Bioreactor (Cat # 353137) in 15 ml of Hybridoma-SFM + 0.5% fetal bovine serum (production media) at 3 million viable cells / ml. The media compartment of the flask contained 350 ml of production media. The bioreactor was incubated at 37°C with 7% CO_2 for 3 days, at which time the cells and media containing nc82 were harvested. 30 million viable cells from the harvest were re-inoculated back into the cell compartment in 30 ml fresh production media. The media in the media compartment was replaced the following day with 650 ml production media. Three days later, the media in the media compartment was replaced with 1,000 ml production media, with the next harvest 3 days later (7 days after the previous harvest). Cells were harvested weekly and fed bi-weekly until the desired amount of monoclonal antibody was reached. After the first harvest, each one contained about 3 mg of monoclonal antibody nc82/ml production media. The harvests to be purified were pooled, centrifuged at 12,855 x g for 15 min. 6.5 mg / run were loaded onto a Cytiva (formerly GE Life Sciences) 1 ml HiTrap Protein G HP antibody purification column (Cat # 29048581) at 1 ml / min. The column was then washed with 0.02 M Sodium Phosphate (pH 7.0) before the monoclonal antibody was eluted with 0.1 M Glycine-HCl (pH 2.7). One ml fractions were collected and immediately neutralized with 60 ml of 1.0 M Tris-HCl (pH 9.0). The harvest, flow through and fractions from the peak were run on an a 10% SDS-PAGE (Bio-Rad Cat # 345-0010) to confirm purity and determine which should be pooled. The pooled fractions of monoclonal antibody were dialyzed into PBS overnight using dialysis tubing (Spectrum™ 132544) with a 50 kDa MWCO. Another 10% SDS-PAGE was run, and the

concentration determined using the absorbance at 280 using an extinction coefficient of 1.43.

Antennal lobe confocal imaging

All brains were imaged using a Zeiss Inverted LSM 880 laser scanning confocal microscope with a 25x / 0.8 NA immersion-corrected objective unless otherwise noted. Glycerol was used as the immersion medium to most closely match the refractive index of the mounting medium Vectashield. Antennal lobes in Figure 2.2, 2.4, 2.5, 3.2, 3.4, 6.1 were imaged at either 1024 x 1024 or 2048 x 2048 pixel resolution in X and Y with 0.5 µm Z-steps for a final voxel size of either 0.0615 x 0.0615 x 0.5 μm^3 or 0.1230 x 0.1230 x 0.5 μm^3. Both conditions oversampled relative to the objective resolution and no differences were noted between imaging conditions. The laser intensity and gain were adjusted along the Z-axis to account for a loss of intensity due to depth and care was taken to avoid saturation and ensure that the deepest glomeruli were visible for segmentation. *3xP3* was used as a promoter to express fluorescent proteins as markers for the knock-ins and *QUAS* transgenes used in this study, and care was taken to distinguish expression derived from the *3XP3* promoter from the expression of the QF2 driver and *QUAS* effector lines under investigation. *3xP3* drives expression in the optic lobes, as well as some cells in the dorsal brain. Neither area overlaps with the antennal lobes, and as reported previously (Matthews *et al.*, 2019), we saw no *3xP3*-driven expression in the antennal lobes in the reporter lines alone (data not shown). Representative antennal lobe images presented in the figures were cropped to remove *3xP3*-driven expression elsewhere in the brain.

Antennal lobe glomerulus quantification

Confocal images of the antennal lobes in Figure 2.2, 2.4, 2.5, 3.2, 3.4, 6.1 were processed in ImageJ/FIJI (Curley et al.). The number of glomeruli was quantified as follows: a single region of interest (ROI) was manually drawn around each glomerulus at a section approximately central along the Z-axis. Every glomerulus was outlined and an ROI set was collected that contained the outlines of all glomeruli. Glomeruli were then separated into two groups, GFP-positive and GFP-negative glomeruli. A count of each was made to determine the number of glomeruli labeled by each line as well as the total number of glomeruli. The ROIs were flattened along the Z-axis to enable representation of the data in two dimensions in Figure 2.4, 2.5, 3.3. The left antennal lobe in 3 brains was analyzed for each genotype in Figure 2.4 except for *Gr3*, for which the left antennal lobe was analyzed in 1 brain, and both left and right antennal lobes were analyzed in an additional 4 brains in Figure 2.5. Although we were able to recognize general regions of the antennal lobe, the interindividual variability made it impossible to identify most glomeruli by shape alone. We therefore have not attempted to name and number every glomerulus in *Ae. aegypti* as has been done in previous studies (Ignell *et al.*, 2005; Shankar and McMeniman, 2020). As noted by Ito et al. (Ito et al., 2014), there is considerable confusion about the use of coordinate axes in the brains of animals in general and insects in particular. The glomeruli in the antennal lobe of *Ae. aegypti* were originally named by Ignell et al. (Ignell *et al.*, 2005) using a set of coordinate axes that differ from those consistently used in *Drosophila melanogaster* (Couto *et al.*, 2005; Fishilevich and Vosshall, 2005; Grabe *et al.*, 2015; Laissue *et al.*, 1999; Stocker *et al.*,

1990a). A recent study of the antennal lobe of *Ae. aegypti* renamed glomeruli to account for this discrepancy in coordinate axes (Shankar and McMeniman, 2020), and throughout this paper we use the same coordinate axes they have implemented. While Shankar and McMeniman renamed most antennal lobe regions and glomeruli, they chose not to rename the MD (Medio-Dorsal) cluster of glomeruli comprising MD1, MD2, and MD3 whose sensory input derives from the maxillary palp. We have observed in our study that the MD glomeruli are medial, but they are not notably dorsal, and therefore refer to them as Glomerulus 1, Glomerulus 2, and Glomerulus 3 in this paper for simplicity. While there is utility in naming glomeruli, we suspect that the *Ae. aegypti* mosquito antennal lobe atlas will be refined in the future with the advent of new genetic tools that will unambiguously allow the field to distinguish and name genetically identifiable glomeruli. We found that the size, shape, and number of antennal lobe glomeruli in *Ae. aegypti* was variable from animal to animal. It is possible that the boundaries between glomeruli are not easily distinguished by synaptic staining and that specific glomeruli will become identifiable once there are genetic tools available that label smaller populations of olfactory sensory neurons. The anatomical variability we see is consistent with both the original map that identified 50 glomeruli (Ignell *et al.*, 2005), which divided glomeruli into 3 classes based on their variability in location, as well as a recent study that looked specifically at the size and shape of glomeruli across animals (Shankar and McMeniman, 2020) and revised the original map to a count of ~80 glomeruli. Shankar and McMeniman named and numbered these glomeruli across animals, but they noted that they were only able to consistently identify 63 glomeruli. This is similar to the ~65 glomeruli we observed in our work. While there is not yet a

clear consensus on the exact number of antennal lobe glomeruli in *Ae. aegypti*, the number of chemosensory receptors expressed in the antenna and maxillary palp is at least twice as large as any of the estimates of glomerulus number. The variability in antennal lobe structure appears at first to contrast with *Drosophila melanogaster*, where each glomerulus can be clearly identified and named. However, we note that the antennal lobe map in *Drosophila melanogaster* has been refined with the advent of new genetic techniques, starting with 35 glomeruli in the original atlas (Stocker *et al.*, 1990a), then modified to 40 glomeruli (Laissue *et al.*, 1999), and further refined in numerous studies (Couto *et al.*, 2005; Fishilevich and Vosshall, 2005; Tanaka *et al.*, 2012) including a recent count of 54 (Grabe *et al.*, 2015) and 58 (Task *et al.*, 2020) glomeruli. We have refrained from naming glomeruli in *Ae. aegypti* at this time because we believe that a more stereotyped arrangement will emerge as new genetic lines are generated that allow cell-type-specific labelling. A recent study in the mosquito *Anopheles gambiae* using mosquitoes that label *Orco*-expressing olfactory neurons also noted that the antennal lobe was variable between animals relative to *Drosophila melanogaster* (Riabinina *et al.*, 2016). It is therefore possible that mosquito antennal lobes are more variable than Drosophilids (Grabe *et al.*, 2015; Prieto-Godino *et al.*, 2017). Variability in olfactory bulb structure is seen even in the mouse, *Mus musculus,* where the principles of olfactory organization were first established (Schaefer *et al.*, 2001; Strotmann *et al.*, 2000; Zou *et al.*, 2009). The exact size and location of glomeruli can vary between animals more than initially appreciated and appears to be determined by both genetic factors and activity in olfactory sensory neurons during the early life of the animal. In *Drosophila melanogaster*, glomerulus size is highly genetically determined and

correlates strongly with the number of olfactory sensory neurons that innervates each glomerulus (Grabe *et al.*, 2015). Whether the variability in glomerulus size in the mosquito is due to activity-dependent changes in structure or other factors remains to be seen.

Additional technical notes on expression and projection patterns of Split-QF2 strains

Ir25a-QF2-AD,Orco-QF2-DBD > QUAS-dTomato-T2A-GCaMP6s: All antennal lobe immunostaining in Figure 3.2, 3.4, was carried out as described above with slight modifications to utilize the *15xQUAS-dTomato-T2A-GCaMP6s* effector line. The same primary antibodies were used because of the structural similarity between GCaMP6s and GFP. Intrinsic dTomato was detected without antibody amplification, as it retained fluorescence throughout fixation and staining. Brp (Cy5), dTomato, and GCaMP6s (Alexa Fluor 488) were imaged as three separate confocal channels as described above. Glomeruli labelled by dTomato completely overlapped with those labelled by GCaMP6s immunofluorescence, so both channels were used during the quantification of positive and negative glomeruli. dTomato labeling was used to generate sample images. There was no staining in the antennal lobes of the individual split effector lines crossed to *15xQUAS-dTomato-T2A-GCaMP6s* (n=3 / genotype, Figure 3.2). Due to an initial observation that certain glomeruli were consistently unlabeled in the *Ir25a-AD;Orco-DBD* line but were labelled in the *Orco-QF2* and *IR25a-QF2* lines, particularly in an anterior region of the brain, we conducted a second experiment to compare glomeruli labelled by the *Orco-QF2, IR25a-QF2* and *IR25a-AD;Orco-DBD* drivers side-

by-side. All drivers were crossed to the *15xQUAS-dTomato-T2A-GCaMP6s* effector (Figure 3.4). 3 brains per genotype were immunostained and imaged as described above.

Antennal lobe anterograde dye fill

For images in Figure 2.2, mosquitoes were anesthetized on ice until immobile and then transferred to a cold dissection dish. A single antenna or maxillary palp was loaded with Texas-red conjugated dextran (Molecular Probes D3328) diluted 10 mg in 100 µL external saline (103 mM NaCl, 3 mM KCl, 5 mM 2-[Tris(hydroxymethyl)methyl]-2-aminoethanesulfonic acid (TES), 1.5 mM $CaCl_2$, 4 mM $MgCl_2$, 26 mM $NaHCO_3$, 1 mM NaH_2PO_4, 10 mM trehalose, 10 mM glucose, pH 7.3, osmolality adjusted to 275 mOsm/kg). To load the dye a small drop (approximately 0.5-1 µL) of dye was placed onto the surface of the dish and the animal was moved such that the intended cut-site on a single antenna or maxillary palp was placed in the drop of dye. The antenna or maxillary palp was then removed with sharp forceps and a fine scalpel (F.S.T 10315-12) while it was submerged in the dye. Care was taken to remove the maxillary palp proximal to the 4^{th} segment, to include all the basiconic sensilla, and to remove the antenna near the base but to leave the antennal pedicel completely intact. The animal remained immobile on ice with the antenna or maxillary palp submerged and the dye was loaded for 2-5 min. After this time the animal was placed in a small soup cup with access to 10% sucrose and returned to standard rearing conditions overnight to give the dye time to diffuse throughout the neurons and fill the length of the axon. The next

morning dissection of adult brains and immunostaining was carried out as described above.

Antennal lobe 3-D reconstructions

In an attempt to develop a map of the *Ae. aegypti* antennal lobe, 3 brains from the Liverpool strain were immunolabeled with Brp to identify the boundaries between antennal lobe glomeruli. The left antennal lobe in each brain was independently reconstructed from confocal sections taken with a Plan-Apochromat 63x/1.40NA oil immersion objective, at 1024 x 1024 pixel resolution in X and Y with 0.5 µm Z-steps for a final voxel size of either 0.1318 x 0.1318 x 0.5 μm^3 using the software Imaris (Bitplane). Although the area previously termed Johnston's organ center was considered a single glomerulus in a previous study (Ignell *et al.*, 2005), we noted anatomical boundaries in this region, suggesting that it contains multiple glomeruli. This observation is consistent with recently published work (Shankar and McMeniman, 2020) and this area was segmented by an individual researcher to generate the final reconstructions. Two of these are shown in Figure 2.2. Each glomerulus was manually segmented into an individual surface using Surpass View. We were consistently able to identify the three glomeruli innervated by the maxillary palp, previously termed MD1, MD2 and MD3 (Ignell *et al.*, 2005) which we refer to in this study as Glomerulus 1, Glomerulus 2, and Glomerulus 3 (Figure 2.2, Figure 6.1). The overall structure of the antennal lobe varied considerably from animal to animal and although we were able to identify certain regions and certain landmark glomeruli including those that are targeted by the maxillary palp, we were unable to assign an unambiguous identity to every

glomerulus, as is possible in *Drosophila melanogaster* (Couto *et al.*, 2005; Fishilevich and Vosshall, 2005). This variability makes it essentially impossible to identify a given glomerulus between animals and we therefore have decided to avoid referring to glomeruli by previous naming schemes, including MD1, MD2, MD3. An authoritative atlas of the *Ae. aegypti* antennal lobe awaits genetic reagents that label subpopulations of sensory neurons that will permit the field to refer to glomeruli by their molecular identity.

Antennal whole mount immunofluorescence

Whole-mount immunostaining of adult antennae was performed as described (Riabinina *et al.*, 2016) with modifications. 7-11 day-old Liverpool mosquitoes were immobilized on ice, decapitated and heads and placed in 1 mL ZnFA fixative solution (0.25% $ZnCl_2$, 2% paraformaldehyde, 135 mM NaCl, 1.2% sucrose and 0.03% Triton X-100) for 20–24 h at room temperature in the dark. Next, the heads were washed three times for 30 min each with HBS buffer (150 mM NaCl, 5 mM KCl, 25 mM sucrose, 10 mM HEPES, 5 mM $CaCl_2$ and 0.03% Triton X-100). Antennae were carefully removed in HBS on ice and placed in 400 µL HBS in 0.5 mL Eppendorf tubes. After a brief wash in HBS, the tissue was incubated in 400 µL 80% methanol/20% dimethyl sulfoxide (DMSO) solution for 1 h at room temperature, washed for 5 min in 400 µL 0.1 M Tris pH 7.4, 0.03% Triton X-100 solution and incubated in 400 µL blocking solution (PBS, 5% normal goat serum (Jackson 005-000-121), 1% DMSO and 0.3% Triton X-100) for at least 3 h at room temperature or overnight at 4^{o}C. Next, the tissue was placed in a 0.5 mL Eppendorf tubes containing 400 µL blocking solution with primary antibodies [rabbit anti-Orco EC2

(Larsson *et al.*, 2004), 1:50, Vosshall lab; chicken anti-GFP,1:200, Aves GFP-1020] and submerged and held in a water bath sonicator (Branson m1800) for 30 sec at the high setting. Next, the tubes were placed on a rotator for 2 days at 4^{o}C in the dark, after which the sonication procedure was repeated. The tubes were placed on a rotator for 2 additional days (for a total of 4 days) at 4^{o}C in the dark. Next, the tissue was washed 5X 30 min each at room temperature in PBS, 1% DMSO and 0.3% Triton X-100. Secondary antibodies (anti-rabbit Alexa Fluor 555 Plus, 1:200, Thermo Fisher A-32732, anti-chicken Alexa Fluor 488, 1:200, Thermo Fisher A-11039) and nuclear dye (TO PRO 3 Iodide, 1:400, Thermo Fisher T3605) were added to the blocking solution, and tubes were sonicated as described above and incubated for 4 days at 4^{o}C in the dark with the sonication repeated after 2 days of incubation. The tissue was then washed 5X 30 min at room temperature in PBS, 1% DMSO and 0.3% Triton X-100, rinsed in PBS and mounted in Slow Fade Diamond for confocal imaging.

Whole mount antennal and maxillary palp RNA *in situ* hybridization

RNA was detected in whole mount antenna and maxillary palp using the hybridization chain reaction (HCR) technique as previously described (Choi *et al.*, 2018) with modifications. Probes, amplifiers, Probe Hybridization Buffer, Amplification Buffer, and Probe Wash Buffer were purchased from Molecular Instruments. 5-8 day-old Liverpool mosquitoes were cold anesthetized, manually decapitated with forceps, and heads with antennae and the proboscis were digested in a chitinase-chymotrypsin solution (119 mM NaCl, 48 mM KCl, 2 mM $CaCl_2$, 2 mM $MgCl_2$, 25 mM HEPES, 5 U/mL chitinase (Sigma-Aldrich C6137-50UN), 100 U/mL alpha-chymotrypsin (Sigma-Aldrich CHY5S-

10VL), 2% DMSO) (Manning and Doe, 2017) at 37°C for 30 min (antennae) or 1 hr (maxillary palps) in a Fisher Isotemp oven and subsequently fixed in 4% paraformaldehyde, 1X PBS, 0.03% Triton X-100 on a rotator at 4°C overnight. Heads were washed 4 times on ice for 10 min each in 0.1% PBS-Tween-20. Antennae or maxillary palps were dissected in 0.1% PBS-Tween-20 on ice and dehydrated with a graded series of methanol/0.1% PBS-Tween: 25% methanol in 0.1% PBS-Tween-20 for 10 min on ice, 50% methanol in 0.1% PBS-Tween-20 for 10 min on ice, 75% methanol in 0.1% PBS-Tween-20 for 10 min on ice, and two washes of 100% methanol for 10 min on ice. Tissues were incubated overnight in 100% methanol at -20°C and were subsequently rehydrated with a series of graded methanol/0.1% PBS-Tween-20: 75% methanol in 0.1% PBS-Tween-20 for 10 min on ice, 50% methanol in 0.1% PBS-Tween-20 for 10 min on ice, 25% methanol in 0.1% PBS-Tween-20 for 10 min on ice, and two washes of 0.1% PBS-Tween-20 for 10 min each on ice. Tissue was digested in 20 µg/mL Proteinase-K (Thermo Fisher AM2548) in 0.1% PBS-Tween for 30 min at room temperature and washed twice with 0.1% PBS-Tween-20 for 10 min each at room temperature. Tissue was fixed in 4% paraformaldehyde in 0.1% PBS-Tween-20 for 20 min at room temperature and washed 3 times for 10 min each in 0.1% PBS-Tween-20 at room temperature. Tissue was incubated in Probe Hybridization Buffer at room temperature for 5 min and then in 37°C pre-warmed Probe Hybridization Buffer rotating in a hybridization oven for 30 min. 8 pmol of each probe set was prepared in 37°C pre-warmed Probe Hybridization Buffer and tissue was incubated in probe solution at 37°C in a hybridization oven for 2 nights. Tissues were washed in 37°C pre-warmed Probe Wash Buffer 5 times for 10 min each at 37°C. Tissues were washed twice in 5X SSC

0.1% Tween-20 at room temperature for 10 min each. Tissues were pre-amplified in room temperature Amplification Buffer for 10 min. 18 pmol hairpins were separately prepared by heating 6 µl of 3 µM stock of hairpins H1 and H2 at 95^{o}C for 90 sec on an Eppendorf Mastercycler and allowing to cool to room temperature in a dark drawer for 30 min. Hairpins were resuspended in 100 µl amplification buffer and tissues were incubated in this hairpin solution in the dark on a rotator at room temperature overnight. Tissues were washed 5 times for 10 min each in 5X SSC 0.1% Tween-20 and mounted in SlowFade Diamond (Thermo Fisher S36972) on glass slides with coverslips for confocal imaging.

Whole mount antennal and maxillary palp dTomato visualization

7-14 day-old *Ir25a-QF2*, *Orco-QF2*, *Ir25a-QF2AD*, *Orco-QFDBD*, and *Ir25a-QF2AD,Orco-QFDBD > 15XQUAS-dTomato-T2A-GCaMP6s* mosquitoes were cold anesthetized, manually decapitated with forceps and heads with antennae and maxillary palps were immediately fixed in 1 mL 4% paraformaldehyde, 1X PBS, 0.03% Triton X-100, on a rotator in the dark at 4^{o}C overnight. Heads were washed 3X 30 min each in 1X PBS, 0.03% Triton X-100 at room temperature, then antennae and maxillary palps were carefully removed and placed in 1X PBS, 0.03% Triton X-100. Next, antennae and maxillary palps were placed in a solution of 1X PBS, 0.03% Triton X-100, 1% DMSO, and a 1:400 dilution of TO PRO 3 (Thermo Fisher T3605) for 24 hr at 4^{o}C in the dark. Antennae and maxillary palps were then washed 5X 30 min each in 1X PBS, 0.03% Triton X-100 at room temperature in the dark, washed once with 1X PBS, transferred to

a well of SlowFade diamond to remove excess PBS, and mounted in SlowFade Diamond for confocal imaging.

Antennal and maxillary palp confocal imaging and cell quantification

Images of peripheral tissues were acquired with a Zeiss Axio Observer Z1 Inverted LSM 880 NLO laser scanning confocal microscope (Zeiss) with a 25x/0.8 NA or 63x/1.4 NA immersion-corrected objective at a resolution of 3096 x 3096 pixels or 2048 x 2048 pixels. When comparing dTomato fluorescence across genotypes, image acquisition parameters were kept consistent. When necessary, tiled images were stitched with 20% overlap. Confocal images were processed in ImageJ (Curley *et al.*). Because the antenna is a cylindrical structure, when whole antennal segments are mounted on a slide and imaged on a confocal microscope, signal can be easily detected from the region closest to the coverslip and confocal objective, but signal is weaker when imaging the side further from the coverslip and objective. For the purposes of consistent quantification, we only quantified cell numbers from the region closest to the coverslip (orange region in Figure 4.1). For quantifying expression in the maxillary palp, only the dorso-lateral region of the 4th maxillary palp segment was analyzed. (yellow region in Figure 5.3). Quantification of co-expression in antennae and maxillary palps was done in ImageJ (Curley *et al.*) using the Cell Counter plugin. Cells in each channel were manually marked independently of the signal in the other channels. After cells in each channel are marked, and markers were then merged. Cells that were labeled with multiple markers (co-expressing cells) were then marked with a third marker. Cell counts were then imported into Microsoft Excel and R for analysis.

In vivo 2-photon GCaMP calcium imaging preparation

Calcium imaging was performed on an Ultima IV two-photon laser-scanning microscope (Bruker Nanosystems) equipped with galvanometers and illuminated by a Chameleon Ultra II Ti:Sapphire laser (Coherent). GaAsP photomultiplier tubes (Hamamatsu) were used to collect emitted fluorescence. Images were acquired with a 60X/1.0N.A. Long Working Distance Water-Immersion Objective (Olympus) at a resolution of 256 x 256 pixels. GCaMP6s was expressed via the *Ir25a-QF2* knock-in which labels all three maxillary palp glomeruli. Preliminary imaging studies were conducted in animals that were wild type at the *Gr3* locus. For 2-photon experiments, *Gr3+/-* and *Gr3-/-* animals were reared and imaged in parallel. Because the *Gr3* mutants were generated in the Orlando wild-type background and all Q-system lines were generated in the Liverpool wild-type background, care was taken to compensate for background effects in the following way. A single stock was created containing the *15x-QUAS-dTomato-T2A-GCamP6s-3xP3-ECFP* transgene (Matthews *et al.*, 2019), the *Ir25a-QF2-3xP3-dsRed* gene-sparing knock-in, and the $Gr3^{ECFP}$ knock-out allele that is marked with ECFP (McMeniman *et al.*, 2014). This parental line was then crossed to either the unmarked $Gr3^{\Delta 4}$ mutant that is in the Orlando background (McMeniman *et al.*, 2014) to generate *Gr3-/-* animals, or to wild-type Orlando to generate *Gr3+/-* animals. The *Gr3* mutation is recessive (McMeniman *et al.*, 2014), so this comparison of heteroallelic and heterozygous animals both controls for genetic background and makes it possible to assay the *Gr3* mutant phenotype. Calcium imaging experiments were performed on 7-14 day-old female mosquitoes. Mosquitoes were fed on 10% sucrose and switched to

water overnight prior to imaging. Mosquitoes were anesthetized at 4°C for dissection. The mosquito was fixed to a custom Delrin plastic holder with UV-curable glue (Bondic). The mosquito was inserted into a hole in the holder, such that the head and thorax were exposed above the surface of the holder, with the rest of the mosquito below. The mosquito was secured with a few points of glue (Bondic) on the thorax and head. The antennae and maxillary palp remained below the plate and were kept free of saline to prevent damage to the tissue. The top of the dish was then filled with external saline, which is based on *Drosophila melanogaster* imaging saline (Fişek and Wilson, 2014) with the following composition: 103 mM NaCl, 3 mM KCl, 5 mM 2-[Tris(hydroxymethyl)methyl]-2-aminoethanesulfonic acid (TES), 1.5 mM $CaCl_2$, 4 mM $MgCl_2$, 26 mM $NaHCO_3$, 1 mM NaH_2PO_4, 10 mM trehalose, 10 mM glucose, pH 7.3, osmolality adjusted to 275 mOsm/kg). A small window was gently opened in the head and the cuticle was removed anterior to the antennal pedicles and the tissue was secured with dental wax to expose the antennal lobes. Opaque non-neural tissue, primarily fat cells, was removed if they obstructed the antennal lobes. Great care was taken not to damage the antennal nerves. The preparation was placed on a custom laser cut acrylic holder that was secured to the stage and placed the mosquito in close proximity to the output port of the olfactometer. Plans for the fabrication of the imaging holder are available on Github: https://github.com/VosshallLab/Younger_Herre_Vosshall2020. On rare occasions mosquitoes showed no movement or odor responses and were discarded. Image volumes were taken at higher resolution to identify glomeruli innervated by the maxillary palp, including the nerves that innervate these glomeruli. Glomerulus 1 was always

easily identifiable by eye. A single plane through the center of each glomerulus was scanned at 4.22 frames per second with a 920 nm excitation wavelength imaged through a 680 nm shortpass infrared (IR) blocking filter, a 565 nm longpass dichroic and 595/50 nm or 525/70 nm bandpass filters. GCaMP6s and dTomato emission was collected simultaneously for at least 70 frames per trial.

In vivo 2-photon GCaMP calcium imaging stimulus delivery

Odor stimulation was achieved by directing a continuous stream (400-800 mL/min) of clean air, originating from a breathing air tank (Praxair), through 0.125 inch inner diameter/0.250 inch outer diameter perfluoroalkoxy alkaline (PFA) tubing. The antenna and maxillary palp of the mosquitoes were positioned close to the tube such that they were exposed to constant air flow (carrier stream). 4-60% of the total airstream was diverted through the headspace of a 20 mL borosilicate glass vial (EnviroWare #03-339-14E) containing the odorant diluted in either paraffin oil or water (odor stream). At a trigger, a custom-built solenoid valve controller system redirected the odor stream from a blank vial to a vial containing various odorants diluted in paraffin oil or water to a final volume of 3 mL. Unless otherwise noted, 40% of the airstream was used for odor delivery. Prior to conducting experiments, a mini-PID (Aurora Scientific, model 201A) was used to measure odorant waveforms and ensure the consistency of odor presentations across trials. CO_2 was introduced into this system from a tank of 5% CO_2 in a 20.9% oxygen/ 79.1% nitrogen balance (Praxair). At a trigger, CO_2 was diverted through the headspace of a second clean 20 mL borosilicate glass vial (CO_2 stream) that was redirected from a bypass stream into the system. This was coupled to a clean

airstream with a matched flow rate that was simultaneously removed from the system. In experiments where odor concentration of CO_2 concentration was varied, the fraction of odor stream directed to the mosquito was adjusted. CO_2 was delivered at 4-60% of the total airstream for total concentrations of 0.2- 3.0% CO_2. For 2-photon imaging experiments, a final concentration of 2% CO2 was used in all experiments. Prior to conducting experiments, a CO_2 meter (Vaisala GM70) was used to measure CO_2 concentration in the final airstream and we found that the expected concentration was delivered. Odor and CO_2 delivery was controlled using custom software written in Matlab R2020a (MathWorks). The odor delivery system and software was based on a previously used system and updated for CO_2 delivery (Cohn et al., 2015). After the mosquito was transferred to the microscope and placed within the airstream, there was a 10-min acclimation period before any imaging began. For each trial, 5 sec of GCaMP6s fluorescence at baseline was imaged and then a one second odor or CO_2 pulse was delivered while imaging continued for at least 10 more sec (at least 70 frames total). There was a one-min delay between imaging trials so that the mosquito could reacclimate to the airstream after exposure to each odor. In an initial experiment we did not see any change in the amplitude of the CO_2 response across multiple trials within an animal. Imaging remained stable during the duration of the imaging session in all animals that were included in this study. We did not notice a decrease in the response to stimuli over time. Odorants were selected for the highest purity available for purchase (greater than 98%) and were either diluted in MilliQ ultrapure water (resistance 18 megaohm) or paraffin oil (EMD Millipore #PX0045-3) depending on solubility. All odorants were diluted into a large stock solution that was used throughout

each entire experiment to avoid variability in concentrations. The odorants used in 2-photon experiments were: R-(-)-1-octen-3-ol (PubChem CID: 6992244, Penta Manufacturing 15-18900) diluted 1:10 in paraffin oil; 3-octanone (PubChem CID: 246782, Sigma 136913) diluted 1:10 in paraffin oil; acetone (PubChem CID: 180 Sigma A4206) diluted to 5%v/v in MilliQ ultrapure water; ammonia (PubChem CID: 222, Suprapur, Supelco 105428) diluted to 2.5% v/v in MilliQ ultrapure water; hexyl amine (PubChem CID: 8102, Sigma 219703) diluted to 1% v/v in MilliQ ultrapure water; triethyl amine (PubChem CID: 1146, Sigma T0886) diluted to 1% v/v in MilliQ ultrapure water.

In vivo 2-photon GCaMP calcium imaging data analysis

All image processing was done using FIJI/ImageJ (Curley *et al.*). Data analysis used Matlab R2020a (MathWorks), Excel (Microsoft), and Prism (GraphPad). Regions of interest were selected based on the dTomato fluorescence intensity and GCaMP6s was normalized to dTomato intensity for analysis. A Gaussian blur with a sigma value of 1 was performed on the GCaMP6s signal. In the calculation of ΔF/F, six frames were averaged before stimulus presentation to determine the baseline fluorescence. To determine maximum ΔF/F, the average of the maximum 3 frames at the peak after stimulus delivery was determined for each sweep.

Quattroport olfactometer behavioral assays

Mosquitoes that were blood fed for behavior were fed on warmed defibrinated sheep's blood (Hemostat Laboratories DSB100) through a parafilm membrane. Animals were sorted by eye to determine if they were blood fed by looking at engorgement of the

abdomen, and non-fed animals were not used in subsequent behavior assays. Blood-fed animals were returned to the same rearing conditions as their non-blood-fed counterparts, and behavior was assayed ~48 hr after they had consumed a blood meal. Quattroport olfactometer experiments were conducted as previously described (Basrur *et al.*, 2020) with modifications to enable the delivery of monomolecular odorants. Details of fabrication and operation of the Quattroport are available at https://github.com/VosshallLab/Basrur_Vosshall2020. All behavioral experiments were carried out in an environmental room set to 25 – 28^{o}C, 70-80% relative humidity, and were carried out between ZT3-14. Trials with identical stimuli were interspersed throughout experimental days to control for circadian rhythm fluctuations. Mosquitoes in the Quattroport began each trial in a start canister, flew through a flight tube, and, if they were attracted to a stimulus, into a trap proximal to the stimulus. Filtered air, with or without additional CO_2, was pumped through the stimulus box and into the flying tube. Mosquitoes were prevented from contacting the stimulus by a mesh barrier, and adjustable gates between each chamber allow the experimenter to count the number of mosquitoes in each compartment. The night before each experiment, approximately 20 7-22 days old mosquitoes were cold-anesthetized and placed in each canister. They were sugar-starved with access to water overnight. The next day, at the start of each trial a set of 4 canisters was attached to the Quattroport and mosquitoes were given 10 min to acclimate with filtered air flowing at the 25 mm setting on the flowmeter throughout the assay (see https://github.com/VosshallLab/Basrur_Vosshall2020 for details on filtered air and CO_2 flowmeter settings). They were then exposed to the stimulus with or without added CO_2 flowing at the 50 mm flowmeter setting for 30 sec,

after which they were given access to the flying tube and attraction trap for 5 min in the continued presence of filtered air with or without added CO_2 and the stimulus. At the end of the trial, the gates enclosing the start canister and the attraction trap were closed, and mosquitoes that remained in the start canister, entered the flying tube, or flew into the attraction trap were counted. For live human host-seeking assays, a single human volunteer placed their forearm in the stimulus box. For the delivery of lactic acid and triethyl amine, the odorant solutions were delivered using 35 mm Petri dishes (Fisher Scientific #08-757-100A) placed within the airstream in the stimulus box. The odorants used in this assay were L-(+)-Lactic acid solution, 88-92% (PubChem CID: 107689, Sigma-Aldrich #27714-500mL) and Triethyl amine (PubChem CID: 1146, Sigma T0886) diluted to 1% v/v in MilliQ ultrapure water. In cases where both odorants were used as a stimulus, care was taken not to mix the liquids when they were placed in the stimulus box. Different volumes of each liquid odorant were delivered to generate the dose response curves in Figure 7.5. Depending on the experiment, between 1 µL and 2 mL of liquid odorant was used. When less than 1 mL of liquid was used, the lid of the Petri dish was inverted, and the liquid odorant was pipetted onto the center of the inverted lid. The inverted lid was then placed on the bottom of the Petri dish, which elevated it slightly, placing the odorants in the path of the airstream that ran through the stimulus box. When 1 mL or greater of liquid was used, the liquid odorant was pipetted into the base of the Petri dish, which was set atop the inverted lid of the Petri dish to elevate it. If the volume of odor was 1 mL or greater for either odorant, they were delivered using 2 separate Petri dishes to avoid possible mixing. If the volume of each liquid was less than 1 mL, both liquid odorants were delivered as separated drops of

liquid on a single inverted Petri dish lid, and the drops remained sperate because of surface tension. When neither lactic acid nor triethyl amine was delivered, an empty Petri dish was placed inside the stimulus box to serve as a control for any odors that might be emitted by the dish itself and/or any perturbations in air flow introduced by the presence of the Petri dish lid and base.

CHAPTER 9. APPENDIX

How is host-seeking behavior regulated after a blood-meal? A female mosquito's host-seeking drive becomes profoundly suppressed for 3-4 days following ingestion of a blood-meal, but the regulatory mechanisms that govern this dramatic, long-timescale change in behavior are not fully characterized (Duvall et al., 2019; Klowden and Lea, 1979; Liesch et al., 2013). The data presented in this Appendix are suggestive of the exciting possibility that the steroid hormone ecdysone may act on olfactory neurons to regulate host-seeking behavior post-blood-meal. However, because these results were dependent on administration of non-physiological doses of a steroid hormone without necessary genetic or pharmacologic controls, at present this phenomenon cannot be confirmed. Further, ecdysone and its receptor, the ecdysone receptor, are required for development, which made generating reagents and manipulating these pathways challenging in adult mosquitoes. I show these data with the hope that they could inform further studies on how endogenous reproductive hormones may affect host-seeking behavior when the experimental toolkit in *Ae. aegypti* is expanded to enable temporal and cell-type-specific manipulation of developmentally required genes.

9.1 An *Ae. aegypti* reproductive hormone may regulate post-blood-meal host-seeking behavior

Insects rely on their sense of smell for all aspects of survival: feeding, mating, and reproduction (Li and Liberles, 2015). Olfaction plays a particularly important role in the

host-seeking behavior of many blood-feeding insects, including the mosquito *Aedes aegypti*, a vector of arboviruses including Zika, chikungunya, yellow fever, and dengue (Bhatt et al., 2013; Kotsakiozi et al., 2017; Kraemer et al., 2015). Female *Ae. aegypti* integrate cues such as CO_2, body heat, and body odor to efficiently locate and bite human hosts, and require a blood-meal to obtain protein to produce eggs (Allan et al., 1987; McMeniman et al., 2014). This potent host-seeking drive is not constant: following a blood meal the female suppresses her host-seeking drive until she lays her eggs 3-4 days later (Klowden, 1981; Liesch et al., 2013). Previous studies found a reduction in the sensitivity of olfactory sensory neurons to attractive odorants coincident with host-seeking suppression (Davis, 1974; Siju et al., 2010). However, the mechanisms that connect blood-feeding behavior and modulation of the olfactory system are unknown.

In invertebrates and mammals, hormones act as important mediators of state-dependent behaviors. Behavioral responses to external cues can change dramatically based on reproductive state (Yang and Shah, 2014), and reproductive hormones have been shown to modulate sensory perception across phyla. For example, female mice are more attracted to male pheromones during particular stages in their estrous cycle, a phenomenon modulated at the sensory neuron level by receptors for reproductive hormones (Dey et al., 2015). Older male *Drosophila* have a competitive courtship advantage over younger males because a reproductive hormone increases sensitivity of odorant receptors required for mating (Lin et al., 2016). A surge of androgens enables sexually mature male stickleback fish to be more sensitive to the color red, a cue of other male competitors, during their breeding season by regulating transcription of

opsins in the retina (Shao et al., 2014). These exciting studies highlight the diversity of contexts and mechanisms that reproductive hormones utilize to directly impact sensory neuron function and by extension, chemosensory behaviors.

The dramatic change in the host-seeking behavior program after a blood-meal in *Ae. aegypti* offers an ideal system to determine the pathways responsible for regulating olfactory sensory neuron activity. Clues to this pathway can be derived from blood-meal-induced physiological changes, because the internal state of an organism is known to influence its perception of external cues. In *Ae. aegypti* mosquitoes, the steroid hormone ecdysone is critical during development and for the adult reproductive cycle. In *Ae. aegypti* mosquitoes, the steroid hormone 20-hydroxyecdysone (20E) is critical during development and for the adult reproductive cycle. Shortly after ingestion of a blood-meal and during the period of host-seeking suppression, female *Ae. aegypti* mosquitoes secrete high levels of ecdysone from their ovaries into the hemolymph (Borovsky et al., 1986; Hagedorn et al., 1975). This hormone precursor is subsequently converted to its active metabolite, 20E, which promotes egg maturation (Hansen et al., 2014; Petryk et al., 2003). While 20E has predominantly been studied for its role in metamorphosis across arthropods (Beckstead et al., 2005; Champlin and Truman, 1998; Mello et al., 2014; Ventura et al., 2017; Warren et al., 2006; Yamanaka et al., 2013), it has also been implicated in several adult chemosensory behaviors including responses to sex pheromone in male *Agrotis ipsilon* moths (Bozzolan et al., 2015) and olfactory learning in *Apis mellifera* honeybees (Geddes et al., 2013). Further, work published in the early 1980's demonstrated that injection of 20E into non-fed *Anopheles gambiae* mosquitoes inhibits their biting behavior (Beach, 1979).

20E binds to the ecdysone receptor (EcR), a nuclear hormone receptor and ligand-dependent transcription factor (Johnston et al., 2011). To activate its transcriptional program, EcR forms a heterodimer with ultraspiracle (USP) upon binding 20E and subsequently translocates into the nucleus (Yao et al., 1992). The EcR-USP transcription factor binds to ecdysone response elements, enhancers composed of DNA motifs that are inverted or direct repeats (Yao et al., 1992). The ecdysone-responsive transcriptional network is vast and is mediated initially by the induction of ecdysone-responsive early genes, including *E75, E93, HR3*, and *Broad-Complex*, which are themselves transcription factors that can have activating or repressive effects on transcription of their downstream targets (Ekoka et al., 2021). In *Ae. aegypti*, two isoforms of EcR have been identified: EcR-A and EcR-B, which have identical DNA-binding domains and ligand binding domains but differ in the activation domains that determine their transcriptional interaction partners (Schwedes et al., 2011). As in *Drosophila melanogaster,* these isoforms are described to vary in function as well as spatiotemporal expression (Ekoka et al., 2021). For example, EcR-A is highly expressed in the fat body 12 to 24 hours post-blood-feeding, while EcR-B levels are higher in the fat body in the pre-blood-feeding state and in the post-egg-laying state (Ekoka *et al.*, 2021).

Critically, 20E and EcR have been demonstrated to be essential for development and reproduction across invertebrates, with knockout or knockdown of EcR or ecdysone biosynthesis genes resulting in abnormal larval development and failure of

metamorphosis to the pupal stage (Kozlova and Thummel, 2003; Ventura et al., 2017; Yamanaka *et al.*, 2013; Yan et al., 2016). Thus, most attention has been devoted to how this steroid hormone pathway coordinates developmental transitions.

When we embarked on this project to understand EcR and 20E's role in post-blood-meal regulation of host-seeking behavior, the lack of understanding of this steroid hormone's role in adult physiology was attractive to me. I had not considered the relative lack of studies on the role of ecdysone in adult invertebrates may be in part due to the challenging nature of manipulating genes required for development. Indeed, genetic tools routinely utilized to gain insight into expression and function of cell populations, such as Gal4 lines, do not exist for EcR or ecdysone biosynthesis genes in *Drosophila*, which could have been an early indicator that making complementary tools in *Aedes* would be extraordinarily difficult. However, we did make progress characterizing the effect of exogenous 20E on behavior, its expression pattern in central and peripheral nervous tissues, and its transcriptional footprint.

9.2 Identification of a transcriptional network in the *Ae. aegypti* brain modulated by blood-feeding state

The ability to locate and draw blood from human hosts is essential for female *Ae. aegypti* mosquitoes, which require this blood-meal to develop eggs. Female mosquitoes

are exquisitely equipped to find human hosts, and are strongly attracted to heat, human body odor, and carbon dioxide (McMeniman et al., 2014). However, this strong host-seeking drive is dramatically suppressed within 30 minutes following a blood-meal and remains suppressed for up to 72 hours, during which time eggs mature (Figure 10.1B). Suppression is released after egg-laying, and the cycle of blood-feeding, suppression, and egg-laying repeats (Figure 10.1A). Previous studies have found that factors secreted into the hemolymph, a circulating fluid analogous to blood in vertebrates, are sufficient to downregulate host-seeking behavior (Klowden and Lea, 1979). The identity of such factors and the physiological mechanism by which they direct sustained and reversible host-seeking suppression are unknown. Because host-seeking suppression can last several days after a blood-meal, the putative mechanism driving this behavioral change is inconsistent with more conventional mechanisms that act at shorter time scales, including immediate-early gene induction, alterations of synaptic release, and insertion or removal of receptors in neuronal membranes. Instead, we hypothesized that hemolymph factors trigger slower changes in brain gene expression that act in a global gene regulatory network to alter female mosquito behavior.

To address how gene regulatory networks could be affected by internal state changes, we used chromatin structure analysis as an entry point to identify the putative transcriptional network that responds to blood-feeding. Prior to this study, our lab carried out comprehensive RNA-sequencing analysis over the course of the female mosquito reproductive cycle and identified thousands of brain transcripts whose expression was modulated by blood-feeding (Matthews *et al.*, 2016). The sustained

timescale of host-seeking suppression led us to hypothesize that secreted factors regulated by the blood-meal act in the brain to trigger specific epigenetic changes in chromatin structure to induce a coordinated program of neuronal gene expression changes.

We characterized regulatory DNA sequences in the female mosquito brain using the Assay for Transposase-Accessible Chromatin Sequencing (ATAC-seq), which identifies regions of open chromatin and has been utilized to identify transcription factors integral to development, metastasis, and immune response (Buenrostro et al., 2013; Daugherty et al., 2016; Denny et al., 2016; Scott-Browne et al., 2016). ATAC-seq has been validated to consistently reproduce known regulatory region maps in *Drosophila* (Davie et al., 2015), but few regulatory regions of any kind have been characterized in *Aedes* (Akbari et al., 2014). To ensure the quality of the ATAC-seq datasets we generated, we examined ATAC peak clustering genome-wide (Figure 10.1C) as well as at the well-characterized *vitellogenin* promoter (Fig 10.1D). ATAC peaks were enriched 1 kb upstream of the first base-pair of the first exon, consistent with previous reports (Buenrostro *et al.*, 2013) (Fig 10.1C). Three ATAC peaks spanning 2 kb upstream of the first *vitellogenin* exon exactly replicate previous characterization of the *vitellogenin* promoter by transgenesis, suggesting successful application of this technique in *Aedes* (Kokoza et al., 2001).

Figure 9.1 Identification of differentially accessible brain chromatin regions by ATAC-seq

(A) The mosquito gonotrophic cycle. Female mosquitoes experience a suppression of host-seeking drive following a blood-meal, during egg development. Following egg-laying, host-seeking drive is restored until she ingests another blood-meal.
(B) Host-seeking behavior in female *Ae. aegypti* measured in the quattroport olfactometer assay at the indicated time after a blood-meal (mean±I.Q.R.., n=17-20 mosquitoes/trial, Data labeled with different letters are significantly different Kruskal-Wallis test with Dunn's multiple comparison, $p<0.05$).
(C) Genome-wide clustering of ATAC-seq peaks near transcription start sites (TSS).
(D) Regulation of chromatin state at the vitellogenin promoter. Proposed vitellogenin promoter unit adapted from Kokoza and Raikhel, 2001 (16).
(C) MA plot of differentially accessible ATAC-seq regions from 48 hours post-blood-meal.
(D) List of transcription factor binding sites enriched in regions modulated by blood-feeding.

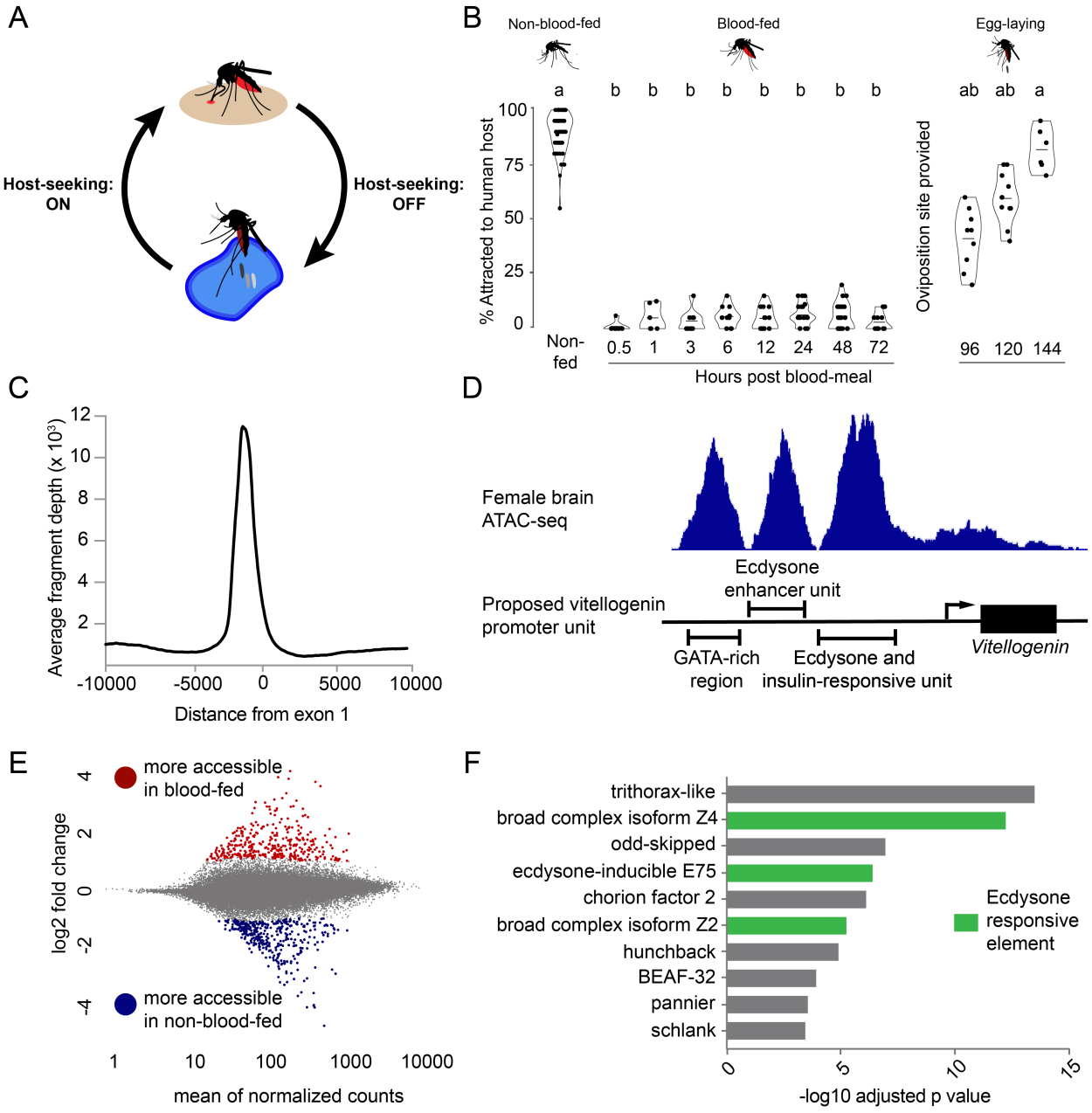
A
Host-seeking: ON
Host-seeking: OFF
B
Non-blood-fed
Blood-fed
Egg-laying
a b b b b b b b b
ab ab a
% Attracted to human host
100
75
50
25
0
Non-fed
0.5 1 3 6 12 24 48 72
Hours post blood-meal
Oviposition site provided
96 120 144
C
Average fragment depth (x 10³)
12
10
8
6
4
2
-10000 -5000 0 5000 10000
Distance from exon 1
D
Female brain ATAC-seq
Ecdysone enhancer unit
Proposed vitellogenin promoter unit
GATA-rich region
Ecdysone and insulin-responsive unit
Vitellogenin
E
more accessible in blood-fed
more accessible in non-blood-fed
log2 fold change
4
2
0
-2
-4
1 10 100 1000 10000
mean of normalized counts
F
trithorax-like
broad complex isoform Z4
odd-skipped
ecdysone-inducible E75
chorion factor 2
broad complex isoform Z2
hunchback
BEAF-32
pannier
schlank
Ecdysone responsive element
0 5 10 15
-log10 adjusted p value

Differential peak analysis was performed on ATAC samples from non-blood-fed and 48 hour post-blood-meal female mosquitoes, when host-seeking behavior is profoundly suppressed (Figure 10.1B). A total of 1,010 differentially accessible regions were identified (Figure 10.1E). Sequences from differentially accessible regions at 48 hours post-blood-meal were then analyzed for transcription factor binding consensus sequences. Binding sites for three ecdysone-responsive transcription factors were enriched: *Broad-Complex* (*br-c*) isoforms *Z2* and *Z4*, as well as the ecdysone-induced transcription factor *E75* (Figure 10.1F). *Br-c* and *E75* have previously been described to coordinate ecdysone-induced transcription in *Drosophila* pupae as well as in *Apis mellifera* honeybee brains and ovaries (Basso et al., 2006; Paul et al., 2006). The identification of binding footprints belonging to ecdysone-responsive factors in differentially accessible regions supported our theory that a coordinated program of gene expression changes in the brain is important in regulating host-seeking behavior. Additionally, it had been known for decades that titers of the active form of ecdysone, 20E, dramatically rise following a blood-meal (Hagedorn et al., 1975), and previous studies demonstrated that injection of ecdysone alone, in the absence of a blood-meal, can induce suppression of host-seeking behavior (Beach, 1979). Thus, this raised the possibility that ecdysone signaling following a blood-meal may contribute to the dramatic suppression of host-seeking drive.

9.3 Administration of exogenous 20E suppresses host-seeking behavior: a physiological or non-physiological effect?

To examine if 20E modulates host-seeking behavior in female *Ae. aegypti* mosquitoes, we fed 20E in a protein-free saline meal that does not lead to egg development or behavioral suppression and observed dose-dependent suppression of host-seeking drive 48 hours after feeding (Figure 10.2A). Importantly, 20E administration does not depress activity levels or participation rates (Figure 10.2B), indicating that feeding exogenous 20E did not make them too sick to engage in the assay.

To determine the time course of this inhibition, we fed 20E and assayed host-seeking drive from 8 to 96 hours after feeding (Figure 10.2C). We found that a single dose of 20E inhibits host-seeking behavior for 36 hours (from 24 hours post-feeding to 60 hours post-feeding). These results indicate that feeding 20E induces a sustained, reversible inhibition of mosquito host-seeking drive. While these results were exciting, administration of 350 ng 20E is approximately 1000x the physiological dose experienced by the mosquito following a blood-meal. While we do not know the bioavailability of fed 20E, steroid hormones, and ecdysone in particular, generally have high bioavailability so it is likely that the mosquito absorbs much of the 20E dose (Saez et al., 2000). This raises the concern that administration of such high doses of 20E cause non-physiological effects. Indeed, non-physiological effects of exogenous ecdysone have been observed in other biological processes in mosquitoes, such as egg

development (Lea, 1964). Further, administration of excess amounts of other developmental hormones in *Drosophila* have generated non-physiological phenotypes (Flatt et al., 2005).

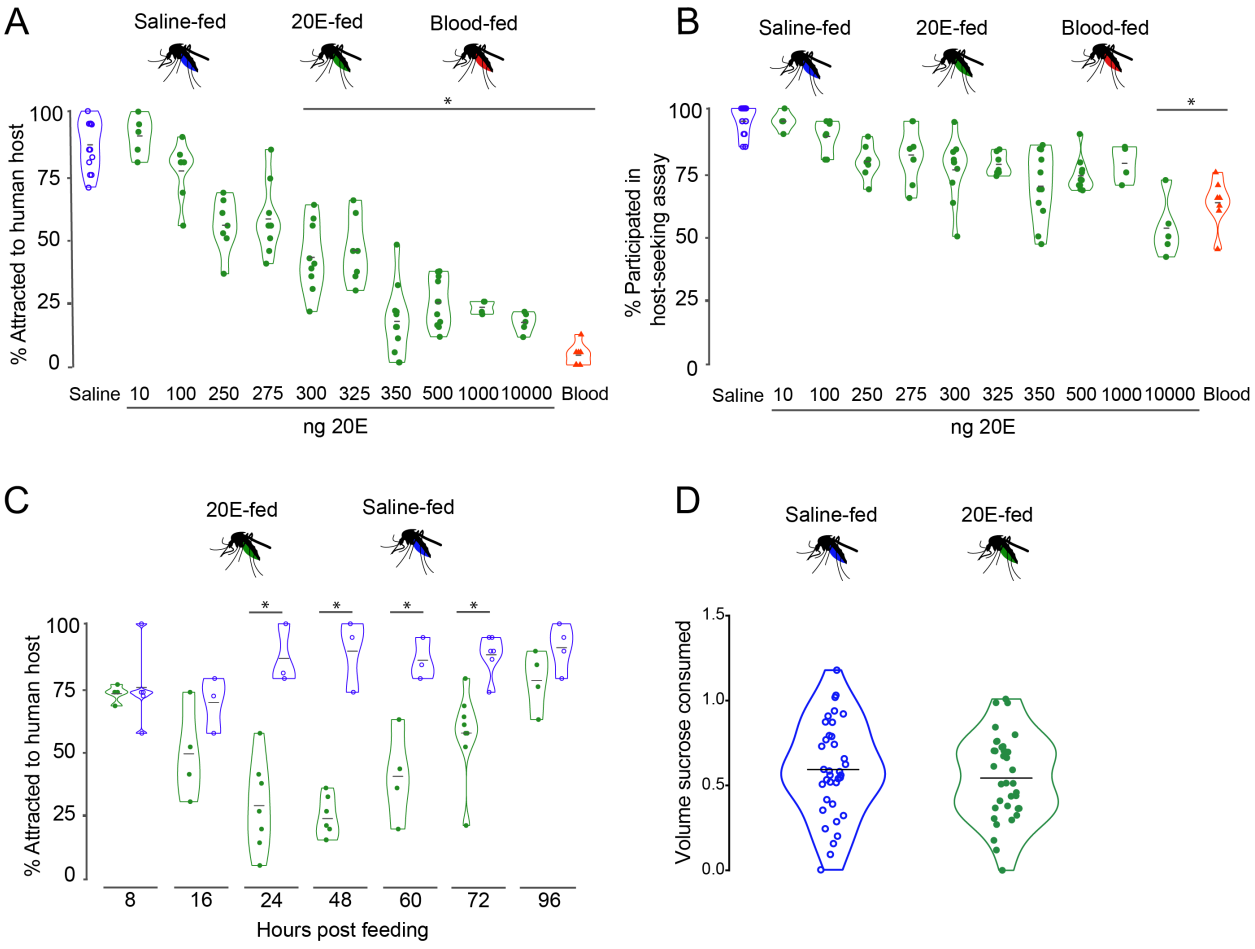

Figure 9.2 Administration of exogenous 20E suppresses host-seeking drive

(A) Rates of attraction to a human host of non-fed, saline-fed (110mM NaCl, 20mM NaHCO3, 1mM ATP), blood-fed (defibrinated sheep's blood, 1mM ATP), and 20E-fed at indicated doses, 110mM NaCl, 20mM NaHCO3, 1mM ATP) female mosquitoes in an olfactometer assay 48 hours post-feeding. Data shown as mean with interquartile range (mean with range, n=17-20 mosquitoes/trial, *significantly different from solvent control by Kruskal-Wallis test with Dunn's multiple correction, $p<0.05$)
(B) Rates of activation in the presence of a human host of non-fed, saline-fed, blood-fed, and 20E-fed female mosquitoes in an olfactometer assay. (mean with range, n=17-

20 mosquitoes/trial, *significantly different from solvent control by Kruskal-Wallis test with Dunn's multiple correction, $p<0.05$)
(C) Timecourse of 20E induced host-seeking suppression measured in the quattroport after being fed 20E or solvent meal. (mean with interquartile range, n=17-20 mosquitoes/trial, Student's T-test performed on timepoints separately, $p<0.05$).
(D) Volume of sucrose ingested 48 hours after fasting.

To investigate whether this suppression of host-seeking drive is specific to human cues, we then assayed sugar-feeding behavior in animals treated with 20E (Figure 10.2D). By adding fluorescein to the sucrose solution laboratory mosquitoes are maintained on, we could quantify individual consumption of sucrose following 20E or saline treatment. We found that 20E administration did not affect hunger for sugar.

It is tempting to conclude that the effect of 20E is therefore specific to inhibiting host-seeking behavior, but several aspects of the host-seeking assay and sugar-feeding assay differ in ways that make these results difficult to compare to each other. The host-seeking assay is a medium-range olfactory assay which tasks mosquitoes to fly through an approximately 1-meter-long tube into a trap proximal to a human arm or other stimulus (Basrur *et al.*, 2020). Meanwhile, the sugar-feeding assay is a very short-range assay, where mosquitoes in a bucket need to fly only approximately 20 cm to a sucrose source. Further, mosquitoes in the host-seeking assay are not starved prior to participating in the assay, whereas mosquitoes in the sugar feeding assay need to be starved for at least 48 hours in order to consume a meal large enough to be quantified. Thus, a superior experiment for determining if sugar hunger is affected by 20E administration is to assay mosquito attraction to sugar or honey odors in the same

medium-range olfactory assay as we use to examine host-seeking behavior (Basrur *et al.*, 2020; DeGennaro *et al.*, 2013).

To address concerns about non-physiological effects of 20E administration, we tried to utilize known 20E agonists and antagonists to modulate and replicate these behaviors (Hu et al., 2018; Oberdorster et al., 2001). However, none were appetitive and thus could not be fed and were either insoluble or lethal at concentrations required for injection. Thus, we could not use pharmacological manipulation of EcR as confirmation for the effects observed upon exogenous 20E administration.

9.4 The ecdysone receptor (EcR) is expressed in olfactory sensory neurons

The receptor for 20-hydroxyedysone (20E), the ecdysone receptor (EcR), is a nuclear hormone receptor and ligand-dependent transcription factor (Johnston *et al.*, 2011). To determine the localization of EcR in the nervous system and chemosensory tissues of *Aedes aegypti*, we used an antibody generated against the *Drosophila melanogaster* A isoform of the ecdysone receptor (EcR-A). This antibody was validated for sensitivity and specificity for *Ae. aegypti* EcR-A by heterologous expression in cell culture, as well as immunoprecipitation followed by mass spectrometry (IP-MS) in mosquito tissues. The EcR-A antibody stains EcR-A-transfected cells but not cells transfected with another EcR isoform, EcR-B, indicating isoform specificity (Figure 10.3A). Immunoprecipitation with the EcR-A antibody in *Ae. aegypti* heads followed by elution and western blotting revealed a band at the expected molecular weight of EcR-

A, 83 kDa (Figure 10.3B). The band in the 75-100 kDa region was then excised and mass spectrometry (MS) was performed to verify the detection of EcR-A (data not shown).

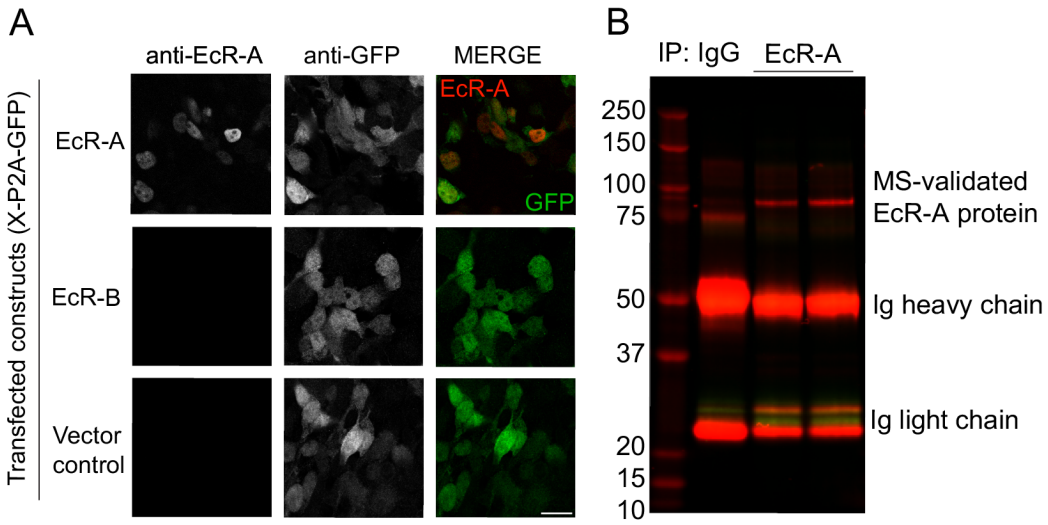

Figure 9.3 Validation of an EcR-A antibody

A) HEK cells transfected with plasmids expressing EcR-A-P2A-eGFP, EcR-B-P2A-eGFP, or P2A-eGFP vector control and stained with anti-EcR-A, anti-EcR-B, and anti-GFP antibodies. (scale bar = 25 μm)
(B) IP-western blot with EcR-A and mouse IgG control antibodies showed an EcR-A specific band at ~80 kDa (predicted MW= 83kDa).

EcR-A immunolabeling revealed specific antennal lobe glomeruli that differed in female and male brains (Figure 10.4B). We observed 4-6 antennal lobe glomeruli labeled in female brains by the EcR-A antibody, with 1-2 labeled in male antennal lobes. Staining in female antennae revealed EcR-A labeling in many Orco/Ir25a co-expressing neurons, definitively indicating this nuclear hormone receptor is expressed in olfactory neurons. These results suggested the exciting possibility that 20E and EcR could modulate gene expression olfactory neurons to affect host-seeking behavior.

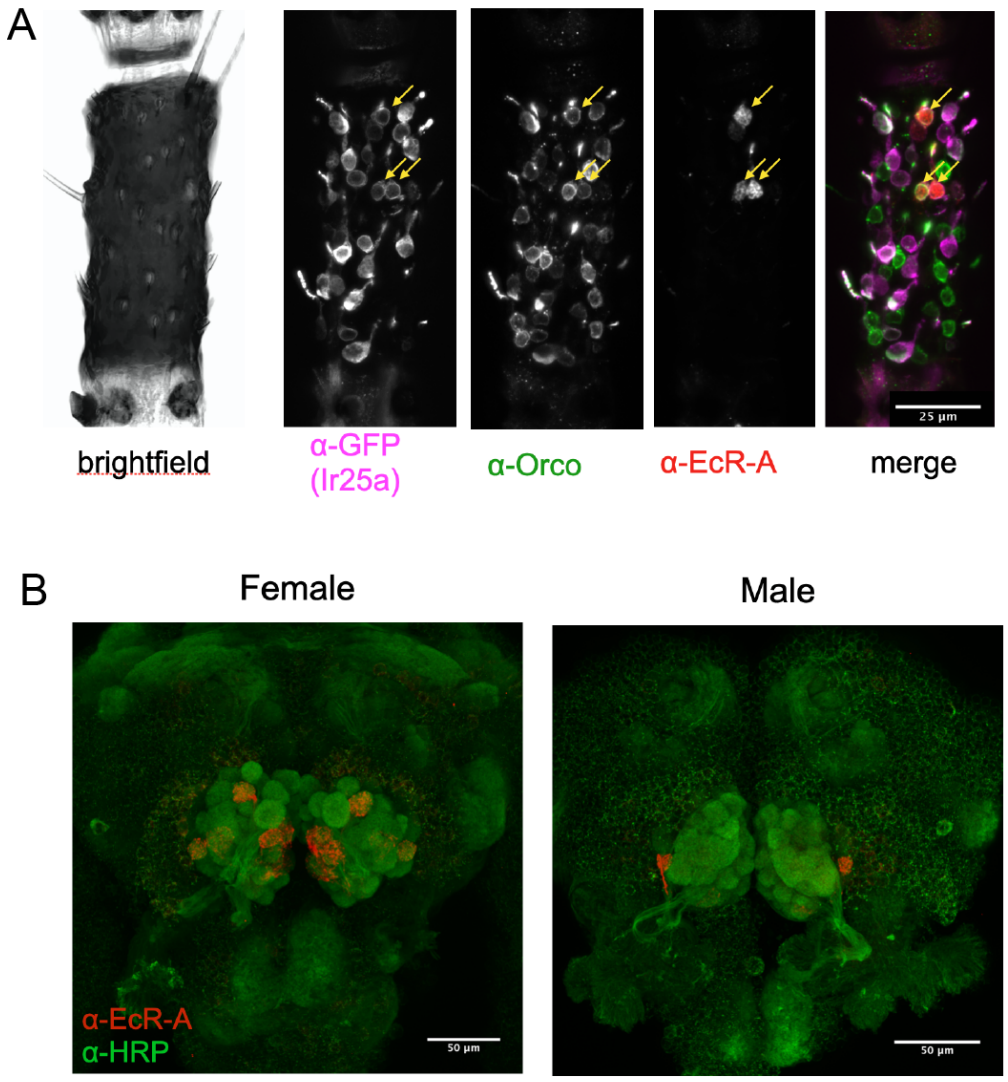

Figure 9.4 EcR-A is expressed in olfactory sensory neurons

(A) Confocal maximum projections of female Ir25a>GFP antennae immunostained with GFP, Orco, and EcR-A antibodies. Yellow arrows indicate EcR neurons. Scale bar = 25 μm.
(B) Confocal maximum projections of representative female and male brains stained with EcR-A antibody. Scale bar = 50 μm.

9.5 Attempted generation of EcR genetic reagents

We next attempted to generate genetic reagents to label, record activity from, and manipulate EcR neurons to confirm and extend these results. We also attempted to knock down EcR in olfactory neurons to determine if suppressing ecdysone signaling in olfactory neurons affects post-blood-meal host-seeking suppression. For reasons known and unknown, generation of these reagents failed. I detail them here to document these attempts to inform future attempts to label and manipulate EcR cells.

EcR-T2A-tdTomato

We first attempted to generate a tdTomato fluorescent protein knock-in to the EcR-A locus to confirm the expression patterns observed in antibody staining. We used CRISPR-Cas9 to insert an in-frame T2A-tdTomato into the EcR-A-specific region of the *EcR* gene as well as a 3xP3-eYFP marker to identify larvae with the insertion. We recovered one 3xP3-eYFP-positive G1 family and confirmed correct in-frame insertion of the T2A-tdTomato. However, the Tomato protein could not be visualized in any tissue and IP-western blots did not recover any Tomato protein (data not shown). Further, the knock-in of the tdTomato disrupted the EcR gene and upon homozygosing knock-in larvae did not survive, indicating manipulation of EcR-A in *Ae. aegypti* is developmentally lethal.

EcR-RNAi

To determine if knockdown of EcR in olfactory neurons affects post-blood-meal host-seeking behavior, we next attempted to adapt a short hairpin strategy for knockdown of EcR transcripts in a cell-type-specific manner. We chose short hairpin RNA (shRNA) for this method because in *Drosophila*, shRNA has been more effective than long hairpin RNA in generating loss-of-function phenotypes in neurons (Bartoletti et al., 2017). Thus, we adapted Valium20, a vector for shRNA in *Drosophila* for use in *Ae. aegypti* (PMID: 21460824). We used hairpin prediction software to target sites previously targeted in *Drosophila* EcR knockdown and chose 4 hairpins. We cloned the Valium20 components into a QUAS backbone such that we could express the shRNAs in cells that express *Ir25a-QF2*. We isolated 6 independent transgenic lines per hairpin, for a total of 24 RNAi line. We developed an RNA extraction method from antennae to quantify EcR knockdown and performed QPCR to assess degree of knockdown. We found no knockdown from any of our 24 lines (Figure 10.5).

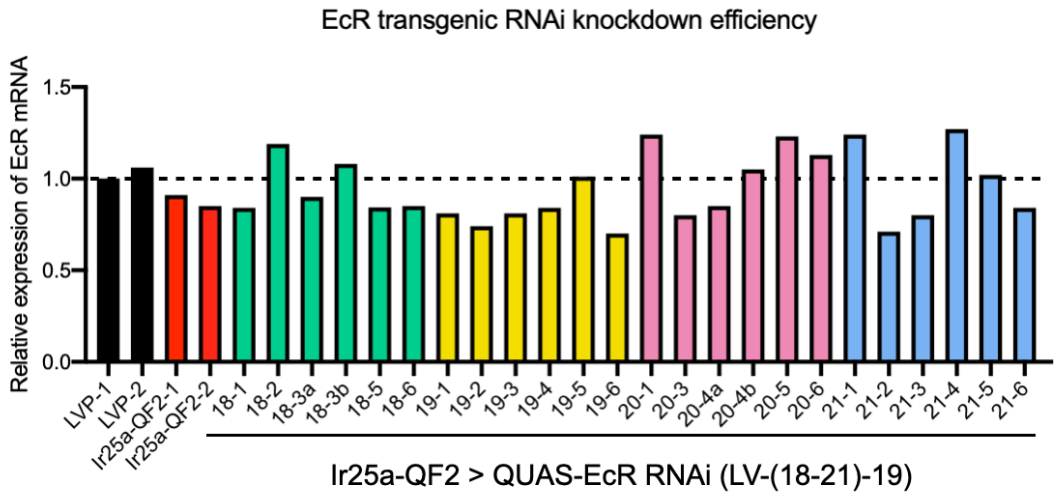

Figure 9.5 EcR RNAi knockdown reagents fail to reduce EcR transcript levels
QPCR analysis of female mosquito antennae from LVP, Ir25a-QF2, and Ir25a-QF2>QUAS-EcR-RNAi lines. Expression of EcR relative to beta-Tubulin.

We do not know why these reagents did not produce desired knockdown. To produce a functional cell-type-specific RNAi system in mosquitoes, the elements of the vector and hairpin may need to be tested first in cell culture systems. I am optimistic that a systematic approach to developing these reagents in *Ae. aegypti* will be functional, as they have shown to be in *Drosophila* and mice.

EcR-QF2-DBD

While our lab has been able to generate many QF driver lines to label cells expressing genes of interest, QF lines were not recovered after being inserted in certain loci. After analysis of successful and failed QF lines, it appeared as though QF expression from genes that are highly expressed in the brain or other tissues caused lethality. Indeed, the QF system had previously been described as potentially toxic and

efforts had been made to modify QF proteins to reduce their toxicity (Riabinina *et al.*, 2015). EcR is highly expressed in the brain and reproductive tissues during development. The expression levels are as high or higher than the expression of genes that had failed attempts at QF integration. To try to avoid QF toxicity, we chose to use the Split-QF system to express the DNA binding domain (DBD) from the EcR locus, as it is hypothesized that the activation domain (AD) of the QF protein is more toxic than the DBD (Lena Riabinina, pers. comm.). Thus, we inserted a T2A-QF-DBD sequence in place of the stop codon of EcR, as well as a 3xP3-EYFP selection marker. We recovered 1 G1 male with the correct insertion and sequence-verified the insertion, but egg morphology of progeny was highly irregular and no larvae with the insertion hatched. EcR is highly expressed in ovaries of female mosquitoes so it is possible that expression of the DBD domain caused toxicity in ovaries, and thus the line could neither be crossed to QUAS effectors or be maintained.

EcR-LexA

Due to the toxicity of the QF system, we next tried another binary expression system, LexA/LexAOP, to label and manipulate EcR cells. In a similar fashion as the QF-DBD line, we inserted a T2A-LexA in place of the EcR stop codon as well as a 3xP3-EYFP selection marker. No G1 larvae were isolated with the insertion. It is unknown if targeting the EcR locus produces lethality, or if LexA is toxic when highly expressed in *Ae. aegypti*.

9.6 Transcriptional regulation by administration of 20E

Next, we attempted to determine the transcriptional footprint of EcR signaling. EcR is a ligand-dependent transcription factor that acts in a complex to regulate transcription of target genes (Johnston et al., 2011; Koelle et al., 1991). Transcriptome analysis published by our lab showed that expression levels for several odorant receptors in the antennae change following a blood-meal (Matthews et al., 2016). The localization of EcR-A in sensory neuron projections raises the exciting possibility that EcR-A and its ligand 20E regulate transcription of olfactory receptors and associated olfactory signaling genes in sensory neurons, which in turn modulates their sensitivity to human cues.

To compare the effects of 20E administration and a blood-meal, which exposes female mosquitoes to high endogenous levels of 20E, we conducted an RNA-seq experiment in nervous and chemosensory tissues: brains, antennae, maxillary palps (Figure 10.6A). We also conducted this experiment in reproductive tissues: ovaries and fat body. We chose these tissues because 20E and blood-feeding have documented effects on reproductive tissues, but 20E's effect on nervous and chemosensory tissues is unknown. By comparing 20E administration and blood-feeding to a saline-meal, we could compare transcriptional changes after a blood-meal to transcriptional changes after 20E administration. If 20E-induced transcription changes are physiological, we expect a high degree of overlap between 20E-induced changes and blood-meal-

induced changes. If 20E-administration induces non-physiological transcriptional changes, we could then expect less overlap.

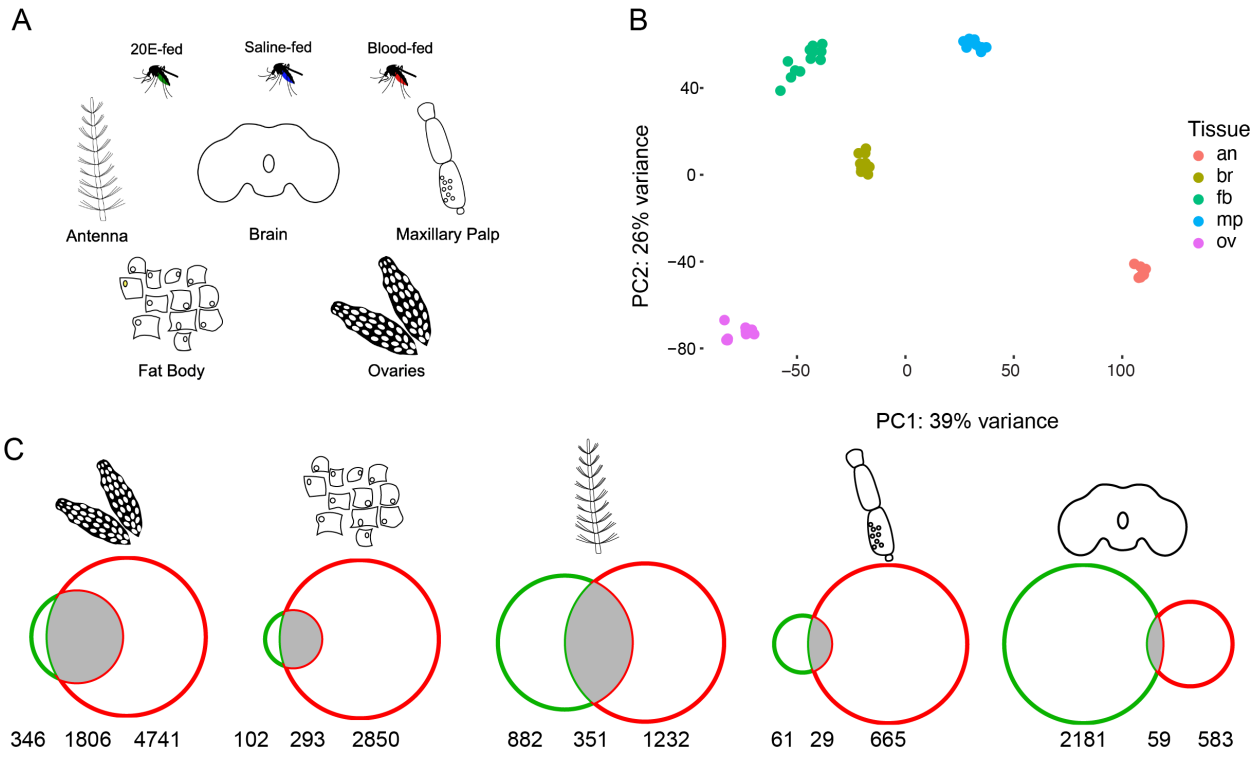

Figure 9.6 Administration of 20E causes transcriptional changes in sensory and reproductive tissues

(A) Schematic of RNA-seq experiment. 20E-fed, saline-fed and blood-fed mosquito tissues were dissected 48 hours after feeding and bulk RNA was isolated for RNA-sequencing.
(B) PCA plot of clusters by tissues. an = antennae, br = brains, fb = fat body, mp = maxillary palp, ov = ovary.
(C) Venn diagrams indicating overlap of differentially expressed genes (DESeq2, LFC > 1, padj > 0.05) between 20E vs saline (green), and blood vs saline (red) for indicated tissues.

As expected, we observed extensive overlap between 20E-induced and blood-meal-induced transcriptional changes in the ovary and fat body (Figure 10.6C).

Encouragingly, there was also overlap between gene expression changes in the

antennae and maxillary palps. However, there was almost no overlap in transcriptional changes in the brain between 20E and blood-feeding, suggesting that 20E may induce non-physiological changes in the brain after administration that could affect behavior.

This extensive dataset deserves further analysis and is being utilized by current lab members to address other questions regarding post-blood-meal reproductive physiology. Some of the gene expression changes observed (for example, modulation of expression of several ORs in the antenna after both blood-feeding and 20E-administration) were exciting, but the inability to generate genetic reagents to confirm the behavior effects of 20E administration are physiological made continuing with this work difficult. We hope that development of reagents that allow for temporal manipulation of EcR cells will shed light on EcR and 20E's potential role in regulating post-blood-meal behavior.

CHAPTER 10. REFERENCES

Abuin, L., Bargeton, B., Ulbrich, M.H., Isacoff, E.Y., Kellenberger, S., and Benton, R. (2011). Functional architecture of olfactory ionotropic glutamate receptors. Neuron *69*, 44-60. 10.1016/j.neuron.2010.11.042.

Abuin, L., Prieto-Godino, L.L., Pan, H., Gutierrez, C., Huang, L., Jin, R., and Benton, R. (2019). In vivo assembly and trafficking of olfactory Ionotropic Receptors. BMC Biol *17*, 34. 10.1186/s12915-019-0651-7.

Ache, B.W., and Young, J.M. (2005). Olfaction: diverse species, conserved principles. Neuron *48*, 417-430.

Acree, F., Jr., Turner, R.B., Gouck, H.K., Beroza, M., and Smith, N. (1968). L-Lactic acid: a mosquito attractant isolated from humans. Science *161*, 1346-1347.

Afify, A., Betz, J.F., Riabinina, O., and Potter, C.J. (2019). Commonly used insect repellents hide human odors from Anopheles mosquitoes. bioRxiv, https://doi.org/10.1101/530964.

Ahn, J.E., Chen, Y., and Amrein, H. (2017). Molecular basis of fatty acid taste in Drosophila. Elife *6*. 10.7554/eLife.30115.

Ai, M., Blais, S., Park, J.Y., Min, S., Neubert, T.A., and Suh, G.S. (2013). Ionotropic glutamate receptors IR64a and IR8a form a functional odorant receptor complex in vivo in *Drosophila*. J Neurosci *33*, 10741-10749. 10.1523/JNEUROSCI.5419-12.2013.

Akbari, O.S., Papathanos, P.A., Sandler, J.E., Kennedy, K., and Hay, B.A. (2014). Identification of germline transcriptional regulatory elements in Aedes aegypti. Sci Rep *4*, 3954. 10.1038/srep03954.

Allan, S.A., Day, J.F., and Edman, J.D. (1987). Visual ecology of biting flies. Annu Rev Entomol *32*, 297-316. 10.1146/annurev.en.32.010187.001501.

Auer, T.O., Khallaf, M.A., Silbering, A.F., Zappia, G., Ellis, K., Alvarez-Ocana, R., Arguello, J.R., Hansson, B.S., Jefferis, G., Caron, S.J.C., et al. (2020). Olfactory receptor and circuit evolution promote host specialization. Nature *579*, 402-408. 10.1038/s41586-020-2073-7.

Bartoletti, R., Capozzoli, B., Moore, J., Moran, J., Shrawder, B., and Vivekanand, P. (2017). Short hairpin RNA is more effective than long hairpin RNA in eliciting pointed loss-of-function phenotypes in Drosophila. Genesis *55*. 10.1002/dvg.23036.

Bashkirova, E., and Lomvardas, S. (2019). Olfactory receptor genes make the case for inter-chromosomal interactions. Curr Opin Genet Dev *55*, 106-113. 10.1016/j.gde.2019.07.004.

Basrur, N.S., De Obaldia, M.E., Morita, T., Herre, M., von Heynitz, R.K., Tsitohay, Y.N., and Vosshall, L.B. (2020). *fruitless* mutant male mosquitoes gain attraction to human odor. BioRxiv *10.1101/2020.09.04.282434*.

Basso, L.R., Jr., de, C.N.M., Monesi, N., and Paco-Larson, M.L. (2006). Broad-Complex, E74, and E75 early genes control DNA puff BhC4-1 expression in prepupal salivary glands. Genesis *44*, 505-514. 10.1002/dvg.20239.

Beach, R. (1979). Mosquitoes: biting behavior inhibited by ecdysone. Science *205*, 829-831. 10.1126/science.205.4408.829.

Beckstead, R.B., Lam, G., and Thummel, C.S. (2005). The genomic response to 20-hydroxyecdysone at the onset of Drosophila metamorphosis. Genome Biol *6*, R99. 10.1186/gb-2005-6-12-r99.

Benton, R., Sachse, S., Michnick, S.W., and Vosshall, L.B. (2006). Atypical membrane topology and heteromeric function of *Drosophila* odorant receptors in vivo. PLoS Biol *4*, e20. 10.1371/journal.pbio.0040020.

Benton, R., Vannice, K.S., Gomez-Diaz, C., and Vosshall, L.B. (2009). Variant ionotropic glutamate receptors as chemosensory receptors in *Drosophila*. Cell *136*, 149-162. 10.1016/j.cell.2008.12.001.

Benton, R., Vannice, K.S., and Vosshall, L.B. (2007). An essential role for a CD36-related receptor in pheromone detection in Drosophila. Nature *450*, 289-293. 10.1038/nature06328.

Bernier, U.R., Booth, M.M., and Yost, R.A. (1999). Analysis of human skin emanations by gas chromatography/mass spectrometry. 1. Thermal desorption of attractants for the yellow fever mosquito (*Aedes aegypti*) from handled glass beads. Anal Chem *71*, 1-7.

Bernier, U.R., Kline, D.L., Allan, S.A., and Barnard, D.R. (2007). Laboratory comparison of *Aedes aegypti* attraction to human odors and to synthetic human odor compounds and blends. J Am Mosq Control Assoc *23*, 288-293. 10.2987/8756-971X(2007)23[288:LCOAAA]2.0.CO;2.

Bernier, U.R., Kline, D.L., Barnard, D.R., Schreck, C.E., and Yost, R.A. (2000). Analysis of human skin emanations by gas chromatography/mass spectrometry. 2. Identification of volatile compounds that are candidate attractants for the yellow fever mosquito (*Aedes aegypti*). Anal Chem *72*, 747-756.

Bhatt, S., Gething, P.W., Brady, O.J., Messina, J.P., Farlow, A.W., Moyes, C.L., Drake, J.M., Brownstein, J.S., Hoen, A.G., Sankoh, O., et al. (2013). The global distribution and burden of dengue. Nature *496*, 504-507. 10.1038/nature12060.

Bisch-Knaden, S., Dahake, A., Sachse, S., Knaden, M., and Hansson, B.S. (2018). Spatial Representation of Feeding and Oviposition Odors in the Brain of a Hawkmoth. Cell Rep *22*, 2482-2492. 10.1016/j.celrep.2018.01.082.

Bohbot, J., Pitts, R.J., Kwon, H.W., Rutzler, M., Robertson, H.M., and Zwiebel, L.J. (2007). Molecular characterization of the *Aedes aegypti* odorant receptor gene family. Insect Mol Biol *16*, 525-537.

Bohbot, J.D., and Dickens, J.C. (2009). Characterization of an enantioselective odorant receptor in the yellow fever mosquito *Aedes aegypti*. PLoS One *4*, e7032. 10.1371/journal.pone.0007032.

Bohbot, J.D., Sparks, J.T., and Dickens, J.C. (2014). The maxillary palp of *Aedes aegypti*, a model of multisensory integration. Insect Biochem Mol Biol *48*, 29-39. 10.1016/j.ibmb.2014.02.007.

Boo, K.S., and McIver, S.B. (1975). Fine structure of sunken thick-walled pegs (sensilla ampullacea and coeloconica) on the antennae of mosquitoes. Can J Zool *53*, 262-266.

Borovsky, D., Whisenton, L.R., Thomas, B.R., and Fuchs, M.S. (1986). Biosynthesis and distribution of ecdysone and 20-OH-ecdysone in Aedes aegypti. Insect Biochemistry and Physiology *3*, 19-30.

Bozzolan, F., Duportets, L., Limousin, D., Wycke, M.A., Demondion, E., Francois, A., Abrieux, A., and Debernard, S. (2015). Synaptotagmin I, a molecular target for steroid hormone signaling controlling the maturation of sexual behavior in an insect. FEBS J *282*, 1432-1444. 10.1111/febs.13231.

Brand, A.H., and Perrimon, N. (1993). Targeted gene expression as a means of altering cell fates and generating dominant phenotypes. Development *118*, 401-415.

Brand, P., and Ramirez, S.R. (2017). The Evolutionary Dynamics of the Odorant Receptor Gene Family in Corbiculate Bees. Genome Biol Evol *9*, 2023-2036. 10.1093/gbe/evx149.

Brand, P., Robertson, H.M., Lin, W., Pothula, R., Klingeman, W.E., Jurat-Fuentes, J.L., and Johnson, B.R. (2018). The origin of the odorant receptor gene family in insects. Elife *7*. 10.7554/eLife.38340.

Buck, L., and Axel, R. (1991a). A novel multigene family may encode odorant receptors: a molecular basis for odor recognition. Cell *65*, 175-187. 10.1016/0092-8674(91)90418-x.

Buck, L., and Axel, R. (1991b). A novel multigene family may encode odorant receptors: a molecular basis for odor recognition. Cell *65*, 175-187.

Buenrostro, J.D., Giresi, P.G., Zaba, L.C., Chang, H.Y., and Greenleaf, W.J. (2013). Transposition of native chromatin for fast and sensitive epigenomic profiling of open chromatin, DNA-binding proteins and nucleosome position. Nat Methods *10*, 1213-1218. 10.1038/nmeth.2688.

Butterwick, J.A., Del Marmol, J., Kim, K.H., Kahlson, M.A., Rogow, J.A., Walz, T., and Ruta, V. (2018). Cryo-EM structure of the insect olfactory receptor Orco. Nature *560*, 447-452. 10.1038/s41586-018-0420-8.

Cao, L.H., Jing, B.Y., Yang, D., Zeng, X., Shen, Y., Tu, Y., and Luo, D.G. (2016). Distinct signaling of Drosophila chemoreceptors in olfactory sensory neurons. Proc Natl Acad Sci U S A *113*, E902-911. 10.1073/pnas.1518329113.

Cao, L.H., Yang, D., Wu, W., Zeng, X., Jing, B.Y., Li, M.T., Qin, S., Tang, C., Tu, Y., and Luo, D.G. (2017). Odor-evoked inhibition of olfactory sensory neurons drives olfactory perception in Drosophila. Nat Commun *8*, 1357. 10.1038/s41467-017-01185-0.

Champlin, D.T., and Truman, J.W. (1998). Ecdysteroid control of cell proliferation during optic lobe neurogenesis in the moth Manduca sexta. Development *125*, 269-277.

Chandrashekar, J., Hoon, M.A., Ryba, N.J., and Zuker, C.S. (2006). The receptors and cells for mammalian taste. Nature *444*, 288-294. 10.1038/nature05401.

Chen, T.W., Wardill, T.J., Sun, Y., Pulver, S.R., Renninger, S.L., Baohan, A., Schreiter, E.R., Kerr, R.A., Orger, M.B., Jayaraman, V., et al. (2013). Ultrasensitive fluorescent proteins for imaging neuronal activity. Nature *499*, 295-300. 10.1038/nature12354.

Chen, Y., and Amrein, H. (2017). Ionotropic Receptors Mediate Drosophila Oviposition Preference through Sour Gustatory Receptor Neurons. Curr Biol *27*, 2741-2750 e2744. 10.1016/j.cub.2017.08.003.

Chess, A., Simon, I., Cedar, H., and Axel, R. (1994). Allelic inactivation regulates olfactory receptor gene expression. Cell *78*, 823-834.

Choi, H.M.T., Schwarzkopf, M., Fornace, M.E., Acharya, A., Artavanis, G., Stegmaier, J., Cunha, A., and Pierce, N.A. (2018). Third-generation *in situ* hybridization chain reaction: multiplexed, quantitative, sensitive, versatile, robust. Development *145*, 10.1242/dev.165753. 10.1242/dev.165753.

Chou, Y.H., Zheng, X., Beachy, P.A., and Luo, L. (2010). Patterning axon targeting of olfactory receptor neurons by coupled hedgehog signaling at two distinct steps. Cell *142*, 954-966. 10.1016/j.cell.2010.08.015.

Clyne, P.J., Warr, C.G., and Carlson, J.R. (2000). Candidate taste receptors in *Drosophila*. Science *287*, 1830-1834. 10.1126/science.287.5459.1830.

Clyne, P.J., Warr, C.G., Freeman, M.R., Lessing, D., Kim, J., and Carlson, J.R. (1999). A novel family of divergent seven-transmembrane proteins: candidate odorant receptors in *Drosophila*. Neuron *22*, 327-338.

Cohn, R., Morantte, I., and Ruta, V. (2015). Coordinated and compartmentalized neuromodulation shapes sensory processing in *Drosophila*. Cell *163*, 1742-1755. 10.1016/j.cell.2015.11.019.

Corfas, R.A., and Vosshall, L.B. (2015). The cation channel TRPA1 tunes mosquito thermotaxis to host temperatures. Elife *4*, 10.7554/eLife.11750. 10.7554/eLife.11750.

Costa-da-Silva, A.L., Navarrete, F.R., Salvador, F.S., Karina-Costa, M., Ioshino, R.S., Azevedo, D.S., Rocha, D.R., Romano, C.M., and Capurro, M.L. (2013). Glytube: a conical tube and parafilm M-based method as a simplified device to artificially blood-feed the dengue vector mosquito, *Aedes aegypti*. PLoS One *8*, e53816. 10.1371/journal.pone.0053816.

Couto, A., Alenius, M., and Dickson, B.J. (2005). Molecular, anatomical, and functional organization of the *Drosophila* olfactory system. Curr Biol *15*, 1535-1547. 10.1016/j.cub.2005.07.034.

Croset, V., Rytz, R., Cummins, S.F., Budd, A., Brawand, D., Kaessmann, H., Gibson, T.J., and Benton, R. (2010). Ancient protostome origin of chemosensory ionotropic glutamate receptors and the evolution of insect taste and olfaction. PLoS Genet *6*, e1001064. 10.1371/journal.pgen.1001064.

Curley, J.P., Rock, V., Moynihan, A.M., Bateson, P., Keverne, E.B., and Champagne, F.A. (2010). Developmental shifts in the behavioral phenotypes of inbred mice: the role of postnatal and juvenile social experiences. Behav Genet *40*, 220-232.

Daugherty, A., Yeo, R., Buenrostro, J., Greenleaf, W., Kundaje, A., and Brunet, B. (2016). Chromatin accessibility dynamics reveal novel functional enhancers in *C. elegans*. bioRxiv, doi: https://doi.org/10.1101/088732.

Davie, K., Jacobs, J., Atkins, M., Potier, D., Christiaens, V., Halder, G., and Aerts, S. (2015). Discovery of transcription factors and regulatory regions driving in vivo tumor development by ATAC-seq and FAIRE-seq open chromatin profiling. PLoS Genet *11*, e1004994. 10.1371/journal.pgen.1004994.

Davis, E.E. (1974). Identification of antennal chemoreceptors of the mosquito, Aedes aegypti: a correction. Experientia *30*, 1282-1283. 10.1007/BF01945187.

Davis, E.E. (1984). Regulation of sensitivity in the peripheral chemoreceptor systems for host-seeking behavior by a haemolymph-borne factor in *Aedes aegypti*. J Insect Physiol *30*, 179-183.

Davis, E.E., and Bowen, M.F. (1994). Sensory physiological basis for attraction in mosquitoes. J Am Mosq Control Assoc *10*, 316-325.

de Bruyne, M., Foster, K., and Carlson, J.R. (2001). Odor coding in the *Drosophila* antenna. Neuron *30*, 537-552.

DeGennaro, M., McBride, C.S., Seeholzer, L., Nakagawa, T., Dennis, E.J., Goldman, C., Jasinskiene, N., James, A.A., and Vosshall, L.B. (2013). *orco* mutant mosquitoes lose strong preference for humans and are not repelled by volatile DEET. Nature *498*, 487-491. 10.1038/nature12206.

Dekker, T., Geier, M., and Carde, R.T. (2005). Carbon dioxide instantly sensitizes female yellow fever mosquitoes to human skin odours. J Exp Biol *208*, 2963-2972. 10.1242/jeb.01736.

Denny, S.K., Yang, D., Chuang, C.H., Brady, J.J., Lim, J.S., Gruner, B.M., Chiou, S.H., Schep, A.N., Baral, J., Hamard, C., et al. (2016). Nfib promotes metastasis through a widespread increase in chromatin accessibility. Cell *166*, 328-342. 10.1016/j.cell.2016.05.052.

Dey, S., Chamero, P., Pru, J.K., Chien, M.S., Ibarra-Soria, X., Spencer, K.R., Logan, D.W., Matsunami, H., Peluso, J.J., and Stowers, L. (2015). Cyclic Regulation of Sensory Perception by a Female Hormone Alters Behavior. Cell *161*, 1334-1344. 10.1016/j.cell.2015.04.052.

Distler, P., and Boeckh, J. (1997). Central projections of the maxillary and antennal nerves in the mosquito *Aedes aegypti*. J Exp Biol *200*, 1873-1879.

Dormont, L., Bessiere, J.M., McKey, D., and Cohuet, A. (2013). New methods for field collection of human skin volatiles and perspectives for their application in the chemical ecology of human-pathogen-vector interactions. J Exp Biol *216*, 2783-2788. 10.1242/jeb.085936.

Duvall, L.B., Ramos-Espiritu, L., Barsoum, K.E., Glickman, J.F., and Vosshall, L.B. (2019). Small-molecule agonists of *Ae. aegypti* neuropeptide Y receptor block mosquito biting. Cell *176*, 687-701. 10.1016/j.cell.2018.12.004.

Ebrahim, S.A., Dweck, H.K., Stokl, J., Hofferberth, J.E., Trona, F., Weniger, K., Rybak, J., Seki, Y., Stensmyr, M.C., Sachse, S., et al. (2015). *Drosophila* avoids parasitoids by sensing their semiochemicals via a dedicated olfactory circuit. PLoS Biol *13*, e1002318. 10.1371/journal.pbio.1002318.

Ekoka, E., Maharaj, S., Nardini, L., Dahan-Moss, Y., and Koekemoer, L.L. (2021). 20-Hydroxyecdysone (20E) signaling as a promising target for the chemical control of malaria vectors. Parasit Vectors *14*, 86. 10.1186/s13071-020-04558-5.

Faller, W.E., and Luttges, M.W. (1995). Method for determining individual neuron size in simultaneous single-unit recordings. Med Biol Eng Comput *33*, 121-130. 10.1007/BF02523029.

Fandino, R.A., Haverkamp, A., Bisch-Knaden, S., Zhang, J., Bucks, S., Nguyen, T.A.T., Schroder, K., Werckenthin, A., Rybak, J., Stengl, M., et al. (2019). Mutagenesis of odorant coreceptor Orco fully disrupts foraging but not oviposition behaviors in the hawkmoth Manduca sexta. Proc Natl Acad Sci U S A *116*, 15677-15685. 10.1073/pnas.1902089116.

Fischler, W., Kong, P., Marella, S., and Scott, K. (2007). The detection of carbonation by the *Drosophila* gustatory system. Nature *448*, 1054-1057.

Fişek, M., and Wilson, R.I. (2014). Stereotyped connectivity and computations in higher-order olfactory neurons. Nat Neurosci *17*, 280-288. 10.1038/nn.3613.

Fishilevich, E., Domingos, A.I., Asahina, K., Naef, F., Vosshall, L.B., and Louis, M. (2005). Chemotaxis behavior mediated by single larval olfactory neurons in *Drosophila*. Curr Biol *15*, 2086-2096.

Fishilevich, E., and Vosshall, L.B. (2005). Genetic and functional subdivision of the *Drosophila* antennal lobe. Curr. Biol. *15*, 1548-1553.

Flanagan, D., and Mercer, A.R. (1989). An atlas and 3-D reconstruction of the antennal lobes in the worker honey bee, *Apis mellifera* L. (Hymenoptera : Apidae). Int J Insect Morphol & Embryol *18*, 145-159.

Flatt, T., Tu, M.P., and Tatar, M. (2005). Hormonal pleiotropy and the juvenile hormone regulation of Drosophila development and life history. Bioessays *27*, 999-1010. 10.1002/bies.20290.

French, A., Ali Agha, M., Mitra, A., Yanagawa, A., Sellier, M.J., and Marion-Poll, F. (2015). Drosophila Bitter Taste(s). Front Integr Neurosci *9*, 58. 10.3389/fnint.2015.00058.

Gallagher, M., Wysocki, C.J., Leyden, J.J., Spielman, A.I., Sun, X., and Preti, G. (2008). Analyses of volatile organic compounds from human skin. Br J Dermatol *159*, 780-791. 10.1111/j.1365-2133.2008.08748.x.

Gao, Q., and Chess, A. (1999). Identification of candidate *Drosophila* olfactory receptors from genomic DNA sequence. Genomics *60*, 31-39.

Geddes, L.H., McQuillan, H.J., Aiken, A., Vergoz, V., and Mercer, A.R. (2013). Steroid hormone (20-hydroxyecdysone) modulates the acquisition of aversive olfactory memories in pollen forager honeybees. Learn Mem *20*, 399-409. 10.1101/lm.030825.113.

Geier, M., Bosch, O.J., and Boeckh, J. (1999). Ammonia as an attractive component of host odour for the yellow fever mosquito, *Aedes aegypti*. Chem Senses *24*, 647-653.

Geier, M., Sass, H., and Boeckh, J. (1996). A search for components in human body odour that attract females of Aedes aegypti. Ciba Found Symp *200*, 132-144; discussion 144-138, 178-183.

Ghaninia, M., Hansson, B.S., and Ignell, R. (2007a). The antennal lobe of the African malaria mosquito, *Anopheles gambiae* - innervation and three-dimensional reconstruction. Arthropod Struct Dev *36*, 23-39.

Ghaninia, M., Ignell, R., and Hansson, B.S. (2007b). Functional classification and central nervous projections of olfactory receptor neurons housed in antennal trichoid

sensilla of female yellow fever mosquitoes, Aedes aegypti. Eur J Neurosci *26*, 1611-1623. 10.1111/j.1460-9568.2007.05786.x.

Ghaninia, M., Majeed, S., Dekker, T., Hill, S.R., and Ignell, R. (2019). Hold your breath - Differential behavioral and sensory acuity of mosquitoes to acetone and carbon dioxide. PLoS One *14*, e0226815. 10.1371/journal.pone.0226815.

Giang, T., He, J., Belaidi, S., and Scholz, H. (2017). Key Odorants Regulate Food Attraction in Drosophila melanogaster. Front Behav Neurosci *11*, 160. 10.3389/fnbeh.2017.00160.

Gillies, M.T. (1980). The role of carbon dioxide in host-finding in mosquitoes (Diptera:Culicidae): a review. Bull Entomol Res *70*, 525-532.

Gomez-Diaz, C., Martin, F., Garcia-Fernandez, J.M., and Alcorta, E. (2018). The Two Main Olfactory Receptor Families in Drosophila, ORs and IRs: A Comparative Approach. Front Cell Neurosci *12*, 253. 10.3389/fncel.2018.00253.

Grabe, V., Strutz, A., Baschwitz, A., Hansson, B.S., and Sachse, S. (2015). Digital in vivo 3D atlas of the antennal lobe of *Drosophila melanogaster*. J Comp Neurol *523*, 530-544. 10.1002/cne.23697.

Grant, A.J., Wigton, B.E., Aghajanian, J.G., and O'Connell, R.J. (1995). Electrophysiological responses of receptor neurons in mosquito maxillary palp sensilla to carbon dioxide. J Comp Physiol [A] *177*, 389-396.

Greer, P.L., Bear, D.M., Lassance, J.M., Bloom, M.L., Tsukahara, T., Pashkovski, S.L., Masuda, F.K., Nowlan, A.C., Kirchner, R., Hoekstra, H.E., and Datta, S.R. (2016). A family of non-GPCR chemosensors defines an alternative logic for mammalian olfaction. Cell *165*, 1734-1748. 10.1016/j.cell.2016.05.001.

Greppi, C., Laursen, W.J., Budelli, G., Chang, E.C., Daniels, A.M., van Giesen, L., Smidler, A.L., Catteruccia, F., and Garrity, P.A. (2020). Mosquito heat seeking is driven by an ancestral cooling receptor. Science *367*, 681-684. 10.1126/science.aay9847.

Grosse-Wilde, E., Kuebler, L.S., Bucks, S., Vogel, H., Wicher, D., and Hansson, B.S. (2011). Antennal transcriptome of *Manduca sexta*. Proc Natl Acad Sci U S A *108*, 7449-7454. 10.1073/pnas.1017963108.

Ha, T.S., and Smith, D.P. (2006). A pheromone receptor mediates 11-*cis*-vaccenyl acetate-induced responses in *Drosophila*. J Neurosci *26*, 8727-8733.

Haga-Yamanaka, S., Ma, L., and Yu, C.R. (2015). Tuning properties and dynamic range of type 1 vomeronasal receptors. Front Neurosci *9*, 244. 10.3389/fnins.2015.00244.

Hagedorn, H.H., O'Connor, J.D., Fuchs, M.S., Sage, B., Schlaeger, D.A., and Bohm, M.K. (1975). The ovary as a source of alpha-ecdysone in an adult mosquito. Proc Natl Acad Sci U S A *72*, 3255-3259. 10.1073/pnas.72.8.3255.

Hagino-Yamagishi, K., Matsuoka, M., Ichikawa, M., Wakabayashi, Y., Mori, Y., and Yazaki, K. (2001). The mouse putative pheromone receptor was specifically activated by stimulation with male mouse urine. J Biochem *129*, 509-512. 10.1093/oxfordjournals.jbchem.a002884.

Hallem, E.A., and Carlson, J.R. (2004). The odor coding system of *Drosophila*. Trends Genet *20*, 453-459.

Hallem, E.A., and Carlson, J.R. (2006). Coding of odors by a receptor repertoire. Cell *125*, 143-160.

Hallem, E.A., Ho, M.G., and Carlson, J.R. (2004). The molecular basis of odor coding in the *Drosophila* antenna. Cell *117*, 965-979.

Hansen, I.A., Attardo, G.M., Rodriguez, S.D., and Drake, L.L. (2014). Four-way regulation of mosquito yolk protein precursor genes by juvenile hormone-, ecdysone-, nutrient-, and insulin-like peptide signaling pathways. Front Physiol *5*, 103. 10.3389/fphys.2014.00103.

Hansson, B.S., and Stensmyr, M.C. (2011). Evolution of insect olfaction. Neuron *72*, 698-711. 10.1016/j.neuron.2011.11.003.

Hong, W., Mosca, T.J., and Luo, L. (2012). Teneurins instruct synaptic partner matching in an olfactory map. Nature *484*, 201-207. 10.1038/nature10926.

Hu, X., Yin, B., Cappelle, K., Swevers, L., Smagghe, G., Yang, X., and Zhang, L. (2018). Identification of novel agonists and antagonists of the ecdysone receptor by virtual screening. J Mol Graph Model *81*, 77-85. 10.1016/j.jmgm.2018.02.016.

Hussain, A., Zhang, M., Üçpunar, H.K., Svensson, T., Quillery, E., Gompel, N., Ignell, R., and Grunwald Kadow, I.C. (2016). Ionotropic chemosensory receptors mediate the taste and smell of polyamines. PLoS Biol *14*, e1002454. 10.1371/journal.pbio.1002454.

Ignell, R., Dekker, T., Ghaninia, M., and Hansson, B.S. (2005). Neuronal architecture of the mosquito deutocerebrum. J Comp Neurol *493*, 207-240.

Illig, K.R., and Haberly, L.B. (2003). Odor-evoked activity is spatially distributed in piriform cortex. J Comp Neurol *457*, 361-373. 10.1002/cne.10557.

Ito, K., Shinomiya, K., Ito, M., Armstrong, J.D., Boyan, G., Hartenstein, V., Harzsch, S., Heisenberg, M., Homberg, U., Jenett, A., et al. (2014). A systematic nomenclature for the insect brain. Neuron *81*, 755-765. 10.1016/j.neuron.2013.12.017.

Jafari, S., and Alenius, M. (2015). Cis-regulatory mechanisms for robust olfactory sensory neuron class-restricted odorant receptor gene expression in *Drosophila*. PLoS Genet *11*, e1005051. 10.1371/journal.pgen.1005051.

Jeanne, J.M., Fisek, M., and Wilson, R.I. (2018). The Organization of Projections from Olfactory Glomeruli onto Higher-Order Neurons. Neuron *98*, 1198-1213 e1196. 10.1016/j.neuron.2018.05.011.

Johnston, D.M., Sedkov, Y., Petruk, S., Riley, K.M., Fujioka, M., Jaynes, J.B., and Mazo, A. (2011). Ecdysone- and NO-mediated gene regulation by competing EcR/Usp and E75A nuclear receptors during Drosophila development. Mol Cell *44*, 51-61. 10.1016/j.molcel.2011.07.033.

Jones, W.D., Cayirlioglu, P., Kadow, I.G., and Vosshall, L.B. (2007). Two chemosensory receptors together mediate carbon dioxide detection in *Drosophila*. Nature *445*, 86-90. 10.1038/nature05466.

Jové, V., Gong, Z., Hol, F.J.H., Zhao, Z., Sorrells, T.R., Carroll, T.S., Prakash, M., McBride, C.S., and Vosshall, L.B. (2020). Sensory discrimination of blood and floral nectar by *Aedes aegypti* mosquitoes. Neuron *10.1016/j.neuron.2020.09.019*.

Karner, T., Kellner, I., Schultze, A., Breer, H., and Krieger, J. (2015). Co-expression of six tightly clustered odorant receptor genes in the antenna of the malaria mosquito *Anopheles gambiae*. Front Ecol Evol *3*, 10.3389/fevo.2015.00026. 10.3389/fevo.2015.00026.

Kaupp, U.B. (2010). Olfactory signalling in vertebrates and insects: differences and commonalities. Nat Rev Neurosci *11*, 188-200. 10.1038/nrn2789.

Keil, T.A., and Steinbrecht, A. (1964). Mechanosensitive and Olfactory Sensilla of Insects. Insect Ultrastructure, 477-516.

Kellogg, F.E. (1970). Water vapour and carbon dioxide receptors in *Aedes aegypti*. J. Insect Physiol. *16*, 99-108.

Kistler, K.E., Vosshall, L.B., and Matthews, B.J. (2015). Genome engineering with CRISPR-Cas9 in the mosquito *Aedes aegypti*. Cell Rep *11*, 51-60. 10.1016/j.celrep.2015.03.009.

Klowden, M. (1981). Initiation and termination of host-seeking inhibition in *Aedes aegypti* during oöcyte maturation. J Insect Physiol *27*, 799-803.

Klowden, M.J., and Lea, A.O. (1979). Humoral inhibition of host-seeking in *Aedes aegypti* during oocyte maturation. J Insect Physiol *25*, 231-235.

Knecht, Z.A., Silbering, A.F., Cruz, J., Yang, L., Croset, V., Benton, R., and Garrity, P.A. (2017). Ionotropic Receptor-dependent moist and dry cells control hygrosensation in Drosophila. Elife *6*. 10.7554/eLife.26654.

Knecht, Z.A., Silbering, A.F., Ni, L., Klein, M., Budelli, G., Bell, R., Abuin, L., Ferrer, A.J., Samuel, A.D., Benton, R., and Garrity, P.A. (2016). Distinct combinations of variant

ionotropic glutamate receptors mediate thermosensation and hygrosensation in Drosophila. Elife *5*. 10.7554/eLife.17879.

Koelle, M.R., Talbot, W.S., Segraves, W.A., Bender, M.T., Cherbas, P., and Hogness, D.S. (1991). The Drosophila EcR gene encodes an ecdysone receptor, a new member of the steroid receptor superfamily. Cell *67*, 59-77. 10.1016/0092-8674(91)90572-g.

Kohl, J., Ostrovsky, A.D., Frechter, S., and Jefferis, G.S. (2013). A bidirectional circuit switch reroutes pheromone signals in male and female brains. Cell *155*, 1610-1623. 10.1016/j.cell.2013.11.025.

Kokoza, V.A., Martin, D., Mienaltowski, M.J., Ahmed, A., Morton, C.M., and Raikhel, A.S. (2001). Transcriptional regulation of the mosquito vitellogenin gene via a blood meal-triggered cascade. Gene *274*, 47-65. 10.1016/s0378-1119(01)00602-3.

Kotsakiozi, P., Gloria-Soria, A., Caccone, A., Evans, B., Schama, R., Martins, A.J., and Powell, J.R. (2017). Tracking the return of Aedes aegypti to Brazil, the major vector of the dengue, chikungunya and Zika viruses. PLoS Negl Trop Dis *11*, e0005653. 10.1371/journal.pntd.0005653.

Kozlova, T., and Thummel, C.S. (2003). Essential roles for ecdysone signaling during Drosophila mid-embryonic development. Science *301*, 1911-1914. 10.1126/science.1087419.

Kraemer, M.U., Sinka, M.E., Duda, K.A., Mylne, A.Q., Shearer, F.M., Barker, C.M., Moore, C.G., Carvalho, R.G., Coelho, G.E., Van Bortel, W., et al. (2015). The global distribution of the arbovirus vectors *Aedes aegypti* and *Ae. albopictus*. Elife *4*, e08347. 10.7554/eLife.08347.

Kreher, S.A., Kwon, J.Y., and Carlson, J.R. (2005). The molecular basis of odor coding in the Drosophila larva. Neuron *46*, 445-456. 10.1016/j.neuron.2005.04.007.

Kwon, H.W., Lu, T., Rutzler, M., and Zwiebel, L.J. (2006). Olfactory responses in a gustatory organ of the malaria vector mosquito *Anopheles gambiae*. Proc Natl Acad Sci U S A *103*, 13526-13531.

Kwon, J.Y., Dahanukar, A., Weiss, L.A., and Carlson, J.R. (2007). The molecular basis of CO_2 reception in *Drosophila*. Proc Natl Acad Sci U S A *104*, 3574-3578. 10.1073/pnas.0700079104.

Laissue, P.P., Reiter, C., Hiesinger, P.R., Halter, S., Fischbach, K.F., and Stocker, R.F. (1999). Three-dimensional reconstruction of the antennal lobe in *Drosophila melanogaster*. J Comp Neurol *405*, 543-552.

Laissue, P.P., and Vosshall, L.B. (2008). The olfactory sensory map in *Drosophila*. Adv Exp Med Biol *628*, 102-114.

Larsson, M.C., Domingos, A.I., Jones, W.D., Chiappe, M.E., Amrein, H., and Vosshall, L.B. (2004). *Or83b* encodes a broadly expressed odorant receptor essential for *Drosophila* olfaction. Neuron *43*, 703-714.

Lea, A.O. (1964). Selection for autogeny in *Aedes aegypti* (Diptera: Culicidae). Ann Entomol Soc Am *57*, 656-657.

Lee, Y., Poudel, S., Kim, Y., Thakur, D., and Montell, C. (2018). Calcium taste avoidance in *Drosophila*. Neuron *97*, 67-74 e64. 10.1016/j.neuron.2017.11.038.

Li, H., Li, T., Horns, F., Li, J., Xie, Q., Xu, C., Wu, B., Kebschull, J.M., McLaughlin, C.N., Kolluru, S.S., et al. (2020). Single-cell transcriptomes reveal diverse regulatory strategies for olfactory receptor expression and axon targeting. Curr Biol *30*, 1189-1198.e1185. 10.1016/j.cub.2020.01.049.

Li, Q., Barish, S., Okuwa, S., Maciejewski, A., Brandt, A.T., Reinhold, D., Jones, C.D., and Volkan, P.C. (2016). A functionally conserved gene regulatory network module governing olfactory neuron diversity. PLoS Genet *12*, e1005780. 10.1371/journal.pgen.1005780.

Li, Q., and Liberles, S.D. (2015). Aversion and attraction through olfaction. Curr Biol *25*, R120-R129. 10.1016/j.cub.2014.11.044.

Li, W., Howard, J.D., Parrish, T.B., and Gottfried, J.A. (2008). Aversive learning enhances perceptual and cortical discrimination of indiscriminable odor cues. Science *319*, 1842-1845. 10.1126/science.1152837.

Liesch, J., Bellani, L.L., and Vosshall, L.B. (2013). Functional and genetic characterization of neuropeptide Y-like receptors in Aedes aegypti. PLoS Negl Trop Dis *7*, e2486. 10.1371/journal.pntd.0002486.

Liman, E.R., Zhang, Y.V., and Montell, C. (2014). Peripheral coding of taste. Neuron *81*, 984-1000. 10.1016/j.neuron.2014.02.022.

Lin, H.H., Cao, D.S., Sethi, S., Zeng, Z., Chin, J.S.R., Chakraborty, T.S., Shepherd, A.K., Nguyen, C.A., Yew, J.Y., Su, C.Y., and Wang, J.W. (2016). Hormonal Modulation of Pheromone Detection Enhances Male Courtship Success. Neuron *90*, 1272-1285. 10.1016/j.neuron.2016.05.004.

Lomvardas, S., Barnea, G., Pisapia, D.J., Mendelsohn, M., Kirkland, J., and Axel, R. (2006). Interchromosomal interactions and olfactory receptor choice. Cell *126*, 403-413.

Lu, T., Qiu, Y.T., Wang, G., Kwon, J.Y., Rutzler, M., Kwon, H.W., Pitts, R.J., van Loon, J.J., Takken, W., Carlson, J.R., and Zwiebel, L.J. (2007). Odor coding in the maxillary palp of the malaria vector mosquito *Anopheles gambiae*. Curr Biol *17*, 1533-1544.

Majeed, S., Hill, S.R., and Ignell, R. (2014). Impact of elevated CO_2 background levels on the host-seeking behaviour of *Aedes aegypti*. J Exp Biol *217*, 598-604. 10.1242/jeb.092718.

Malaspina, D.C., C. Goudsmit, N. (2006). The Impact of Olfaction on Human Social Function. In Olfaction and the Brain, W.C. Brewer, D. Pantelis, C., ed. (Cambridge University Press), pp. 220-232.

Malnic, B., Hirono, J., Sato, T., and Buck, L.B. (1999). Combinatorial receptor codes for odors. Cell *96*, 713-723.

Manning, L., and Doe, C.Q. (2017). Immunofluorescent antibody staining of intact *Drosophila* larvae. Nat Protoc *12*, 1-14. 10.1038/nprot.2016.162.

Marder, E., and Goaillard, J.M. (2006). Variability, compensation and homeostasis in neuron and network function. Nat Rev Neurosci *7*, 563-574. 10.1038/nrn1949.

Maresh, A., Rodriguez Gil, D., Whitman, M.C., and Greer, C.A. (2008). Principles of glomerular organization in the human olfactory bulb--implications for odor processing. PLoS One *3*, e2640. 10.1371/journal.pone.0002640.

Martelli, C., Carlson, J.R., and Emonet, T. (2013). Intensity invariant dynamics and odor-specific latencies in olfactory receptor neuron response. J Neurosci *33*, 6285-6297. 10.1523/JNEUROSCI.0426-12.2013.

Matthews, B.J., Dudchenko, O., Kingan, S.B., Koren, S., Antoshechkin, I., Crawford, J.E., Glassford, W.J., Herre, M., Redmond, S.N., Rose, N.H., et al. (2018). Improved reference genome of *Aedes aegypti* informs arbovirus vector control. Nature *563*, 501-507. 10.1038/s41586-018-0692-z.

Matthews, B.J., McBride, C.S., DeGennaro, M., Despo, O., and Vosshall, L.B. (2016). The neurotranscriptome of the *Aedes aegypti* mosquito. BMC Genomics *17*, 32. 10.1186/s12864-015-2239-0.

Matthews, B.J., Younger, M.A., and Vosshall, L.B. (2019). The ion channel *ppk301* controls freshwater egg-laying in the mosquito *Aedes aegypti*. Elife *8*, e43963. 10.7554/eLife.43963.

McBride, C.S. (2016). Genes and odors underlying the recent evolution of mosquito preference for humans. Curr Biol *26*, R41-46. 10.1016/j.cub.2015.11.032.

McBride, C.S., Baier, F., Omondi, A.B., Spitzer, S.A., Lutomiah, J., Sang, R., Ignell, R., and Vosshall, L.B. (2014). Evolution of mosquito preference for humans linked to an odorant receptor. Nature *515*, 222-227. 10.1038/nature13964.

McIver, S.B. (1972). Fine structure of pegs on the palps of female culicine mosquitoes. Can J Zool *50*, 571-576. 10.1139/z72-078.

McIver, S.B. (1982). Sensilla of mosquitoes (Diptera: Culicidae). J Med Entomol *19*, 489-535.

McIver, S.B., and Hutchinson, S.A. (1972). Coeloconic sensilla on the antennae of the yellow fever mosquito, Aedes aegypti (L.). Experientia *28*, 323.

McKenzie, S.K., and Kronauer, D.J.C. (2018). The genomic architecture and molecular evolution of ant odorant receptors. Genome Res *28*, 1757-1765. 10.1101/gr.237123.118.

McLaughlin, C.N., Brbić, M., Xie, Q., Li, T., Horns, F., Kolluru, S.S., Kebschull, J.M., Vacek, D., Xie, A., Li, J., et al. (2020). Single-cell transcriptomes of developing and adult olfactory receptor neurons in *Drosophila*. BioRxiv *10.1101/2020.10.08.332130*.

McMeniman, C.J., Corfas, R.A., Matthews, B.J., Ritchie, S.A., and Vosshall, L.B. (2014). Multimodal integration of carbon dioxide and other sensory cues drives mosquito attraction to humans. Cell *156*, 1060-1071. 10.1016/j.cell.2013.12.044.

Mello, T.R., Aleixo, A.C., Pinheiro, D.G., Nunes, F.M., Bitondi, M.M., Hartfelder, K., Barchuk, A.R., and Simoes, Z.L. (2014). Developmental regulation of ecdysone receptor (EcR) and EcR-controlled gene expression during pharate-adult development of honeybees (Apis mellifera). Front Genet *5*, 445. 10.3389/fgene.2014.00445.

Meyer, J.M., Ejendal, K.F., Avramova, L.V., Garland-Kuntz, E.E., Giraldo-Calderon, G.I., Brust, T.F., Watts, V.J., and Hill, C.A. (2012). A "genome-to-lead" approach for insecticide discovery: pharmacological characterization and screening of *Aedes aegypti* D(1)-like dopamine receptors. PLoS Negl Trop Dis *6*, e1478. 10.1371/journal.pntd.0001478.

Min, S., Ai, M., Shin, S.A., and Suh, G.S. (2013). Dedicated olfactory neurons mediating attraction behavior to ammonia and amines in *Drosophila*. Proc Natl Acad Sci U S A *110*, E1321-1329. 10.1073/pnas.1215680110.

Misof, B., Liu, S., Meusemann, K., Peters, R.S., Donath, A., Mayer, C., Frandsen, P.B., Ware, J., Flouri, T., Beutel, R.G., et al. (2014). Phylogenomics resolves the timing and pattern of insect evolution. Science *346*, 763-767. 10.1126/science.1257570.

Mombaerts, P. (1996). Targeting olfaction. Curr Opin Neurobiol *6*, 481-486.

Mombaerts, P., Wang, F., Dulac, C., Chao, S.K., Nemes, A., Mendelsohn, M., Edmondson, J., and Axel, R. (1996). Visualizing an olfactory sensory map. Cell *87*, 675-686.

Montell, C. (2009). A taste of the *Drosophila* gustatory receptors. Curr Opin Neurobiol *19*, 345-353. 10.1016/j.conb.2009.07.001.

Moon, S.J., Lee, Y., Jiao, Y., and Montell, C. (2009). A *Drosophila* gustatory receptor essential for aversive taste and inhibiting male-to-male courtship. Curr Biol *19*, 1623-1627. 10.1016/j.cub.2009.07.061.

Nagel, K.I., and Wilson, R.I. (2011). Biophysical mechanisms underlying olfactory receptor neuron dynamics. Nat Neurosci *14*, 208-216. 10.1038/nn.2725.

Neuhaus, E.M., Gisselmann, G., Zhang, W., Dooley, R., Stortkuhl, K., and Hatt, H. (2005). Odorant receptor heterodimerization in the olfactory system of *Drosophila melanogaster*. Nat Neurosci *8*, 15-17.

Ni, L., Bronk, P., Chang, E.C., Lowell, A.M., Flam, J.O., Panzano, V.C., Theobald, D.L., Griffith, L.C., and Garrity, P.A. (2013). A gustatory receptor paralogue controls rapid warmth avoidance in *Drosophila*. Nature *500*, 580-584. 10.1038/nature12390.

Ni, L., Klein, M., Svec, K.V., Budelli, G., Chang, E.C., Ferrer, A.J., Benton, R., Samuel, A.D., and Garrity, P.A. (2016). The Ionotropic Receptors IR21a and IR25a mediate cool sensing in Drosophila. Elife *5*. 10.7554/eLife.13254.

Niimura, Y. (2009). Evolutionary dynamics of olfactory receptor genes in chordates: interaction between environments and genomic contents. Hum Genomics *4*, 107-118. 10.1186/1479-7364-4-2-107.

Niimura, Y., Matsui, A., and Touhara, K. (2014). Extreme expansion of the olfactory receptor gene repertoire in African elephants and evolutionary dynamics of orthologous gene groups in 13 placental mammals. Genome Res *24*, 1485-1496. 10.1101/gr.169532.113.

Oberdorster, E., Clay, M.A., Cottam, D.M., Wilmot, F.A., McLachlan, J.A., and Milner, M.J. (2001). Common phytochemicals are ecdysteroid agonists and antagonists: a possible evolutionary link between vertebrate and invertebrate steroid hormones. J Steroid Biochem Mol Biol *77*, 229-238. 10.1016/s0960-0760(01)00067-x.

Okumu, F.O., Killeen, G.F., Ogoma, S., Biswaro, L., Smallegange, R.C., Mbeyela, E., Titus, E., Munk, C., Ngonyani, H., Takken, W., et al. (2010). Development and field evaluation of a synthetic mosquito lure that is more attractive than humans. PLoS One *5*, e8951. 10.1371/journal.pone.0008951.

Omer, S.M., and Gillies, M.T. (1971). Loss of response to carbon dioxide in palpectomized female mosquitoes. Ent Exp & Appl *14*, 251-252.

Paul, R.K., Takeuchi, H., and Kubo, T. (2006). Expression of two ecdysteroid-regulated genes, Broad-Complex and E75, in the brain and ovary of the honeybee (Apis mellifera L.). Zoolog Sci *23*, 1085-1092. 10.2108/zsj.23.1085.

Petryk, A., Warren, J.T., Marques, G., Jarcho, M.P., Gilbert, L.I., Kahler, J., Parvy, J.P., Li, Y., Dauphin-Villemant, C., and O'Connor, M.B. (2003). Shade is the Drosophila P450 enzyme that mediates the hydroxylation of ecdysone to the steroid insect molting

hormone 20-hydroxyecdysone. Proc Natl Acad Sci U S A *100*, 13773-13778. 10.1073/pnas.2336088100.

Potter, C.J., Tasic, B., Russler, E.V., Liang, L., and Luo, L. (2010). The Q system: a repressible binary system for transgene expression, lineage tracing, and mosaic analysis. Cell *141*, 536-548. 10.1016/j.cell.2010.02.025.

Price, J.L., and Powell, T.P. (1970). The mitral and short axon cells of the olfactory bulb. J Cell Sci *7*, 631-651.

Prieto-Godino, L.L., Rytz, R., Cruchet, S., Bargeton, B., Abuin, L., Silbering, A.F., Ruta, V., Dal Peraro, M., and Benton, R. (2017). Evolution of acid-sensing olfactory circuits in Drosophilids. Neuron *93*, 661-676.e666. 10.1016/j.neuron.2016.12.024.

Raji, J.I., Melo, N., Castillo, J.S., Gonzalez, S., Saldana, V., Stensmyr, M.C., and DeGennaro, M. (2019). *Aedes aegypti* mosquitoes detect acidic volatiles found in human odor using the *IR8a* pathway. Curr Biol *29*, 1253-1262 e1257. 10.1016/j.cub.2019.02.045.

Rattanarithikul, R., Harbach, R.E., Harrison, B.A., Panthusiri, P., and Coleman, R.E. (2007). Illustrated keys to the mosquitoes of Thailand V. Genera Orthopodomyia, Kimia, Malaya, Topomyia, Tripteroides, and Toxorhynchites. Southeast Asian J Trop Med Public Health *38 Suppl 2*, 1-65.

Ray, A., van der Goes van Naters, W., and Carlson, J.R. (2008). A regulatory code for neuron-specific odor receptor expression. PLoS Biol *6*, e125.

Reeves, L.E., Holderman, C.J., Blosser, E.M., Gillett-Kaufman, J.L., Kawahara, A.Y., Kaufman, P.E., and Burkett-Cadena, N.D. (2018). Identification of *Uranotaenia sapphirina* as a specialist of annelids broadens known mosquito host use patterns. Commun Biol *1*, 92. 10.1038/s42003-018-0096-5.

Ressler, K.J., Sullivan, S.L., and Buck, L.B. (1994). Information coding in the olfactory system: evidence for a stereotyped and highly organized epitope map in the olfactory bulb. Cell *79*, 1245-1255.

Riabinina, O., Luginbuhl, D., Marr, E., Liu, S., Wu, M.N., Luo, L., and Potter, C.J. (2015). Improved and expanded Q-system reagents for genetic manipulations. Nat Methods *12*, 219-222, 215 p following 222. 10.1038/nmeth.3250.

Riabinina, O., Task, D., Marr, E., Lin, C.C., Alford, R., O'Brochta, D.A., and Potter, C.J. (2016). Organization of olfactory centres in the malaria mosquito *Anopheles gambiae*. Nat Commun *7*, 13010. 10.1038/ncomms13010.

Riabinina, O., Vernon, S.W., Dickson, B.J., and Baines, R.A. (2019). Split-QF system for fine-tuned transgene expression in *Drosophila*. Genetics *212*, 53-63. 10.1534/genetics.119.302034.

Rimal, S., and Lee, Y. (2018). The multidimensional ionotropic receptors of Drosophila melanogaster. Insect Mol Biol *27*, 1-7. 10.1111/imb.12347.

Robertson, H.M., Gadau, J., and Wanner, K.W. (2010). The insect chemoreceptor superfamily of the parasitoid jewel wasp *Nasonia vitripennis*. Insect Mol Biol *19 Suppl 1*, 121-136. 10.1111/j.1365-2583.2009.00979.x.

Robertson, H.M., Warr, C.G., and Carlson, J.R. (2003). Molecular evolution of the insect chemoreceptor gene superfamily in *Drosophila melanogaster*. Proc Natl Acad Sci U S A *100 Suppl 2*, 14537-14542.

Rose, N.H., Sylla, M., Badolo, A., Lutomiah, J., Ayala, D., Aribodor, O.B., Ibe, N., Akorli, J., Otoo, S., Mutebi, J.P., et al. (2020). Climate and Urbanization Drive Mosquito Preference for Humans. Curr Biol *30*, 3570-3579 e3576. 10.1016/j.cub.2020.06.092.

Roth, L.M. (1951). Loci of sensory end-organs used by mosquitoes (*Aedes aegypti* (L.) and *Anopheles quadrimaculatus say*) in receiving host stimuli. Ann Entomol Soc Am *44*, 59-74.

Saez, E., Nelson, M.C., Eshelman, B., Banayo, E., Koder, A., Cho, G.J., and Evans, R.M. (2000). Identification of ligands and coligands for the ecdysone-regulated gene switch. Proc Natl Acad Sci U S A *97*, 14512-14517. 10.1073/pnas.260499497.

Sanchez-Alcaniz, J.A., Silbering, A.F., Croset, V., Zappia, G., Sivasubramaniam, A.K., Abuin, L., Sahai, S.Y., Munch, D., Steck, K., Auer, T.O., et al. (2018). An expression atlas of variant ionotropic glutamate receptors identifies a molecular basis of carbonation sensing. Nat Commun *9*, 4252. 10.1038/s41467-018-06453-1.

Sato, K., Pellegrino, M., Nakagawa, T., Nakagawa, T., Vosshall, L.B., and Touhara, K. (2008). Insect olfactory receptors are heteromeric ligand-gated ion channels. Nature *452*, 1002-1006.

Schaefer, M.L., Finger, T.E., and Restrepo, D. (2001). Variability of position of the P2 glomerulus within a map of the mouse olfactory bulb. J Comp Neurol *436*, 351-362.

Schneider, D. (1964). Insect Antennae. Annu Rev Entomol *9*, 103-122.

Schwedes, C., Tulsiani, S., and Carney, G.E. (2011). Ecdysone receptor expression and activity in adult Drosophila melanogaster. J Insect Physiol *57*, 899-907. 10.1016/j.jinsphys.2011.03.027.

Scott, K., Brady, R., Jr., Cravchik, A., Morozov, P., Rzhetsky, A., Zuker, C., and Axel, R. (2001). A chemosensory gene family encoding candidate gustatory and olfactory receptors in *Drosophila*. Cell *104*, 661-673.

Scott-Browne, J.P., Lopez-Moyado, I.F., Trifari, S., Wong, V., Chavez, L., Rao, A., and Pereira, R.M. (2016). Dynamic changes in chromatin accessibility occur in CD8+ T cells responding to viral infection. Immunity *45*, 1327-1340. 10.1016/j.immuni.2016.10.028.

Seki, Y., Dweck, H.K.M., Rybak, J., Wicher, D., Sachse, S., and Hansson, B.S. (2017). Olfactory coding from the periphery to higher brain centers in the Drosophila brain. BMC Biol *15*, 56. 10.1186/s12915-017-0389-z.

Semmelhack, J.L., and Wang, J.W. (2009). Select *Drosophila* glomeruli mediate innate olfactory attraction and aversion. Nature *459*, 218-223. 10.1038/nature07983.

Shaner, N.C., Campbell, R.E., Steinbach, P.A., Giepmans, B.N., Palmer, A.E., and Tsien, R.Y. (2004). Improved monomeric red, orange and yellow fluorescent proteins derived from *Discosoma sp.* red fluorescent protein. Nat Biotechnol *22*, 1567-1572.

Shankar, S., and McMeniman, C.J. (2020). An updated antennal lobe atlas for the yellow fever mosquito *Aedes aegypti*. PLoS Negl Trop Dis *14*, e0008729. 10.1371/journal.pntd.0008729.

Shao, Y.T., Wang, F.Y., Fu, W.C., Yan, H.Y., Anraku, K., Chen, I.S., and Borg, B. (2014). Androgens increase lws opsin expression and red sensitivity in male three-spined sticklebacks. PLoS One *9*, e100330. 10.1371/journal.pone.0100330.

Shyu, W.H., Chiu, T.H., Chiang, M.H., Cheng, Y.C., Tsai, Y.L., Fu, T.F., Wu, T., and Wu, C.L. (2017). Neural circuits for long-term water-reward memory processing in thirsty Drosophila. Nat Commun *8*, 15230. 10.1038/ncomms15230.

Siju, K.P., Hill, S.R., Hansson, B.S., and Ignell, R. (2010). Influence of blood meal on the responsiveness of olfactory receptor neurons in antennal sensilla trichodea of the yellow fever mosquito, *Aedes aegypti*. J Insect Physiol *56*, 659-665. 10.1016/j.jinsphys.2010.02.002.

Silbering, A.F., Rytz, R., Grosjean, Y., Abuin, L., Ramdya, P., Jefferis, G.S., and Benton, R. (2011). Complementary function and integrated wiring of the evolutionarily distinct *Drosophila* olfactory subsystems. J Neurosci *31*, 13357-13375. 10.1523/JNEUROSCI.2360-11.2011.

Smallegange, R.C., Knols, B.G., and Takken, W. (2010). Effectiveness of synthetic versus natural human volatiles as attractants for Anopheles gambiae (Diptera: Culicidae) sensu stricto. J Med Entomol *47*, 338-344. 10.1603/me09015.

Smallegange, R.C., Qiu, Y.T., van Loon, J.J., and Takken, W. (2005). Synergism between ammonia, lactic acid and carboxylic acids as kairomones in the host-seeking behaviour of the malaria mosquito *Anopheles gambiae sensu stricto* (Diptera: Culicidae). Chem Senses *30*, 145-152.

Smith, C.N., Smith, N., Gouck, H.K., Weidhaas, D.E., Gilbert, I.H., Mayer, M.S., Smittle, B.J., and Hofbauer, A. (1970). L-lactic acid as a factor in the attraction of *Aedes aegypti* (Diptera: Culicidae) to human hosts. Ann Entomol Soc Am *63*, 760-770.

Soffan, A., Subandiyah, S., Makino, H., Watanabe, T., and Horiike, T. (2018). Evolutionary Analysis of the Highly Conserved Insect Odorant Coreceptor (Orco)

Revealed a Positive Selection Mode, Implying Functional Flexibility. J Insect Sci *18*. 10.1093/jisesa/iey120.

Steib, B.M., Geier, M., and Boeckh, J. (2001). The effect of lactic acid on odour-related host preference of yellow fever mosquitoes. Chem Senses *26*, 523-528.

Stocker, R.F. (1994). The organization of the chemosensory system in *Drosophila melanogaster*: a review. Cell Tissue Res *275*, 3-26.

Stocker, R.F., Lienhard, M.C., Borst, A., and Fischbach, K.F. (1990a). Neuronal architecture of the antennal lobe in *Drosophila melanogaster*. Cell Tissue Res *262*, 9-34. 10.1007/bf00327741.

Stocker, R.F., Lienhard, M.C., Borst, A., and Fischbach, K.F. (1990b). Neuronal architecture of the antennal lobe in *Drosophila melanogaster*. Cell Tissue Res. *262*, 9-34.

Strotmann, J., Conzelmann, S., Beck, A., Feinstein, P., Breer, H., and Mombaerts, P. (2000). Local permutations in the glomerular array of the mouse olfactory bulb. J Neurosci *20*, 6927-6938. 10.1523/jneurosci.20-18-06927.2000.

Syed, Z., and Leal, W.S. (2007). Maxillary palps are broad spectrum odorant detectors in *Culex quinquefasciatus*. Chem Senses *32*, 727-738. 10.1093/chemse/bjm040.

Takken, W., and Kline, D.L. (1989). Carbon dioxide and 1-octen-3-ol as mosquito attractants. J Am Mosq Control Assoc *5*, 311-316.

Takken, W., and Verhulst, N.O. (2013). Host preferences of blood-feeding mosquitoes. Annu Rev Entomol *58*, 433-453. 10.1146/annurev-ento-120811-153618.

Talay, M., Richman, E.B., Snell, N.J., Hartmann, G.G., Fisher, J.D., Sorkac, A., Santoyo, J.F., Chou-Freed, C., Nair, N., Johnson, M., et al. (2017). Transsynaptic mapping of second-order taste neurons in flies by trans-Tango. Neuron *96*, 783-795 e784. 10.1016/j.neuron.2017.10.011.

Tanaka, N.K., Awasaki, T., Shimada, T., and Ito, K. (2004). Integration of chemosensory pathways in the *Drosophila* second-order olfactory centers. Curr. Biol. *14*, 449-457.

Tanaka, N.K., Endo, K., and Ito, K. (2012). Organization of antennal lobe-associated neurons in adult *Drosophila melanogaster* brain. J Comp Neurol *520*, 4067-4130. 10.1002/cne.23142.

Task, D., Lin, C.C., Afify, A., Li, H., Vulpe, A., Menuz, K., and Potter, C.J. (2020). Widespread polymodal odorant receptor expression in *Drosophila* olfactory neurons. bioRxiv *10.1101/2020.11.07.355651*.

Tauxe, G.M., MacWilliam, D., Boyle, S.M., Guda, T., and Ray, A. (2013). Targeting a dual detector of skin and CO_2 to modify mosquito host seeking. Cell *155*, 1365-1379. 10.1016/j.cell.2013.11.013.

Thorne, N., Chromey, C., Bray, S., and Amrein, H. (2004). Taste perception and coding in *Drosophila*. Curr Biol *14*, 1065-1079. 10.1016/j.cub.2004.05.019.

Trible, W., Olivos-Cisneros, L., McKenzie, S.K., Saragosti, J., Chang, N.C., Matthews, B.J., Oxley, P.R., and Kronauer, D.J.C. (2017). orco Mutagenesis Causes Loss of Antennal Lobe Glomeruli and Impaired Social Behavior in Ants. Cell *170*, 727-735 e710. 10.1016/j.cell.2017.07.001.

Troemel, E.R., Chou, J.H., Dwyer, N.D., Colbert, H.A., and Bargmann, C.I. (1995). Divergent seven transmembrane receptors are candidate chemosensory receptors in *C. elegans*. Cell *83*, 207-218.

Turner, S.L., Li, N., Guda, T., Githure, J., Carde, R.T., and Ray, A. (2011). Ultra-prolonged activation of CO_2-sensing neurons disorients mosquitoes. Nature *474*, 87-91. 10.1038/nature10081.

Turner, S.L., and Ray, A. (2009). Modification of CO2 avoidance behaviour in Drosophila by inhibitory odorants. Nature *461*, 277-281. 10.1038/nature08295.

Vassar, R., Chao, S.K., Sitcheran, R., Nunez, J.M., Vosshall, L.B., and Axel, R. (1994). Topographic organization of sensory projections to the olfactory bulb. Cell *79*, 981-991.

Ventura, A.K., and Worobey, J. (2013). Early influences on the development of food preferences. Curr Biol *23*, R401-408. 10.1016/j.cub.2013.02.037.

Ventura, T., Bose, U., Fitzgibbon, Q.P., Smith, G.G., Shaw, P.N., Cummins, S.F., and Elizur, A. (2017). CYP450s analysis across spiny lobster metamorphosis identifies a long sought missing link in crustacean development. J Steroid Biochem Mol Biol *171*, 262-269. 10.1016/j.jsbmb.2017.04.007.

Verhulst, N.O., Takken, W., Dicke, M., Schraa, G., and Smallegange, R.C. (2010). Chemical ecology of interactions between human skin microbiota and mosquitoes. FEMS Microbiol Ecol *74*, 1-9.

Vidal, B., Aghayeva, U., Sun, H., Wang, C., Glenwinkel, L., Bayer, E.A., and Hobert, O. (2018). An atlas of *Caenorhabditis elegans* chemoreceptor expression. PLoS Biol *16*, e2004218. 10.1371/journal.pbio.2004218.

von Frisch, K. (1923). Über die ‚Sprache' der Bienen. Eine tierpsychologische Untersuchung. Zoologische Jahrbücher *40*, 1-186.

Vosshall, L.B., Amrein, H., Morozov, P.S., Rzhetsky, A., and Axel, R. (1999). A spatial map of olfactory receptor expression in the *Drosophila* antenna. Cell *96*, 725-736.

Vosshall, L.B., Wong, A.M., and Axel, R. (2000). An olfactory sensory map in the fly brain. Cell *102*, 147-159.

Vythilingam, I., Chiang, G.L., and Chan, S.T. (1992). Evaluation of carbon dioxide and 1-octen-3-ol as mosquito attractants. Southeast Asian J Trop Med Public Health *23*, 328-331.

Wagh, D.A., Rasse, T.M., Asan, E., Hofbauer, A., Schwenkert, I., Dürrbeck, H., Buchner, S., Dabauvalle, M.C., Schmidt, M., Qin, G., et al. (2006). Bruchpilot, a protein with homology to ELKS/CAST, is required for structural integrity and function of synaptic active zones in *Drosophila*. Neuron *49*, 833-844. 10.1016/j.neuron.2006.02.008.

Wang, F., Nemes, A., Mendelsohn, M., and Axel, R. (1998). Odorant receptors govern the formation of a precise topographic map. Cell *93*, 47-60.

Wang, J.W., Wong, A.M., Flores, J., Vosshall, L.B., and Axel, R. (2003). Two-photon calcium imaging reveals an odor-evoked map of activity in the fly brain. Cell *112*, 271-282.

Wang, Z., Singhvi, A., Kong, P., and Scott, K. (2004). Taste representations in the *Drosophila* brain. Cell *117*, 981-991.

Ward, A., Hong, W., Favaloro, V., and Luo, L. (2015). Toll receptors instruct axon and dendrite targeting and participate in synaptic partner matching in a Drosophila olfactory circuit. Neuron *85*, 1013-1028. 10.1016/j.neuron.2015.02.003.

Warren, J.T., Yerushalmi, Y., Shimell, M.J., O'Connor, M.B., Restifo, L.L., and Gilbert, L.I. (2006). Discrete pulses of molting hormone, 20-hydroxyecdysone, during late larval development of Drosophila melanogaster: correlations with changes in gene activity. Dev Dyn *235*, 315-326. 10.1002/dvdy.20626.

Weiss, L.A., Dahanukar, A., Kwon, J.Y., Banerjee, D., and Carlson, J.R. (2011). The molecular and cellular basis of bitter taste in *Drosophila*. Neuron *69*, 258-272. 10.1016/j.neuron.2011.01.001.

WHO (2020). Vector-borne diseases. World Health Organization, Geneva, http://www.who.int/mediacentre/factsheets/fs387/en/.

Wicher, D., and Miazzi, F. (2021). Functional properties of insect olfactory receptors: ionotropic receptors and odorant receptors. Cell Tissue Res *383*, 7-19. 10.1007/s00441-020-03363-x.

Wicher, D., Schafer, R., Bauernfeind, R., Stensmyr, M.C., Heller, R., Heinemann, S.H., and Hansson, B.S. (2008). *Drosophila* odorant receptors are both ligand-gated and cyclic-nucleotide-activated cation channels. Nature *452*, 1007-1011.

Xu, P., Zhu, F., Buss, G.K., and Leal, W.S. (2015). 1-Octen-3-ol - the attractant that repels. F1000Res *4*, 156. 10.12688/f1000research.6646.1.

Yamagata, N., Ichinose, T., Aso, Y., Placais, P.Y., Friedrich, A.B., Sima, R.J., Preat, T., Rubin, G.M., and Tanimoto, H. (2015). Distinct dopamine neurons mediate reward signals for short- and long-term memories. Proc Natl Acad Sci U S A *112*, 578-583. 10.1073/pnas.1421930112.

Yamanaka, N., Rewitz, K.F., and O'Connor, M.B. (2013). Ecdysone control of developmental transitions: lessons from Drosophila research. Annu Rev Entomol *58*, 497-516. 10.1146/annurev-ento-120811-153608.

Yan, H., Opachaloemphan, C., Mancini, G., Yang, H., Gallitto, M., Mlejnek, J., Leibholz, A., Haight, K., Ghaninia, M., Huo, L., et al. (2017). An Engineered orco Mutation Produces Aberrant Social Behavior and Defective Neural Development in Ants. Cell *170*, 736-747 e739. 10.1016/j.cell.2017.06.051.

Yan, T., Chen, H., Sun, Y., Yu, X., and Xia, L. (2016). RNA Interference of the Ecdysone Receptor Genes EcR and USP in Grain Aphid (Sitobion avenae F.) Affects Its Survival and Fecundity upon Feeding on Wheat Plants. Int J Mol Sci *17*. 10.3390/ijms17122098.

Yang, C.F., and Shah, N.M. (2014). Representing sex in the brain, one module at a time. Neuron *82*, 261-278. 10.1016/j.neuron.2014.03.029.

Yao, C.A., Ignell, R., and Carlson, J.R. (2005). Chemosensory coding by neurons in the coeloconic sensilla of the *Drosophila* antenna. J. Neurosci. *25*, 8359-8367.

Yao, T.P., Segraves, W.A., Oro, A.E., McKeown, M., and Evans, R.M. (1992). Drosophila ultraspiracle modulates ecdysone receptor function via heterodimer formation. Cell *71*, 63-72. 10.1016/0092-8674(92)90266-f.

Yarmolinsky, D.A., Zuker, C.S., and Ryba, N.J. (2009). Common sense about taste: from mammals to insects. Cell *139*, 234-244. 10.1016/j.cell.2009.10.001.

Zhang, Y.V., Ni, J., and Montell, C. (2013). The molecular basis for attractive salt-taste coding in Drosophila. Science *340*, 1334-1338. 10.1126/science.1234133.

Zhao, Z., and McBride, C.S. (2020). Evolution of olfactory circuits in insects. J Comp Physiol A Neuroethol Sens Neural Behav Physiol *206*, 353-367. 10.1007/s00359-020-01399-6.

Zhao, Z., Zung, J.L., Kriete, A.L., Iqbal, A., Younger, M.A., Matthews, B.J., Merhof, D., Thiberge, S., Strauch, M., and McBride, C.S. (2020). Chemical signatures of human odour generate a unique neural code in the brain of *Aedes aegypti* mosquitoes. bioRxiv *10.1101/2020.11.01.363861*.

Zou, D.J., Chesler, A., and Firestein, S. (2009). How the olfactory bulb got its glomeruli: a just so story? Nat Rev Neurosci *10*, 611-618. 10.1038/nrn2666.